Università degli Studi di Salerno

Dipartimento di Ingegneria Elettronica ed Ingegneria Informatica

Dottorato di Ricerca in Ingegneria dell'Informazione
XI Ciclo – Nuova Serie

TESI DI DOTTORATO

Planning and Control of Electric Distribution Networks with Integration of Wind Turbines

CANDIDATO: **GEEV MOKRYANI**

TUTOR: **PROF. PIERLUIGI SIANO**
PROF. ANTONIO PICCOLO

COORDINATORE: **PROF. ANGELO MARCELLI**

Anno Accademico 2011 – 2012

Acknowledgments

Dedication

This thesis is dedicated to my father, Esmaeil, my mother, Fatemeh, and my sister, Golpar.

Table of Contents

List of Figures

List of Tables

Chapter 1

Background, Motivation and Contribution

1.1   Introduction

Recently, the wind power penetration into power systems has been increased. The increase in installing wind capacity in the network introduces different challenges to the operation and planning of the network. Nevertheless, wind generation is relied on the wind speed at a specified instant, which is not easy to forecast in advance. The stochastic nature of wind makes its planning a complex problem and therefore there is a need for the existing analytical methods to model the uncertainties related to wind speed properly.

In this chapter, the motivation for the developed methods, a comprehensive literature review and the main contributions of this thesis are described. In addition, the outline of the thesis is provided and the published papers are also listed.

1.2   Background and Motivation

Wind power is one of the most important types of renewable energy sources (RES) for electricity generation in order to reach aims such as the reduction of carbon-dioxide emission, energy autonomy and improved infrastructure reliability.

The intermittent nature of wind introduces some technical and economic challenges that must be overcome in order to integrate wind turbines (WTs) into the electricity networks. Moreover, wind producer has to hedge against the uncertainty and balance the profit variability because of significant wind unpredictability.

The market organization must provide mechanisms to cover energy imbalances caused by wind generation in competitive markets. Wind producers should be able to reduce the costs of imbalances

throughout a market participation that allows them to reinforce their competitiveness.

The impact of uncertainty in wind production can be eliminated by a balancing mechanism in order to compensate the uncertainty of wind power production. Generally, the balancing mechanism is supported by expensive energy sources such as combined cycle gas turbines. Therefore, a main concern of wind producers is that of decreasing the need for energy balancing [1].

Many European countries follow strategies to increase the exploitation of wind energy through incentives and financial alternatives. WTs integration into the grid creates several challenges to distribution network operators (DNOs) such as voltage deviation, power losses and voltage stability [2]. This is mainly due to the mismatch between the WTs place and the potential of local grid to site the new distributed generators (DGs) in the network.

Hence, appropriate placement of DGs in distribution networks has an important role in the improvement of the system operation. The optimal allocation of DGs is one of the most significant aspects for the distribution system planning.

The major role of a DNO is to supply loads at an acceptable voltage and loading level. A DNO has to develop a rational operating strategy taking into account dispatching DGs, interrupting loads, and purchasing power from the wholesale market while keeping system security. In some cases, DNOs play the role of retailers which buy power on the wholesale market at volatile prices and sell it again at fixed tariffs to small consumers. DNOs and retailers are separate market entities with different purposes, networks, and sizes [3].

European Directives 2005/89/EC and 2003/54/EC imply that DNOs should take into consideration the DG placement for planning the expansion of distribution systems. Nevertheless, they do not determine how this will be implemented without coordination between the planners of distribution system and the generation companies. Since the current capacity of distribution system will not be sufficient to deliver the required generated power, different rules have been provided in which a utility is permitted to locate DGs at strategic places on the grid to defer the cost of network upgrade and reduce energy supply costs at peak hours [3].

Supposing that the DNOs aim is to maximize their benefits, two diverse regulatory cases can be taken into account: 1) DG-owning DNO – permitted to possess DG and can exploit the financial benefits considering new generation as a choice for distribution system investments, 2) Unbundled DNO – forbidden to own DG but it can maximize the financial profits considering a number of incentives [4].

The US method for the ownership of DG is driven by the conventional structure of distribution networks in which they are responsible for supplying consumers throughout purchasing power from various sources besides possessing and operating the wires. The financial profits of DG placement to the utility from deferred generation and distribution investments are well recognized and utilities are permitted to place DG at optimal places in the network to defer costs of network upgrade [5].

On the other hand, WTs are typically located in remote and rural areas. In these areas, the feeders are long and operated at a low or medium voltage level characterized by a high R/X ratio and unbalanced voltage situations. Furthermore, weak grids are usually referred to have a 'low short-circuit level' or a 'low fault level'. In a weak network a change in either active or reactive power can cause a considerable change in the voltage. The impact relies on the strength of the network and the output power of the WTs [6]. Integration of WTs into weak grids will cause the steady state voltage level to go beyond its acceptable limits. Therefore, it can be a constraint for the exploitation of wind energy resources. Another constraint is related to the effect of the power generated by WTs on the voltage quality. Voltage level limitations and accurate control systems are required to control voltage variations as well as to improve voltage quality [7].

In this dissertation, various methods are utilized for planning, management and control of distribution networks with high penetration of WTs.

1.3   Literature Review

Optimal planning methods of distribution networks comprise deterministic and probabilistic methods. In section 1.3.1, previous works that have been carried out to seek the optimal capacities and

locations of DGs with deterministic and probabilistic methods are reviewed. In Section 1.3.2, the methods of control and management of distribution networks during voltage variations are reviewed.

1.3.1 Optimal Planning of Distribution Networks with DG

1.3.1.1 Deterministic Methods

In [8,9], the authors proposed a genetic algorithm (GA)-based method to determine the optimal sizes and locations of multiple DGs in order to minimize the network losses considering network constraints. In [10], a Tabu search method to obtain the optimal sizes and locations of DGs has been proposed. In [11], the authors proposed a cost based model to allocate DGs in distribution networks in order to minimize DG investment and total operation costs of the network. The objective function is solved using an Ant Colony Optimization method. In [12], a novel method for optimal allocation of DGs in distribution systems to minimize the network losses and to guarantee the acceptable reliability level and voltage profile has been proposed. A particle swarm optimization (PSO) based method for DG placement has been proposed in [13]. The main advantage of this method is that it can be easily implemented and typically the results obtained by this method are converged faster than GA. In [14-16], the use of active management schemes such as the coordinated voltage regulation of on-load tap-changers and the power factor control of DGs, including WTs and diesel generators, integrated in the optimal power flow (OPF) for the optimization of objective function have been investigated. In [17] an optimization technique is suggested to establish the maximum wind power injected into the grid with fixed transmission capacity taking into account the network security. In [18], a numerical algorithm is proposed to estimate the maximum wind energy exploitation in independent electric island networks. In [19], the differences in the improvement patterns of offshore wind power in Europe and US are discussed. In [20] the authors provided an investigation for the wind power investment in Turkey inspiring the

interest of wind investment and evaluating the wind generation costs in this country. In [21], a linear programming model is suggested to specify the optimal technology mix, taking into account wind power production as a negative load that influences the variability of the load profile and therefore the network operation.

1.3.1.2 Probabilistic Methods

In [22], a stochastic formulation of load margin considering power injection uncertainty from RES into the network was proposed. In [23], the authors proposed a single auction market model to evaluate the effect of wind production on market prices and total generation costs for different wind penetration levels and wind farm locations. In [24], a probabilistic reliability criterion considering uncertainties related to component outage in the expansion planning has been proposed. Moreover, the method minimizes the investment budget for constructing new transmission lines considering the uncertainties of the transmission system. In [25], a probabilistic method was proposed to find the wind power capacity limits with regards to the power transfer and voltage constraints in the network. In [26], a stochastic optimization algorithm was proposed to minimize the power losses by controlling the power factor of WTs. Some methods such as point estimation and Fast Fourier transform (FFT) are computationally low-cost while these are less accurate than using Monte Carlo simulation (MCS). In [27], the MCS is used to combine the correlated load demands and wind power generations by using the multivariate distribution to choose random variables. In [28], the authors proposed a hybrid optimization method to minimize the annual power losses to find optimal locations and capacities of WTs. The method combines GA, gradient-based constrained nonlinear optimization algorithm and sequential MCS. The authors in [29] established a well-founded statistical analysis to evaluate the impact of day-ahead wind power forecasts on the performance and the distributional properties of the price in the Western Danish area of the Nord Pool's Elspot market. In [30], a method for optimal placement of WTs in distribution networks to minimize the annual energy losses has been proposed. The method is based on generating a probabilistic generation-load model that

combines all possible operating circumstances of the WTs and load levels with their probabilities. The problem is formulated as mixed integer non-linear programming to minimize annual energy losses.

Although in [31-34] the impact of wind generations on electricity prices has been investigated, however, there is a lack of mathematical models capable to imitate the amount of the related impact. In [35], the authors provided a review of different computer tools to analyze the integration of renewable sources.

In [36], a hybrid possibilistic–probabilistic tool to assess the impact of DG units on technical performance of distribution network is proposed. The uncertainty of electric loads, DG operation/investments are also considered.

1.3.2 Control of Distribution Networks

In [37], the authors have proposed a mathematical model of the doubly fed induction generator (DFIG) for the analysis of active and reactive power performances of a wind farm (WF). A proportional-integral (PI)-based control algorithm to control the reactive power produced by WTs has been proposed in [38]. In [39], the relation between reactive and active power to maintain the DFIG's operation within the maximum rotor and stator currents has been studied. In [40], the authors have proposed a fuzzy controller to manage the operation of a Flywheel energy storage system (ESS) connected to a DC bus.

On the other hand, by regulating the rotor blades during abnormal conditions or high wind speed, the active power generated by a WT can be regulated. There are many previous works on pitch angle control. A linear quadratic Gaussian (LQG) control method for controlling the pitch angle has been proposed in [41]. A good robustness in gain and phase margins has been achieved. In [42], the authors proposed a linear matrix inequality (LMI) method for controlling the pitch angle in order to reduce the fluctuations in the power generated by WTs. A robust pitch angle control method has been proposed in [43] for smoothing the variations of the power

generated by WTs. The robustness of system has been obtained by using a LMI method.

Recently, the penetration of WTs into the grids has been increased and the performance of the WTs under faults has become an important issue, especially for DFIGs. Several grid codes prescribed to demand the ability of WTs to stay connected to the grid during faults and voltage variations, referred as fault ride-through (FRT) capability [44]. One of the common FRT capability improvement solutions is to set up a crowbar circuit across the rotor terminals [45]. In [46], the authors have achieved a FRT capability improvement by using hardware modification and inserting an additional voltage source converter connected at the generator terminal. A control strategy for improving the FRT capability by using flexible AC transmission system (FACTS) devices and ESS has been proposed in [47]. In [48], the authors have proposed a new feed-forward transient current control (FFTCC) method applied to rotor side converter for improving the FRT capability. In [49], a fuzzy controller to manage the rotor speed oscillations and the DC-link voltage variations of the DFIG has been proposed.

1.4   Contributions

The main contributions of this thesis are:
1. The review of the main economic and technical challenges of WTs integration into the distribution networks.
2. To provide hybrid deterministic methods for optimal planning of distribution networks with integration of WTs considering wind and load uncertainties. The uncertainties pertaining to wind and load as well as the correlation among different wind speeds are modeled by using time-series analysis.
3. To provide a probabilistic methodology for assessing the amount of wind power that can be injected into the grid as well as the impact of wind power penetration on locational marginal prices (LMPs) throughout the network within market environment considering uncertainties. The uncertainties due to stochastic nature of wind speed and WTs offer price and quantity are modeled by using MCS approach.

4. Policy recommendations for both DNOs and WTs' developers to better allocate WTs in the network as well as in terms of technical and economic effects.
5. To design a fuzzy controller to improve FRT capability of DFIG based WTs according to Danish grid code. The controller is designed to compensate the voltage variations at the point of common coupling by simultaneously controlling the reactive and active power generated by WTs.

1.5   Thesis Outline

The chapters of the thesis are outlined as follows:

Chapter 2 introduces an overview of the main challenges originated from the increasing penetration of wind power in distribution systems, and motivates the problems dealt with in this dissertation.

Chapter 3 describes deterministic methods for the planning of distribution systems within market environment from the points of view of both WTs' developers and DNOs. The uncertainty in load and wind is modeled by using time series analysis method.

Chapter 4 provides a probabilistic methodology to simulate the amount of wind power that can be injected into the grid as well as the effect of wind power penetration on LMPs through the network considering uncertainties within market environment. The method is conceived for DNOs to evaluate the amount of wind power that can be injected into the grid.

Chapter 5 describes a fuzzy controller in order to enhance FRT capability of WTs in distribution networks. The controller is designed to compensate the voltage sages and swells by simultaneously controlling the reactive and active power generated by WTs.

Chapter 6 concludes the thesis and gives suggestions for future work.

Chapter 2

Wind Power Challenges

2.1   Summary

The climate change issue has sparked discussion on the profits of confining industrial greenhouse gases emissions compared to the costs that modifications would involve. Reaching an agreement on this debatable topic looks to be hard because of the time scales and uncertainties. For the time being, climate change can only be rigorously assessed in relation to the planned effects for the upcoming decades and centuries of swelling temperatures, rising sea levels and heat waves.

Governments in developed countries are at present dependent on public view asking actions to prevent the worst effects of climate change. A major part of these fundamental modifications is to be done in the generation part, where restricting greenhouse gases emissions creates global warming that is currently one of the most important issues. The measures carried out to meet emission reduction goals have principally involved in increasing the penetration level of RES [50-51].

Actually, the US Department of Energy (DOE) defines in [52] a model-based scenario where wind energy caters the 20% of the electricity in the US in 2030, and discusses a group of technical and economic challenges that require to be prevailed for this scenario. The European Union is presently following the execution of its ambitious 20/20/20 goals, which aim by 2020 to decrease greenhouse gas emissions by 20%, compared to 1990; increase the amount of RES to 20% of the supply of energy, and the energy consumption decrement by 20% by means of energy efficiency schemes [53]. Numerous European countries, for instance, Germany, Spain, Portugal, and Denmark, have already achieved high wind power integration into the network in the range of 7 to 20% of electricity consumption. The rapid

growing of installed capacity of wind power is predicted to carry on in Europe and the United States [54-56]. It is expected that Asia will become the area in the world with the greatest development of installed wind capacity in the near future. This development will be mostly obtained by China, which has been increasing its installed capacity each year for the preceding few years, and is set to carry on the fast increment of its wind capacity to become the world's biggest annual market. Actually, annual augmentations are anticipated to reach more than 20 GW in China by 2014 [57]. This great advance is vigorously stimulated by government strategies intended to promote the supply change, inspire the development of the domestic industry, and undertake the network planning and strengthening needed to acquire the electricity to the market.

2.2   A Stimulus for Researchers: Challenges

Wind power has no emissions and assists sustainable growth. The wind generation is renewable source and geopolitically generous, encouraging the self-reliance in energy of states. Furthermore, it doesn't use water. As WTs do not use fuel, costs can be reduced and they can be a barrier against the volatility of fuel price. Note that wind power plants have low enforced interruption rates and can help to diminish the requirement for contaminating generation sources.

Nevertheless, because of the uncertainty of wind power it can't be dispatched in a conventional sense. Accordingly, as wind power is variable and uncertain, the high penetration of wind power into a network creates challenges for network operators and planners in about all the fields of the electrical power systems [58-61].

In fact, the handling of uncertainties in a network isn't new for specialists. Note that loads are also stochastic and variable and the network operators have been tackling the variability and uncertainty of loads.

2.2.1   A Long Way Ahead

The wind power integration into a grid requires taking into account a greater amount of uncertainty and variability in the grid operation. This fundamental fact becomes of the most importance if considering the crucial wind power integration into the grid denotes that numerous countries all over the world have set out to reach.

The wind power production variability entails the power system operation with a greater flexibility degree to coordinate the load variation that is described as the difference between the total energy consumption and the total wind energy production. This flexibility characterizes the grid capability to integrate wind power. The requisite for improving the flexibility to embed the variability of wind is depending on a number of features of a power system as explained in the following.

2.2.2   Wind and Load Correlation

If the daily pattern of wind power production coincides with that of demand, wind variability can be absorbed by consumers, with the subsequent decrease in net load variations.

Generally, load and wind availability are not correlated, for example, in Northern Europe, albeit the historical archives disclose that wind power production in winter is greater than that in the summer, there is not a notable coincidence of winter periods with high load and high wind generation [62]. Correlation between wind speeds at two diverse places typically decreases with their distance [63]. Furthermore, the variations of wind farms output power, fed with uncorrelated winds, are neutralized and consequently, the variability of total wind generation reduces. Hence, the geographical distribution of wind farms has a smoothing impact on wind power fluctuations. However, decisions on the location of WTs are usually limited to the wind availability that can be beneficially used.

2.2.3   Generation Mix

Indeed, the capability of a power system to integrate wind power is toughly reliant on its generation mix. Production technologies

capable to proficiently change their power output as needed by the net load fluctuations are of required to withstand supply paradigm mainly based on renewable energy sources. Actually, generally when there is unfavorable correlation between wind and load, not only the necessity for cycling units is increased considerably but also the operating system of the units will be changed considerably. In this regard, flexibility on the generation-side of a power system generally results in operating conventional units at levels of productions greater or less than their optimal to accommodate the intrinsic variability of wind generation by ramping up or down. Moreover, the ramping expeditions may mostly end up with the start-up or shut-down of conventional generators. Accordingly, if great fluctuations of wind generation are to be accommodated by the conventional generation, this may lead to conventional power plants work in a less proficient way, therefore decreasing the amount of pollutant emissions that are decreased by the wind energy integration into the grid [64]. The pollution reduction reached by wind integration is reliant on the type of production and fuel that is substituted when WTs are generating.

Note that wind power integration has an important effect on the generation mix of a power system. The appropriate assessment of this impact needs calculating the wind generation's capacity credit [65].

The capacity credit is a criterion to measure of the volume of conventional generation that is substituted by the intermittent generation without decreasing the reliability of the system. However, when the reliability of the power plant is less than 100%, there always exists a confined risk of not having sufficient capacity accessible to satisfy the demand, and wind generation may be accessible at the crucial moment when load is high and other generators may fail. Actually, it implies that 1 MW of installed wind capacity is not enough to cover 1MWof demand in a reliable and safe way, but it is sufficient to effectively satisfy a specified percentage of it [66].

2.2.4   Demand Side Management

If wind generation and demand are not correlated and the weather conditions cannot be changed, a technique is introducing demand response method to utilize the real-time pricing (RTP) [67-70], according to which retail prices alter mostly to reflect fluctuations in

the energy dispatch and the cost of supplied load. If wind is high/low, the demand will increase/decrease because of low/high prices while when wind is low the demand will decrease due to high prices. The accomplishment of demand-side management schemes will be significantly facilitated by the constitution of smart grids [71], which are considered to enable consumers to play a significant role in optimization of power systems operation by means of intelligent monitoring, control, and communication.

2.2.5   Controllable loads

The controllable loads could be added to the grid to use the unused wind power production. For instance, some kinds of these loads comprise electric heating, and boilers, fuel production such as hydrogen heating; and the electric vehicles or plug-in hybrid vehicles (PHV) that is becoming a hopeful potential in large-scale applications [72,73]. The implication of vehicle-to-grid (V2G) refers to a system where PHVs connect to the network to cater services of demand response by injecting/absorbing power into/from the grid [74, 75].

2.2.6   Electricity Storage

The technical community decides that the high penetration of RES can be significantly simplified by increasing significant storage capabilities. Albeit currently there are numerous energy storage technologies that can afford to achieve this goal such batteries, flywheels, electric vehicles, superconducting magnetic energy storage systems, compressed air, pumped hydro storage systems [76, 77]. Innovative developments and more incentives in this arena are still required for the huge electricity storage to become a reality in the requisite terms [77, 78].

2.2.7   Wind Technology Upgrading

A part of electricity supply side requires to be supplied by generators to cater the ancillary services needed to guarantee the safe operation of the power system. If WTs are not equipped with the proper technology to help the voltage control devices, wind curtailments will be unavoidable in conditions where the sum of the

wind generation and the conventional generation is essential for safety reasons exceed energy consumption. In some countries, grid companies are forcing generators to set up tools for voltage and reactive power control [65]. Furthermore, the significant amount of wind power penetration into the grid requires that WTs stay connected to the grid during fault.

2.2.8   Power System Operation

As previously stated, wind power encompasses uncertainty and variability in the power system operation. A part of the uncertainty can be expected several hours or days ago and can be absorbed by an optimal energy dispatch of the network operators according to their elasticity. Essentially, a generator or load that caters reserve want to change its generation as needed in a short time. Reserves needed to incorporate unexpected wind power variations are basically slow, i.e., the activation times are about or more than 15 minutes [60].

The extension of reserves results in comparatively fast energy re-dispatches, which considerably augments the need for elasticity of power system elements. Accordingly, wind uncertainty includes also operating costs [60, 61] that can be minimized by proper reserve placement and deployment. Briefly, tools for the optimal energy and reserve scheduling are critical to optimal use of wind power in order to avoid unnecessary wind power curtailments and reducing the costs of expected or unexpected uncertainty.

In most countries, the wind energy development is happening in a reconstructed electricity area are controlled by market rules. Electricity transactions are therefore complied in a market to which generators and loads submit their bids to maximize their benefits or minimize the procurement costs. A third party, generally referred to as market operator (MO), is responsible to determine the accepted bids of producers and consumers as well as the electricity price. The aim of MO is maximizing SW by using a market-clearing tool. The competitive transaction of the electricity is challenging by itself because of the constraints forced by the grids and their agents, and they will be influenced by uncertainties. The aim of the market is augmenting the financial performance of grids while ensuring a safe action of the electrical structure.

2.2.9 Market Design and Clearing tools

Every electricity market is established adversely. Usually, electricity markets comprise numerous trading areas to assist energy transactions between producers and consumers in the long and short run. Trading levels for short-term energy trading encompass a day-ahead market, numerous adjustment and balancing markets.

The set of these serially organized short-term trading levels is typically referred to as the pool. In the day-ahead market, energy trading to be happened in the following day is discussed. The adjustment markets allow market operators to change the energy sold or purchased in the day-ahead market with regards to modifications in their expected generations or consumptions. The balancing markets, so-called real-time markets, enable last minute energy trading to tackle with real situations and assure the actual balance between generation and load. The Electricity Market of the Iberian Peninsula, for example, comprises one day-ahead market, six adjustment markets consecutively organized over the delivery horizon, and hourly balancing markets [79].

The results of an electricity market are depending on the market clearing procedure utilized by the market operator. Presently, there are different market-clearing methods such as single auction methods and complex mechanisms for the concurrent energy provision and reserve by means of an OPF. Generally, the market-clearing device's complication depends on the properties of the network that are taken into account in the procedure. Therefore, the techniques for market clearing may consider inter-temporal constraints such as the ramping capabilities or the minimum up and down times of generators. The tool for pricing is dependent on the market clearing mechanism. Therefore, the network modeling in the process to clear the market results in the concept of LMP in which, the LMP at each bus of the network is diverse because of active power losses or network congestion [76,80,81]. On the contrary, if the constraints of the network are neglected, a unique price is attained.

Chapter 3

Planning of Distribution Networks by Using Deterministic Methods

This chapter introduces deterministic methods for optimal planning of distribution networks within a distribution market with integration of wind turbines. Section 3.1 introduces the objectives of DNOs and DG developers. Section 3.2 introduces an innovative method for optimal placement of WTs in distribution network by using OPF. Model formulation is explained in Section 3.3. Test system description and simulation results of this method are provided in Section 3.4. In Section 3.6, the GA implementation for annual energy losses minimization from the DNOs viewpoint is explained. DNO acquisition market is introduced in Section 3.7. Section 3.8 discusses the net present value (NPV) maximization from the point of view of wind turbines' developers. The discussion and conclusions are provided in Section 3.9.

3.1   The Objectives of DNOs and DG Developers

This section investigates the DNOs and developers incentives, which they are two main actors in DG market. The objectives of DG developers are maximizing returns from electricity sales and minimizing the imported energy cost when there are combined heat and power (CHP). These will tend to be met with augmented installed capacity but they are considerably affected by the strategies of DNO on connection and use of system charges.

The incentives for installing DG are different. Some countries such as Australia and Ireland use deep charging while some others like Italy, France and Norway apply shallower charges [82, 83]. In the United States, customers are responsible for paying costs beyond a regulator-specified connection "allowance" [82]. Most systems do not

presently apply Distribution Use of System (DUoS) charges to DG except in a few cases such as Sweden and the U.K., DG placement in the distribution systems of U.K, before April 2005, was charged the full capital costs of connection, and capitalized operation and maintenance costs instead of DUoS charges [84].

The charges encourage the DNO to site DG by catering a return more than the normal regulated return rate in which there is a rational take up level and use of connected generation and the costs of connection are comparatively low [83]. Finally, the cost of network connection and usage is driven by the match between the DG capacity and the network to which it connects. According to the U.K. incentives for DNOs, there is profit to DNOs and DG developers in reducing the capital costs related to reinforcement. Although active network management schemes [85] make a major contribution, identifying and encouraging DG connections at sites and capacities that make the best use of the network is required [86-89].

However, 7% of electricity produced in the U.K. is lost as power losses. Although losses are unavoidable, they can be controlled via investment in low loss tools and more efficient network configuration [90]. Moreover, losses can be considerably affected by DGs: power injections at low voltages reduce losses but losses may increase generally when the injected power is higher than demand. Though the DG effect on losses is site and time specific, losses track a U-shaped trajectory [91]. Till 2005, the DNO incentives to reduce losses were by loss adjustment factors (LAFs) [92] with site-specific LAFs applied at 33 kV and above. The price control motivates DNOs to control losses through catering rewards for loss reductions and penalties for increases compared with a target level. The annual target of DNO is set by Office of Gas and Electricity Market (Ofgem) and values losses at 60 €/MWh (according to 2004 values). DNOs are encouraged to be responsible the essential investment to reduce the losses [83]. The low amount of DG penetration to reduce the power losses can motivate DNOs to confine connections within their networks. It should be noted that DG developers are not fully incentivized for their impact on losses.

3.2   Optimal Placement of WTs by Using Market-based Optimal Power Flow

In this section, a novel method for optimal allocation of WTs by using market-based OPF to maximize the system SW is proposed. The market-based OPF uses constrained cost variable (CCV) approach to generate the appropriate helper variable, cost term, and related constraints for any piecewise linear costs. The method is conceived for DG-owning DNOs to find the optimal numbers and sizes of WTs among different potential combinations. WTs and dispatchable loads (DLs) are owned or managed by the DG-owning DNO. The objective function is solved by using step-controlled primal dual interior point method (SCPDIPM) considering network constraints.

The proposed method considers SW maximization for the optimal allocation of WTs, thus, its maximization implies not only the minimization of the energy production costs but also the maximization of the consumers' benefit.

By using the proposed method, WTs can be, in fact, optimally allocated at buses where they are more advantageous, i.e. near higher loads or in parts of the network where the loads have the higher values and the consumers' benefit is higher. The method can help DG-owning DNOs to better allocate WTs by considering cost reduction and consumers' benefits.

3.2.1   The Structure of the Proposed Method

The structure of the proposed method for optimal allocation of WTs is shown in Fig.3.1. The method maximizes the SW by using market-based OPF for different combinations of load demand and wind power generation considering network constraints.

Different combinations of wind power generation and load demand is considered via scenarios. Each demand level is characterized by six wind generation levels. There are four load demand levels, i.e. 30%, 50%, 70%, 90%, and six wind generation levels, i.e. 0%, 20%, 40%, 60%, 80%, and 100%. Therefore, jointly considering the load demand and wind generation levels results in 24

scenarios, i.e. four load demand levels, with two blocks per level with different sizes and the same price, by six wind generation levels with four blocks per level with the same size and the same price for all blocks.

The maximum number of WTs that can be allocated at a given bus is represented by an equivalent number of blocks in the WT's offer. At each candidate bus it is assumed that maximum four WTs can be allocated; therefore, for each generation level there are four blocks with the same price and the same size equal to the rated power of the WTs for all blocks. With regards to the bids for DLs, it is assumed that there are two blocks per load with different sizes and the same price for all blocks, respectively.

The market-based OPF uses CCV method to generate the appropriate helper variable, cost term, and related constraints for any piecewise linear costs. WTs' offers and bids of DLs are taken and treated as marginal cost and marginal benefit functions, respectively, then by using the CCV method they are converted to the equivalent total cost and total benefit functions and plugged into a matrix as piecewise linear costs. The method is applied by DNOs to find the optimal numbers and capacities of WTs among different potential combinations.
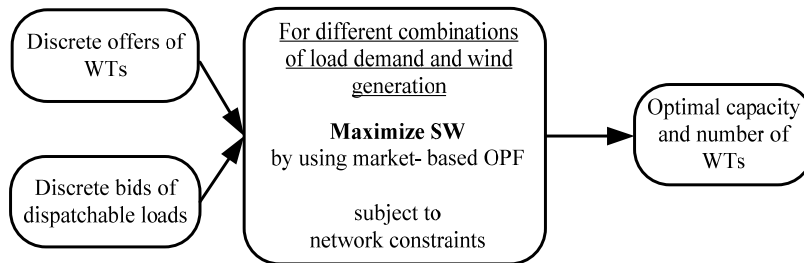
Fig.3.1.The structure of the proposed method

3.3   Model Formulation

In this section, the mathematical formulation of SW maximization is discussed. Maximization of SW implies not only the minimization

of the energy production costs but also the maximization of the consumers' benefit. The SW is formulated as follows:

$$\text{Maximize} \quad SW = \sum_j B_j(d_j) - \sum_i C_i(g_i) \tag{3.1}$$

where

$$B_j(d_j) = \frac{1}{2} m_d d_j^2 + b_j d_j \tag{3.2}$$

$$C_i(g_i) = \frac{1}{2} m_g g_i^2 + b_i g_i \tag{3.3}$$

The $C_i(g_i)$ and $B_j(d_j)$ are the production cost and benefit of consumers, respectively

$$p_i = b_i + m_g g_i, \text{ for } i = 1,2,\cdots I \tag{3.4}$$

where

b_i is the intercept (reservation price $b_i > 0$) in €/MWh,

m_g is the slope ($m_g > 0$) in €/MW²h,

p_i is the price at which producer i is willing to supply in €/MWh,

g_i is the supply in MW,

$$p_j = b_j + m_d d_j, \text{ for } j = 1,2,\cdots J \tag{3.5}$$

where

b_j is the intercept (reservation price $b_j > 0$) in €/MWh,

m_d is the slope ($m_d < 0$)in €/MW²h,

p_j is the price at which consumer j is willing to pay in €/MWh,

d_j is the demand in MW.

3.3.1   Constraints

3.3.1.1   Active and reactive power constraints for the interconnection to the external network (slack bus):

$$P_b^{\min} \le P_b \le P_b^{\max}, \quad Q_b^{\min} \le Q_b \le Q_b^{\max} \tag{3.6}$$

where P_b and Q_b are active and reactive power of the slack bus, respectively.

3.3.1.2 Voltage level constraints at the buses

$$V_i^{\min} \leq V_i \leq V_i^{\max} \qquad (3.7)$$

where $V_i^{\min}$ and $V_i^{\max}$ are the lower and upper bounds of the bus voltage, respectively.

3.3.1.3 Thermal limits of the lines connecting the buses

The thermal capacity $S_k^{\max}$ of network also bounds the maximum apparent power transfer, S_k :

$$S - S_k^{\max} \leq 0 \qquad (3.8)$$

3.3.1.4 WTs power constraint

$$0 \leq P_g \leq P_g^{\max} \qquad (3.9)$$

It is assumed that WTs operate at constant power factor.

$$\cos\varphi = \frac{P_g}{\sqrt{P_g^2 + Q_g^2}} = \text{constant.} \qquad (3.10)$$

where P_g and Q_g are the generated active and reactive powers by WTs, respectively.

3.3.1.5 DLs power constraints

$$P_d^{\min} \leq P_d \leq 0 \qquad (3.11)$$

It is assumed that DLs operate at constant power factor.

$$\cos\varphi = \frac{P_d}{\sqrt{P_d^2 + Q_d^2}} = \text{constant.} \qquad (3.12)$$

where P_d and Q_d are active and reactive power of DLs, respectively.

3.3.2   Dispatchable Load Modeling

One way to model price-sensitive or DLs is modeling them as negative generators with related negative costs. This is carried out by determining a generator with a negative output in a range from a minimum injection equivalent to the negative of the highest load value to a maximum injection of zero [93,94]. Here, it is supposed that DLs have a fixed power factor and an equality constraint to impose a fixed power factor for a negative generator is utilized for a DL modeling. It should be noted that with the description of a DL as a negative generator, if the negative cost relates to the consumer's benefit function, the minimization of generation cost is equal to SW maximization.

Furthermore, an additional equality constraint to enforce a constant power factor for any "negative generator" is utilized to model a DL. In the following, an example of a DL is provided whose marginal benefit function is shown in Fig. 3.2 (a). This relates to a negative generator with the piecewise linear cost curve as shown in Fig.3.2 (b). It should be noted that this approach assumes that the demand blocks can be partially dispatched or split.

(a)

(b)
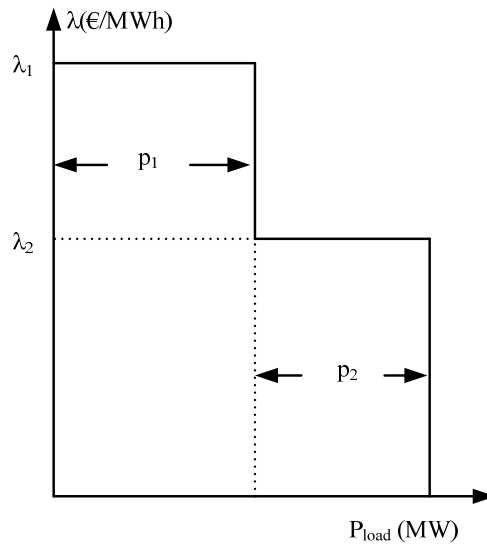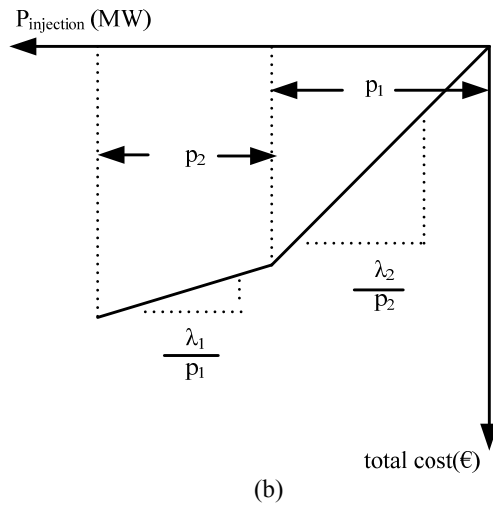
Fig.3.2. (a) Bid function, (b) total cost function for negative injection

3.3.3   Constrained Cost Variable Formulation

The conventional OPF formulation is not capable to solve the non-smooth piecewise linear cost functions result from discrete offers and bids, thus, when such cost functions are convex they can be modeled by CCV method [95-97].

The market-based OPF uses CCV method to generate the appropriate helper variable, cost term, and related constraints for any piecewise linear costs. CCV is an alternative OPF formulation that is suggested to enhance the market-based OPF scalability computation. The piecewise linear cost function $c(x)$ is replaced with a helper variable y and linear constraints that produce a convex "basin" needs the cost variable y to put into the function $c(x)$. A convex n-segment piecewise linear cost function is shown in Fig. 3.3.
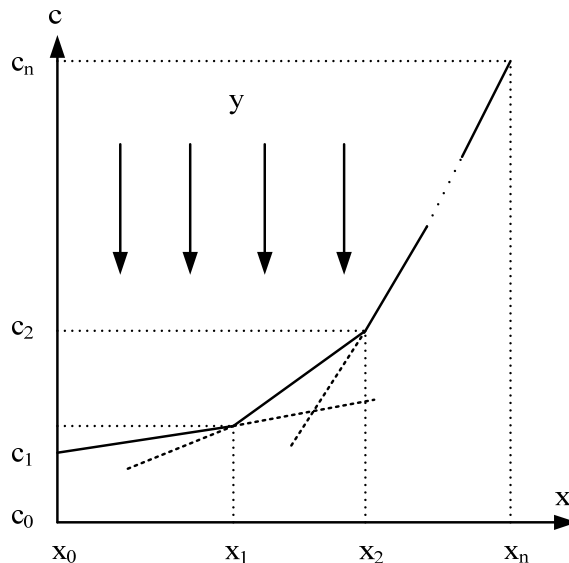
Fig.3.3. Constrained cost variable

$$c(x) = \begin{cases} m_1(x - x_1) + c_1, & x \le x_1 \\ m_2(x - x_2) + c_2, & x_1 < x \le x_2 \\ \vdots \\ m_n(x - x_n) + c_n, & x_{n-1} < x \end{cases} \tag{3.13}$$

A convex n-segment piecewise linear cost function is defined by a sequence of points (x_j, c_j), $j = 0 \cdots n$ where m_j denotes the slope of the jth segment,

$$m_j = \frac{c_j - c_{j-1}}{x_j - x_{j-1}}, \quad j = 1, \cdots, n \tag{3.14}$$

and $x_0 < x_1 < \cdots < x_n$ and $m_1 \le m_2 \le \cdots < m_n$.

The "basin" related to the cost function is generated through the following n constraints on the helper variable y.

$$y \ge m_j(x - x_j) + c_j, \qquad j = 1, \cdots, n \tag{3.15}$$

The variable y is added to the objective function instead of $c(x)$. By using CCV method, the piecewise linear costs of active or reactive power can be converted into the appropriate helper variable and the related constraints.

Furthermore, every piecewise function in the objective is substituted with a helper variable and for every piece of the piecewise function inequality constraints are imposed on that variable. CCV is a way that formulates a piecewise linear cost function on a new variable that is linearly constrained.

In this thesis, the offers of WTs and bids of DLs are taken and treated as marginal cost and marginal benefit functions, respectively, then by using CCV method they are converted into the equivalent total cost and total benefit functions by integrating the marginal cost and benefit functions and plugged into a matrix as piecewise linear costs.

3.3.4   Step-Controlled Primal Dual Interior Point Method

The Primal Dual Interior Point method (PDIPM) and its numerous variations have become the algorithms of choice for solving OPFs in the last years [95-97].
Even if the PDIPM fits properly with classical OPFs that utilize smooth polynomial cost function, it is not able to solve the market-based OPFs with non-differentiable piecewise cost. When piecewise cost is considered, the gradient and Hessian variables change from iteration to iteration considerably. Also, the descending of Newton steps is not obtained. The SCPDIPM [93, 94] that is used in this paper overcomes this difficulty by monitoring the accuracy of the quadratic approximation of the Lagrangian during the OPF computation and reducing the Newton step if any unexpected change of derivative results in an inaccurate approximation. It is efficient applying such step control method when the normal PDIPM step is not able to improve the gradient condition. By adjusting steps, SCPDIPM is able to reduce both system cost and gradients.

3.3.5   Variables

For the objective function (3.1) the optimization variable including vector L= $[V_i, \theta_i, P_g, P_d]$ where V_i and θ_i are voltage and voltage angle at the buses, respectively. P_g is active power generated by WTs and P_d is active power of DLs.

λ and μ are Langrangian multipliers and uses the Newton's method to solve the Karush–Kuhn–Tucker (KKT) conditions [93-95].

3.4   Test System Description and Simulation Results

In this section, the distribution system used to test the proposed method is described. The following analyses are based on an 83-bus 11.4-kV radial distribution system whose data given in [4]. The eleven feeders are supplied by two 20 MVA, 33/11.4 kV transformers. The one line diagram of the distribution system is shown in Fig.3.4. The candidate buses in the test system are included in the set {6, 9, 14, 28, 30, 38, 40, 45, 47, 54, 56, 62, 64, 81, 83}. The WTs operate at power factor of 0.95 lagging. Voltage limits are taken to be ±6% of nominal value, i.e. V_{max}= 1.06 p.u. and V_{min}= 0.94 p.u., and the feeders' thermal limits are given in Table 3.1 and vary between 40 and 480 A. Dispatchable and fixed loads, with constant power factor equal to 0.95, are served by both the grid and the WTs. The total maximum fixed load is 5.4 MW. The loading level for each band is given in Table 3.2.
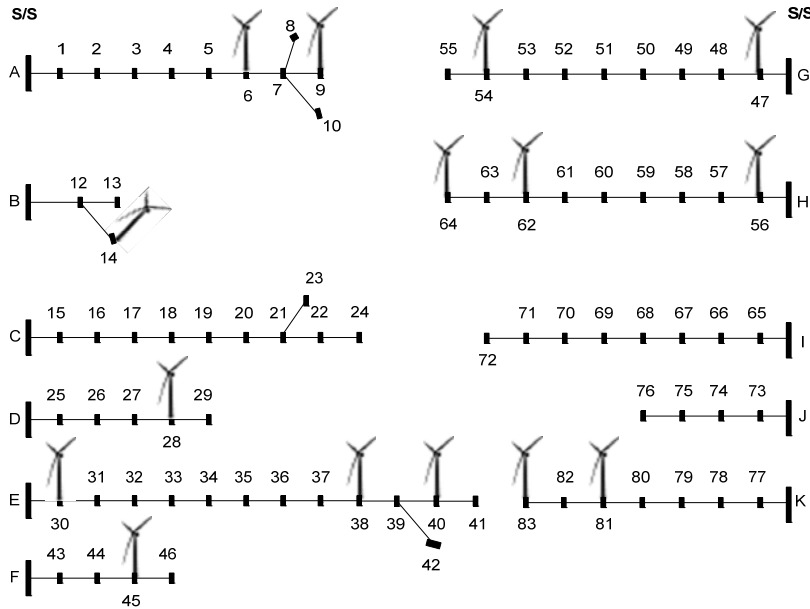
Fig.3.4. 83- bus radial distribution network with candidate locations for WTs

Table 3.1 Existing wires

Wires	Amps
A-1, 1-2, 2-3, 3-4, 4-5, 5-6, B-11, 12-13, C-15, D-25, E-30, 31-32, F-43, 44-45, G-47, 48-49, 57-58, I-65, 66-67, J-73, K-77, 78-79	480
7-8, 13-15, 16-17, 17-18, 19-20, 20-21, 26-27, 27-28, 32-33, 33-34, 34-35, 35-36, 36-37, 37-38, 38-39, 49-50, 50-51, 51-52, 52-53,57-58, 58-59, 59-60, 60-61,67-68, 68-69, 79-80, 80-81	330
21-22,21-23, 28-29, 41-42, 53-54, 61-62, 62-63, 69-70, 70-71, 71-72, 74-75, 75-76	180
H-56	60
7-9, 46-47, 63-64	50
7-10, 12-14, 22-24, 38-39, 39-40, 45-46, 54-55, 81-82, 82-83	40

Table 3.2 Loading level

Load demand level (%)	Active Power (MW)
30	16.50
50	27.50
70	39.00
90	55.00

In this case study, only WTs of a size of 660 kW are considered by the DG-owning DNO even if considering different sizes simultaneously is also possible. This requirement is regulated by the accessible land for WTs' building. The maximum generated active power by the WTs for different wind generation levels is given in Table 3.3.

Table 3.3 Wind generation level

Wind generation level (%)	Active Power (kW)
0	00.00
20	99.60
40	280.00
60	405.00
80	538.00
100	660.00

The maximum number of WTs that can be allocated at a given bus is represented by an equivalent number of blocks in the WT's offer. At each candidate bus it is assumed that maximum four WTs of each size can be allocated, thus, for each generation level there are four blocks of the same size equal to the rated power of the selected WTs and the same price of 70 €/MWh. In the following subsection, the method of calculating WT's offer price from the point of view of DNOs is explained.

The offers are assumed at price of 120 €/MWh for the bus connecting the distribution network to the transmission one. Regarding the bids for DLs, it is assumed that there are two blocks per demand bid with different sizes as presented in Table 3.4 and the same price of 250 €/MWh for all blocks.

Table 3.4 Bids of dispatchable loads

Load No.	Bus No.	Block 1 (MW)	Block 2 (MW)	Load No.	Bus No.	Block 1 (MW)	Block 2 (MW)
1	6	0.84	0.84	16	44	2.10	1.05
2	9	0.84	0.84	17	46	2.10	1.05
3	14	0.84	0.84	18	51	2.10	1.05
4	28	0.84	0.84	19	53	2.10	4.20
5	30	0.84	0.84	20	55	2.10	4.20
6	38	0.84	0.84	21	59	4.20	2.10
7	40	0.84	0.84	22	63	4.20	2.10
8	45	0.84	0.84	23	67	2.10	0.84
9	47	2.10	1.05	24	69	2.10	0.84
10	54	2.10	1.05	25	73	2.10	2.10
11	56	2.10	1.05	26	75	4.20	2.10
12	62	2.10	1.05	27	77	0.84	0.84
13	64	2.10	1.05	28	79	4.20	2.10
14	81	2.10	2.10	29	82	0.84	0.84
15	83	1.05	1.05				

3.4.1   WTs' Offers Price Calculation from the Point of View of DNO

In order to calculate the price of WTs' offers, financial data, i.e. WTs' life time, installation cost, depreciation time, interest rate, are considered as summarized in Table 3.5 [98,99]. The annual cost for WTs is calculated as follows [99]:

$$Ann\_Cost = \frac{i(1+i)^n}{(1+i)^n - 1} \times Inst\_Cost \qquad (3.16)$$

where i is the interest rate, n is the depreciation period in years, $Inst\_Cost$ is the installation cost, and Ann_Cost is the annual cost for depreciation. The capacity factor is evaluated according to the wind generation data and the WTs capability curves. For example, for a 660 kW WT the capacity factor is about 45%, i.e. 4010 MWh/MW. Therefore, by dividing Ann_Cost by equivalent number of hours i.e. 4010 h, the WT's offer price with no subsidy is about 70 €/MWh. Therefore, the 660 kW WT's offer price, without subsidies, is assumed as 70 €/MWh.

Table 3.5 Financial Data for Estimating WT's Offer Price

Life time (years)	20
Installation cost (€/kW)	1700
Depreciation time (years)	10
Interest rate (%)	10
Number of equivalent hours (MWh/MW)	4010
Capacity factor (%)	45
Annual cost (€/kW-year)	280
Calculated offer (€/MWh)	**70**

3.4.2 Simulation Results

The proposed method is applied to the abovementioned distribution network. The method has been implemented in MATLAB® incorporating some features of MATPOWER suite [93, 94].

In order to determine the optimal numbers and capacities of WTs, DNOs assume the worst-case situation of minimum load and maximum generation. When a WT operates at maximum generation and minimum load it leads, in fact, to large reverse power flows with large local voltage variations [100]. So, the mentioned case is assumed as worst-case situation. The optimal numbers and capacities of WTs are obtained in this case as provided in Table 3.6. The simulation results for different combinations of load demand and wind power generation considering the optimal number of WTs obtained in the aforementioned case, as given in Table 3.6, is shown in Figs.3.5 to 3.7.

Table 3.6 Optimal number and capacity of allocated WTs

Bus No.	Total capacity (MW)	Number of allocated WTs
6	2.64	4
9	1.32	2
14	0.66	1
28	2.64	4
30	1.32	2
38	2.64	4
40	0.66	1
45	2.64	4
47	0.66	1
54	2.64	4
56	0.66	1
62	2.64	4
64	1.32	2
81	2.64	4
83	0.66	1
Total	**25.74**	**39**

Buses 6, 28, 38, 45, 54, 62, and 81 have the largest WT capacity (2.64 MW) while buses 14, 40, 47, 56 and 83 have the lowest ones (0.66 MW). The installed capacity of WTs is, in fact, limited by voltage and thermal limits as well as by the bids of DLs at each bus. The installed capacity at bus 40, for example, is limited to one WT. It is mainly due to the lowest value of both thermal limit of the line connecting the buses 39-40 (i.e. 40 A) and the DLs' bids if compared to those at the other lines and buses, respectively.

At bus 64, with the higher thermal limit of the lines 63-64 connecting the buses (i.e. 50 A), and the higher bids of DLs if compared to previous case, the installed capacity is 1.32 MW corresponding to two WTs. In addition, at buses 54 and 62 the thermal limits of the lines 53-54 and 61-62 connecting the buses are 180 A and the DLs' bids are higher if compared to previous cases. This determines that voltage and thermal limits are not binding (active) and consequently the installed capacity at these buses is 2.64 MW corresponding to four WTs.

As regards with the SW, it increases proportionally to the both load demand and wind power generation as shown in Fig. 3.5. It is

worth mentioning that, in all scenarios, the SW is higher if compared to that without WTs in the network.

It is evident that in the case of minimum load, i.e. 30%, and maximum wind generation level, i.e. 100%, the SW is equal to about 3000 €/h and in the case of maximum load and minimum wind generation, the SW is equal to about 2000 €/h while in the case of maximum wind generation level and maximum load demand this value is equal to around 4000 €/h which is higher if compared to previous cases.

Fig. 3.6 shows the total dispatched active power by WTs in different scenarios of wind generations and load demands. It is seen that the dispatched active power has the direct relation with both load demand and wind power generation. In all scenarios, the dispatched active power is higher if compared to that with no WTs in the network.

The supplied loads, shown in Fig. 3.7, evidences its direct relation with wind generation and its inverse relation with load demand due to the network constraints that limit load increase when constraints are binding. It is worth pointing out that, in all scenarios, the value of supplied loads is higher if compared to that without WTs in the network.

The method is computationally very fast, i.e. it takes about 45 seconds, for all scenarios, measuring the CPU time consumption on a laptop with core i7, 1.6 GHz processor and 4 GB of RAM.
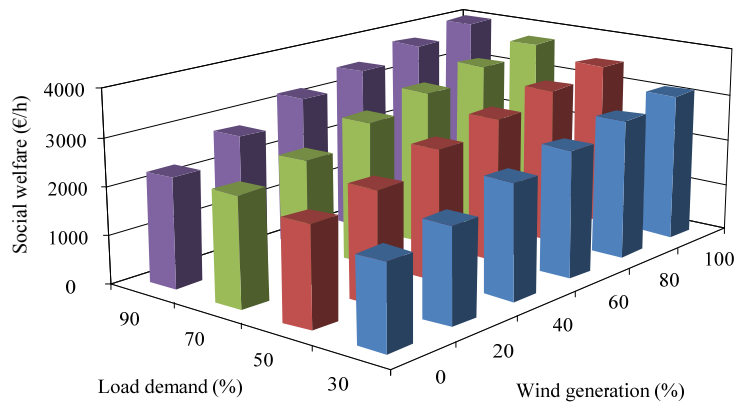
Fig.3.5. Social welfare
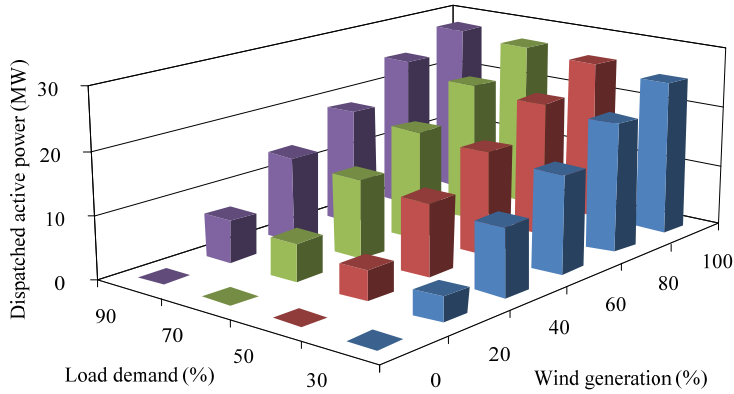
Fig.3.6. Dispatched active power
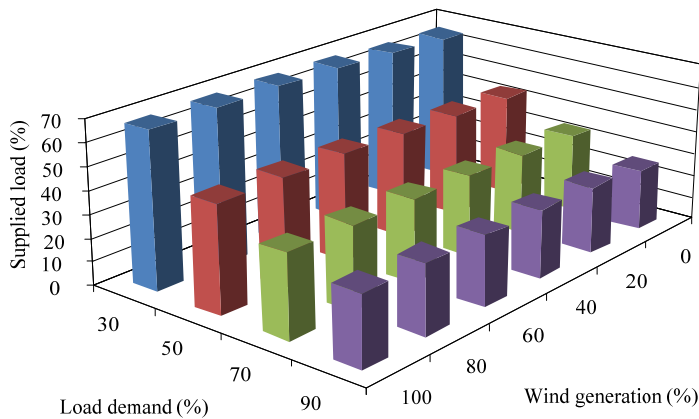
Fig.3.7. Supplied load

3.5   Distribution System Planning within Market Environment

3.5.1   Aim and Approach

In this section, deterministic methods for optimal placement of WTs in distribution networks within a DNO acquisition market environment are proposed. The methods include: 1) hybrid GA and market-based OPF for annual energy losses minimization from the

point of view of DNO; 2) hybrid PSO and market-based OPF for NPV maximization from the viewpoint of WTs' developers.

The uncertainty in wind power generation and load demand is modeled through hourly time-series model of load demand and wind generation. The interrelationships between demand and generation potential are preserved with their joint probability defining the number of coincident hours over the target year.

To the best of our knowledge, no wind power investment methods in distribution level in market environment by using abovementioned hybrid methods have been reported in the literature. The contributions of this section are as follows:

1) Providing a hybrid optimization method for wind power investment in distribution level by using market-based OPF and GA/PSO within a DNO acquisition market environment. Note that market-based OPF is also used to clear the DNO acquisition market. Furthermore, the DNO is the market operator of the DNO acquisition market.

2) Using the GA/PSO to choose the optimal size and the market-based OPF to determine the optimal number of WTs.

3) Modeling wind generation and load demand as well as correlation among different wind speeds through time series analysis approach.

3.5.2   Modeling of Time-Varying Load Demand and Wind Power Generation

The planning horizon consists in a target year where the wind generation and load demand are modeled at each bus of the network through hourly time series analysis as shown in Fig.3.8. The method reduces hourly time-series data to a number of scenarios where the load demand and wind generation for every hour are assigned to a series of bins. Describing the number of coincident hours over the target year preserves the interrelationships between potential of load demand and wind power generation with their joint probability [16, 101].

In order to reduce the computational burden of a full time series analysis, wind generation and load demand are aggregated into a

controllable number of scenarios on the basis of their joint probability of happening. The number of coincident hours is represented by the duration of each hour as shown in Fig.3.8 (bottom).

It splits the demand and generation into a series of bins. In order to show the procedure, ten ranges for demand (i.e. [0, 10%], (10%, 20%],…, (90%,100%]) and 11 ranges for wind generation (i.e. {0}, (0,10%], (10%,20%],…, (90%,100%]) are used. It is seen that with demand higher than 30%, 74 non-zero scenarios are considered in the analysis. Furthermore, low load demand, i.e. 40%, and high wind generation, i.e. 60% to 100%, present few coincident hours. The uncertainty in wind power generation and load demand are represented via scenarios. Each demand level is characterized by eleven wind generation levels, i.e. 0% to 100%. There are seven load demand and eleven wind generation levels. Therefore, jointly considering the load demand and wind power generation levels results in 77 scenarios, i.e. seven load demand levels, with two blocks per level with different sizes and the same price, by eleven wind power generation levels with four blocks per level with the same size and the same price for all blocks.

The method is capable to provide for more than one wind speed profile. A second wind profile can also be taken into account in order to demonstrate this. For each generation level, as shown in Fig. 3.9 (left), first wind profile, a "layer" with the coincident hours of demand/generation is created for the second wind power profile. Though this method is able to generate a great number of scenarios, because of the geographical correlation of the wind data, only 146 periods comprise non-zero number of hours as shown in Fig. 3.9 (right).
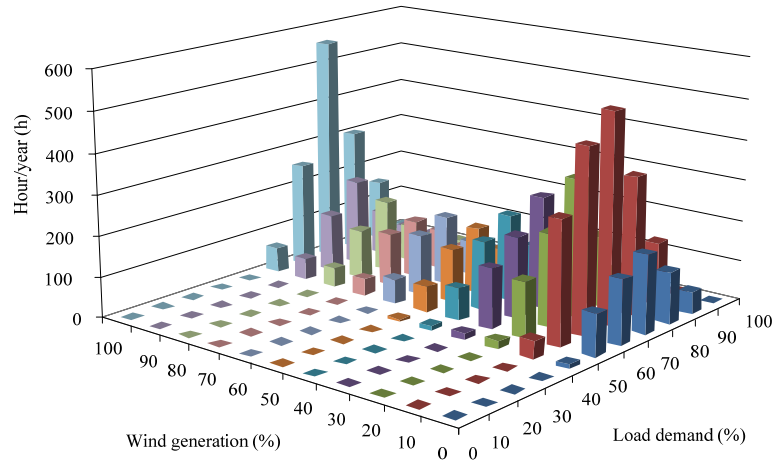
10	103	158	192	127	53	2	0
43	303	451	515	339	156	11	10
20	136	226	336	175	73	15	20
16	147	201	276	138	45	6	30
11	79	170	212	113	41	4	40
7	63	130	161	84	33	7	50
0	60	147	172	85	41	4	60
1	40	132	143	95	33	4	70
0	48	123	176	90	42	8	80
2	54	144	212	110	48	6	90
0	63	257	559	305	152	16	100

% of generation capacity

| 40 | 50 | 60 | 70 | 80 | 90 | 100 |

% of peak demand

Fig.3.8. Coincident hours for demand/generation scenarios

Percentage of Generation Capacity (Wind Profile 1)

Percentage of Peak Demand

Percentage of Generation Capacity (Wind Profile 2)

Percentage of Generation Capacity (Wind Profile 1)

Percentage of Generation Capacity (Wind Profile 2)

Percentage of Peak Demand

0							
1	60	80	114	78	39	2	0
9	35	78	78	49	14	0	10

10							
30	211	319	356	238	100	8	10
13	92	132	159	101	56	3	20

20							
7	50	71	104	45	22	6	20
12	78	132	200	115	47	8	30
1	8	23	32	15	4	1	40

30							
0	9	19	25	6	2	0	30
7	88	139	181	98	29	4	40
9	50	43	70	34	14	2	50

40							
4	57	113	167	71	23	4	50
7	22	57	45	42	18	0	60

50							
5	34	84	114	54	18	5	60
2	29	46	47	30	15	2	70

60							
0	21	66	76	33	18	3	70
0	39	81	96	52	23	1	80

70							
1	24	57	79	48	10	1	80
0	16	75	64	47	23	3	90

80							
0	48	105	157	76	35	8	90
0	0	18	19	14	7	0	100

90							
2	54	144	212	110	48	6	100

100							
0	0	8	4	10	11	0	0
0	63	249	555	295	141	16	100

Percentage of Peak Demand

Fig.3.9. Schematic example of the coincident hours for two wind profiles (left) and the scenarios (right)

3.6   GA Implementation for Annual Energy Losses Minimization from the Point of View of DNOs

3.6.1   The Structure of the Proposed Method

The maximum number of WTs that can be allocated at a given bus is represented by an equivalent number of blocks in the WT's offer. It is assumed that at each candidate bus maximum four WTs can be allocated; therefore, for each generation level there are four blocks with the same size equal to the power output of WTs and the same price for all blocks.

With regards to the bids for DLs, it is assumed that there are two blocks per load with different sizes and the same price for all blocks, respectively.

WTs' offers and bids of DLs are taken and treated as marginal cost and marginal benefit functions, respectively, then by using the CCV method they are converted to the equivalent total cost and total benefit functions and plugged into a matrix as piecewise linear costs.

The method jointly minimizes the total energy losses over the target year and maximizes the SW for each scenario. The structure of the proposed hybrid optimization method for optimal allocation of WTs is shown in Fig.3.10.
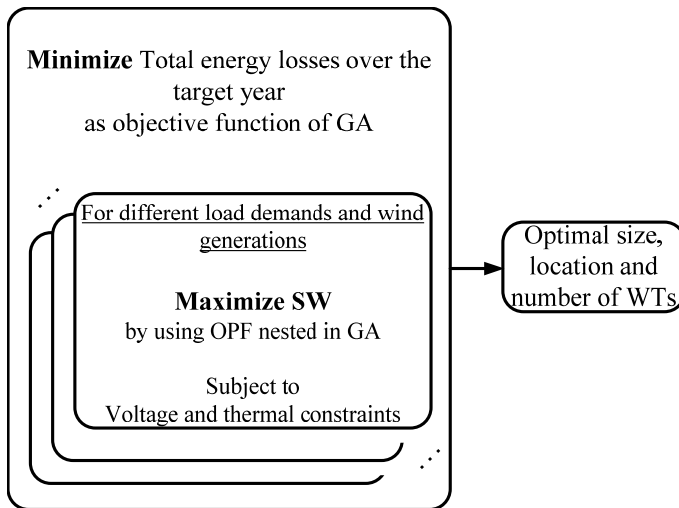
Fig.3.10.The structure of the proposed method

The WTs' sizes and locations are represented by the variable of the GA: a vector of integers, called chromosome, in the range [0, N_{sizes}] with a length equal to the number of candidate buses N_c such that each element of the vector is associated to a candidate bus as

shown in Fig. 3.11. In such a way, different vectors allow representing different investments in WTs both in terms of selected locations and sizes.

Different sizes of WTs identified with a label in the range [0, N_{sizes}] are considered on the basis of their rating power and power coefficients. Three different sizes of WTs of sizes 1.2, 2 and 3 MW, namely sizes A, B and C, respectively, are considered by the DNO. For example, WTs of size A are related to the first element of the vector while WTs of sizes B and C are related to the last two elements of the vector. According to this formulation, WTs of the same size can be allocated at a candidate bus.

For each chromosome, the annual energy losses are evaluated considering the different scenarios: the energy losses in coincidence with a given scenario derived from the SW maximization.

The GA is able to find the optimal locations and sizes of WTs while the market-based OPF, nested in the GA, can determine the optimal number of WTs of a given size to be selected at a chosen location. In particular, the optimal number is the maximum number of WTs identified by the market-based OPF among all the 77 scenarios.

Note that the purpose of using the market-based OPF is threefold: 1) to determine the optimal number of WTs; 2) to clear the DNO acquisition market; 3) to maximize SW.

By solving the abovementioned problems the optimal locations, sizes and numbers of WTs to be allocated at candidate buses are determined.
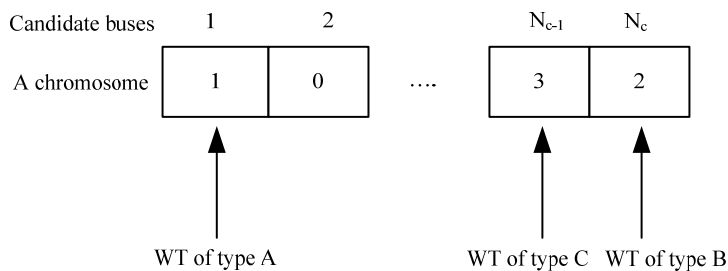
Fig.3.11. Schematic of the GA chromosome

3.6.2   Implementation of GA

The GA starts with an initial population whose elements are called chromosomes. Chromosomes encode candidate solutions and evolve to better ones. The evolution begins from a number of arbitrarily generated chromosomes. During each iteration, called generation, the objective function for each chromosome in the population is assessed and, based on this assessment; a new population of candidate solution is formed. The new population generated in the next iteration is usually better than those in the current population. The GA uses three kinds of rules at every step including selection rules, crossover rules and mutation rules to produce the next generation from the current population and it continues until some stopping criteria is reached [102].

The GA generates the initial populations by defining a set of vector in the range [0, 3]. The number of chromosomes and iterations are set. Each chromosome has a size N_c, where N_c is the number of candidate buses. A number of new improved individuals, according to their objective function, at each generation are created by choosing the individuals. After the selection of new population the genetic operators are applied to chosen chromosomes. The iteration procedure is repeated until one of the following stopping criteria is reached: 1) the maximum generation is more than 300, 2) an enhancement in the objective function for five consecutive generations cannot be obtained, and 3) the cumulative change in the fitness function for five consecutive iterations is less than $1e^{-6}$.

Sensitivity analyses have been carried out to consider different values for the GA parameters such as stopping criteria, population size and genetic operators. From these analyses, it can be seen that the values used here guarantee the convergence of the algorithm to a satisfactory solution.

The energy losses over the target year to be minimized are represented as follows:

$$\text{Minimize} \qquad E_{loss}(x) = \sum_{k=1}^{8760} E_{loss}^k(x) \qquad\qquad (3.17)$$

where

$E_{loss}(x)$ is the energy losses over the study period, $E_{loss}^{k}(x)$ is the total system energy losses during *k-th* hour and *x* is the decision variable of the GA that is a vector of integers in the range [0, N_sizes] with a length equal to the number of candidate buses. For each chromosome, hourly energy losses are obtained considering the DNO acquisition market formulation as is described in the following Section for all the considered scenarios.

3.7   DNO Acquisition Market

Usually, the energy is purchased from the wholesale market and delivered to final customers by DNO and it manages the services and buys energy throughout bilateral contracts and in the Pool. Nonetheless, due to the power system reconstructing and emerging DGs such as WTs, the business of traditional DNO is unbundled into technical and economic tasks.

A DNO energy acquisition market model, called the DNO acquisition market, with WTs and DL is presented here under a distribution market structure based on Pool and bilateral contracts within DNO's control area at low voltage level. The DNO is defined as the market operator of the acquisition market, which determines the price estimation and the optimization process for the acquisition of active power. DLs and WTs send active power offers and bids to the DNO acquisition market in form of blocks for each hour [103].

The DNO combines DL bids and WTs' offers to construct supply and demand curves, respectively. The supply curve is constructed by stacking energy offers in increasing order of offer price. The demand curve is likewise constructed by stacking energy quantities in decreasing order of bid price. The intersection of these curves determines the market clearing price.

The wholesale market of the whole interconnected network set up a price margin with DNO acquisition market. In other words, the wholesale market provides energy at a specified or approximated price. The price of wholesale market is considered as the DNO approximated acquisition price for active power from the interconnected network.

The DNO's aim is maximizing the consumers' benefit function and minimizing the costs of energy producers when buying active and reactive power from the grid. When selling active and reactive power to the grid, the purpose of DNO is maximizing revenues by exchanging power with the grid [16].

Under the assumed DNO acquisition market, the market clearing quantity and price are determined by maximizing the social welfare while keeping the distribution network's security. In other words, the market clearing is carried out by solving the social welfare maximization as is formulated in the following. Furthermore, the DNO is the responsible for achieving this task. Social welfare maximization implies not only the minimization of the costs related to energy production but also the maximization of the consumers' benefit function. The formulation was provided in Section 3.3.

3.7.1   Simulation Procedure

The proposed hybrid optimization method to determine the optimal locations, sizes and numbers of WTs runs as follows.

1)   Define GA parameters and WTs types (size and speed-power curves) to be allocated by the DG-owning DNO.
2)   Set the candidate buses according to wind energy availability.
3)   Model uncertainties through hourly time series analysis for target year as explained in Section 3.5.2.
4)   Calculate the power output of different sizes of WTs based on their speed-power curves and calculate WTs' offer price.
5)   For each chromosome, maximize the SW for the considered scenarios and evaluate the hourly energy losses.
6)   Evaluate the annual energy losses.
7)   If one of the stopping criteria is reached go to step 9) otherwise repeat steps 5)-7) until one of the stopping criteria is reached.
8)   The by-product of the proposed method is the optimal locations, sizes and numbers of WTs.
9)   Print the solution.

3.7.2   Test System Description

The same distribution network as shown in Fig.3.6 with the same assumptions is considered, except here the feeders' thermal limits are given in Table 3.7 and vary between 90 and 480 A. The different sizes of WTs of 1.2, 2 and 3 MW are considered by the DNO. At each candidate bus it is assumed that maximum four WTs of each size can be allocated; this requirement is regulated by the accessible land for building WTs. Thus, for each generation level there are four blocks of the same size equal to the rated power of the selected WTs and the same price of 60 €/MWh. The same method as explained in Section 3.4.1 was applied with the data provided in Table 3.8 for a 1.2 MW WT.

Table 3.7 Existing wires

Wires	Amps
A-1, 1-2, 2-3, 3-4, 4-5, 5-6, 6-7, 8-11, B-11, 12-13, C-15, 18-19, D-25, 26-27, E-30, 31-32, F-43, G-47, 48-49, H-56, 57-58, I-65, 66-67, J-73, 74-75,K-77, 78-79	480
7-8, 13-15, 16-17, 17-18, 27-28, 32-33, 33-34, 34-35, 35-36, 36-37, 37-38, 38-39, 44-45, 49-50, 50-51, 51-52, 52-53, 58-59, 59-60, 60-61, 61-62, 67-68, 68-69, 70-71, 79-80, 80-81	330
19-20, 20-21, 21-22, 22-23, 22-24, 28-29, 39-42, 53-54, 54-55, 62-63, 69-70, 71-72, 75-76	180
8-9, 8-10, 13-14, 39-40, 40-41, 45-46, 63-64, 81-82, 82-83	90

The maximum number of WTs that can be allocated at a given bus is represented by an equivalent number of blocks in the WT's offer. The offers are assumed at price of 80 €/MWh for the bus connecting the distribution network to the transmission one. With regards to the bids for DLs, there are two blocks per demand bid with different sizes as presented in Table 3.4 and the same price of 140 €/MWh for all blocks.

The capacity factor is evaluated according to the wind generation data and the WTs capability curves. For example, for a 1.2 MW WT the capacity factor is about 40%, i.e. 3504 MWh/MW. Therefore, by dividing *Ann_Cost* by equivalent number of hours i.e. 3504 h, the WTs' offers with no subsidy is about 56 €/MWh. Therefore, the 1.2 MW WTs' offers, without subsidies, are assumed as 60 €/MWh. The same approach can be applied considering WTs of different sizes and

capacity factors. In order to simplify the analysis, the same offers are considered for all the sizes of WTs.

Table 3.8 Financial data for estimating the offers
for a 1.2 MW WT

Life time (years)	20
Installation cost (€/kW)	1200
Depreciation time (years)	10
Interest rate (%)	10
Number of equivalent hours (h)	3504
Capacity factor (%)	40
Annual cost (€/kW-year)	195.27

3.7.3   Simulation Results

The proposed method is applied to the abovementioned distribution network. After a sensitivity analysis, the best parameters for the GA have been chosen as provided in Table 3.9. Note that these parameters have been obtained from several trial runs where 50 runs have been carried out.

Table 3.9 GA parameters

Number of chromosomes	Population size	Number of iterations	Crossover Fraction	Mutation uniform
15	20	300	0.95	0.05

The method has been implemented in MATLAB® incorporating some features of MATPOWER suite [93,94] and MATLAB® toolbox for GA [104] on a laptop with core i7, 1.6 GHz processor and 4 GB of RAM.

The minimum energy losses over the year are about 7532 MWh. The optimal sizes and numbers of WTs at each candidate bus found by the proposed method are given in Table 3.10.

Table 3.10 The optimal numbers, sizes and capacities of
WTs obtained by the proposed method

Bus No.	Size	Number	Capacity (MW)
6	-	-	-
9	C	1	3
14	A	2	2.4
28	-	-	-
30	C	1	3
38	A	4	4.8
40	-	-	-
45	A	4	4.8
47	-	-	-
54	B	4	8
56	B	2	4
62	B	4	8
64	-	-	-
81	B	4	8
83	-	-	-
Total capacity			**46**

It is evident from Table 3.10 that buses 54, 62, and 81 have the largest installed capacity (i.e. 8 MW) while bus 14 has the lowest one (i.e. 2.4 MW). The installed capacity, in fact, is limited by voltage and thermal limits as well as by the bids' values at each bus. For instance, the installed capacity at bus 14 is limited to 2.4 MW (two WTs of size A) and this is mainly due to the lowest value of both thermal limit of the line connecting the buses 13-14 (i.e. 90 A) and the bids' values of DLs if compared to those at the other lines and buses.

The installed capacity at buses 38 and 45 is 4.8 MW (four WTs of size A). These buses have the same bid values and the higher thermal limits (i.e. 330 A) of the lines 37-38 and 44-45 connecting the WTs if compared to previous case.

At buses 62 and 81, the DL bids are higher and the thermal limits of the lines 61-62 and 80-81 are the same if compared to the previous case; consequently, the highest capacity is installed at these buses (i.e. four WTs of size B).
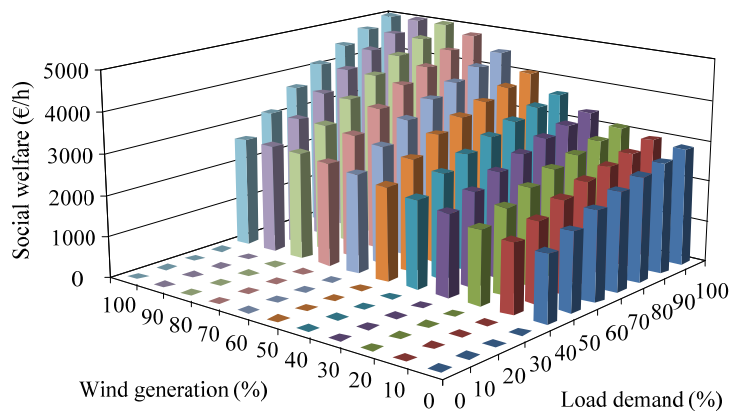
Fig.3.12. Social welfare
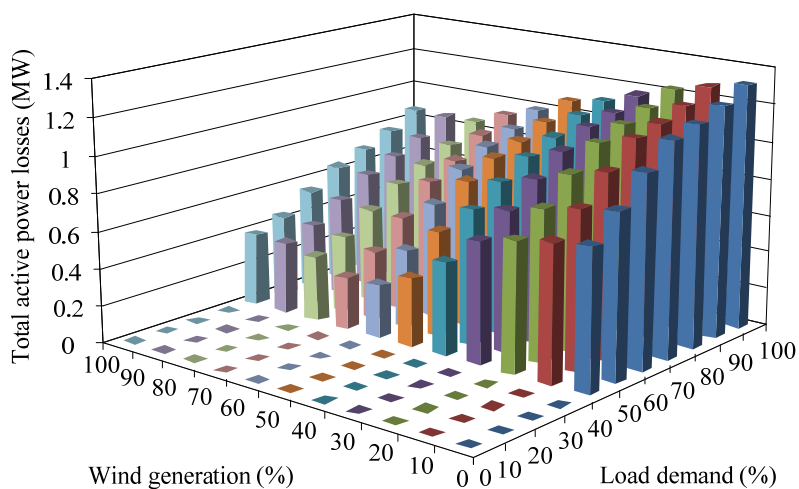
Fig. 3.13. Total active power losses

As regards with the SW, it increases proportionally to both load demand and wind generation as shown in Fig. 3.12. It is worth mentioning that, in all scenarios, the SW is higher if compared to that without WTs in the network. In the case of minimum load (i.e. 40%) and maximum wind generation level (i.e. 100%), the SW is equal to about 2500 €/h and in the case of maximum load and minimum wind generation level the SW is equal to about 3000 €/h. Instead, in the case of maximum wind generation level and maximum load demand this value is equal to around 5000 €/h.

It is seen from Fig. 3.13 that by increasing the generation, active power losses are decreased. In all scenarios, the total active power losses are lower if compared to the case with no WTs in the network. In the case of maximum wind power generation and minimum load demand the total active power losses are reduced by about 50% if compared to the case with no WTs in the network. It is evident that total active power losses have inverse relation with the wind generation and direct relation with load demand.
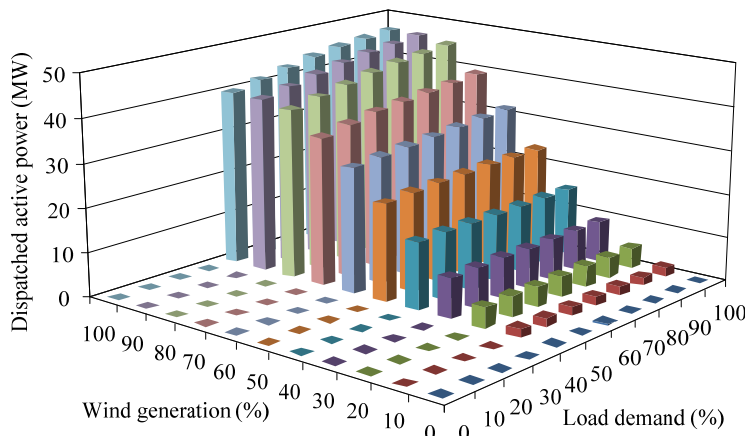
Fig.3.14. Dispatched active power

Fig. 3.14 shows the total dispatched active power by WTs in different scenarios of wind generations and load demands. It is evident that the dispatched active power has the direct relation with both load demand and wind generation.

The supplied loads, shown in Fig. 3.15, evidences its direct relation with wind generation and its inverse relation with load demand due to the network constraints that limit load increase when constraints are binding. The cases considering different wind energy potential at candidate buses can be addressed by considering different capacity factors for each location and calculating the WTs' offers.
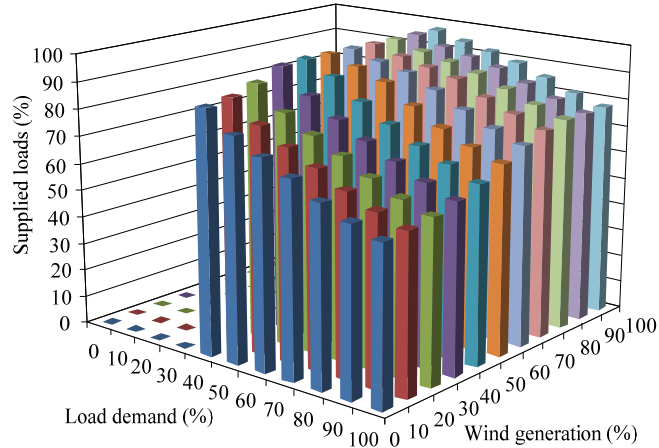
Fig.3.15. Percentage of supplied loads

3.8   NPV Maximization from the Point of View of WTs' Developers

PSO is a population-based method introduced by Kennedy and Eberhart in 1995 [105]. This method handles a population of individuals in parallel to explore areas of n-dimensional space where the optimal solution is searched. The individuals are called particles and the population is called swarm. Each particle in the swarm moves toward the optimal point with adaptive velocity [106]. In n-dimensional space, the position and velocity of each individual are illustrated as the vectors, $X_i = [P_{i,1}, P_{i,2},...,P_{i,n}]$ and $V_i = [V_{i,1}, V_{i,2},...,V_{i,n}]$, respectively. Alternatively, the best position related to the best value of the objective function for each particle is represented as $Pbest_i = (Pbest_{i,1}, Pbest_{i,2},...., Pbest_{i,n})$ and the global best position among all particles or best *pbests* is denoted as $Gbest_i = (Gbest_{i,1}, Gbest_{i,2},...., Gbest_{i,n})$. During the iteration procedure, the velocity and position of particles are updated.

3.8.1   **Implementation of PSO Algorithm**

The number of population, the number of particles and iterations are set. The population of particles X_j as well as their velocity V_j in the search space is initialized. The velocity of each component is selected in the range $[V_{min}, V_{max}]$ randomly. Here, V_{min} and V_{max} of 0 and 3 have been selected for the PSO process, respectively. After calculation of the objective function (OF), the best position associated to each member of particles is assessed. The objective function related to each particle in the population in the current iteration is compared with that from the previous iteration and the particle's position which has a higher value of objective function is taken as *Pbest* for the current iteration and is recorded as

$$Pbest_j^{k+1} = \begin{cases} Pbest_j^k & \text{if} \quad OF_j^{k+1} \leq OF_j^k \\ X_j^{k+1} & \text{if} \quad OF_j^{k+1} > OF_j^k \end{cases} \qquad (3.18)$$

where k is the number of iterations, and OF_j^k is the objective function assessed for particle j at iteration k.

The best objective function associated with the *Pbests* among all particles in the current iteration is compared with that from the previous iteration and the higher value is chosen as the current overall *Gbest*:

$$Gbest_j^{k+1} = \begin{cases} Gbest_j^k & \text{if} \quad OF_j^{k+1} \leq OF_j^k \\ Pbest_j^{k+1} & \text{if} \quad OF_j^{k+1} > OF_j^k \end{cases} \qquad (3.19)$$

After calculation of *Pbest* and *Gbest*, the velocity of particles for the next iteration will be modified by using the following equation.

$$V_j^{k+1} = \omega V_j^k + c_1 rand_1 \times (Pbest_j^k - X_j^k)$$
$$+ c_2 rand_2 \times (Gbest_j^k - X_j^k) \qquad (3.20)$$

where

V_j^k velocity of particle j at iteration k;

ω inertia weight factor;

c_1, c_2 acceleration coefficients;

X_j^k position of particle j at iteration k;

$Pbest_j^k$ best position of particle j at iteration k;

$Gbest_j^k$ best position among all particles at iteration k.

In each iteration the acceleration coefficients c_1 and c_2 control how far an individual is moved in each iteration. The inertia weight, ω, is used to control the convergence behavior of the PSO during the training step according to the following:

$$\omega = \omega_{max} - \frac{\omega_{max} - \omega_{min}}{k_{max}} \times k \tag{3.21}$$

where

k current iteration number;

k_{max} maximum iteration number;

ω_{max} initial inertia weight factor;

ω_{min} final inertia weight factor.

The position of each particle at the $k+1$ (next iteration) is modified as

$$X_j^{k+1} = X_j^k + V_j^{k+1} \tag{3.22}$$

If $X_j^{k+1} - X_j^k \prec \varepsilon$ or $k = k_{max}$, the program is terminated and the results are printed, otherwise, the iteration process continues until one of the stopping criteria is reached. The flowchart of the proposed PSO based algorithm is shown in Fig.3.16.
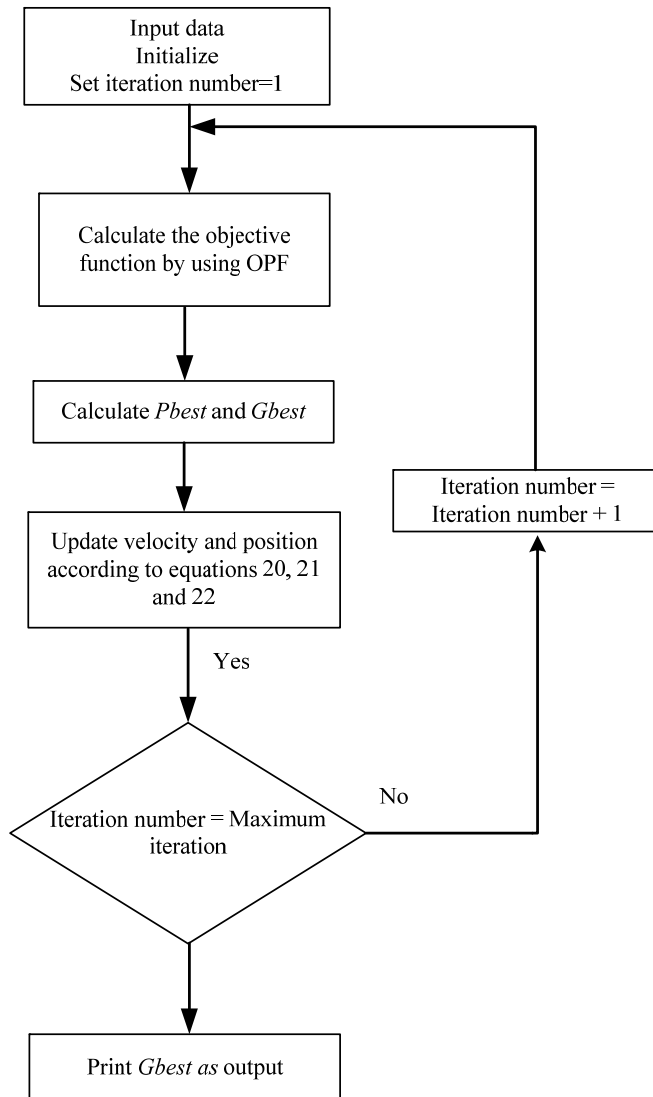
Fig.3.16. Flowchart of the proposed PSO based algorithm

In order to investigate the profitability of the WTs investment, the NPV is used as the objective function of the PSO. It is defined as the difference between the discounted cash flows and the investment cost. The NPV to be maximized as the objective function of PSO is expressed as follow:

Maximize $NPV(x) = FA \times FC(x) - IC(x)$ (3.23)

where FA is annual factor, FC is the total revenue obtained by selling energy into the DNO acquisition market over the target year and IC is the initial investment cost. FA and FC are calculated as follows:

$$FA = \frac{(1+r)^n - 1}{r(1+r)^n}$$ (3.24)

$$FC(x) = \sum_{h=1}^{8760} E_d^h(x) \times \lambda_h(x)$$ (3.25)

where n is the lifetime of WTs and r is the discount rate. Here, n and r are assumed as 20 years and 10%, respectively. $FC(x)$ is the annual revenue and x is the decision variable of the PSO that is a vector of integers in the range [0, N_{sizes}] with a length equal to the number of candidate buses. E_d^h is the energy dispatched by the installed WTs at a given hour h and λ_h is the Langrangian multiplier (LMP) that is obtained from market-based OPF. For each particle, hourly revenue (i.e. multiplication of WTs' dispatched energy by LMP at a given hour h) is obtained considering the DNO acquisition market formulation for all the considered scenarios. It has been, in fact, assumed that the WTs' developers sell energy at LMPs. Therefore, according to (3.23), the NPV will depend on the energy dispatched by the WTs, the LMPs and the initial investment cost.

3.8.2   Simulation Procedure

The proposed hybrid optimization method to determine the optimal locations, sizes and numbers of WTs runs as follows.
1) Define PSO parameters and WTs types (size and speed-power curves) to be allocated by WTs' developers.
2) Set the candidate buses according to wind energy availability.
3) Model uncertainties through hourly time series analysis for a target year as explained in Section 3.5.2.
4) Calculate the power output of different sizes of WTs based on their speed-power curves and calculate WTs' offer price.

5) For each particle, maximize the SW for the considered scenarios and evaluate the hourly revenue (i.e. multiplication of WTs' dispatched energy by the LMP for each hour) and initial investment cost.
6) Evaluate the annual revenue and the NPV.
7) If one of the stopping criteria is reached go to step 9) otherwise repeat steps 5)-7) until one of the stopping criteria is reached.
8) The by-product of the proposed method is the optimal locations, sizes and numbers of WTs.
9) Print the solution.

3.8.3   Simulation Results

After a sensitivity analysis, the best parameters for the PSO have been chosen as provided in Table 3.11. The capital costs of the three sizes of WTs are listed in Table 3.12.The optimal sizes and numbers of WTs at each candidate bus found by the proposed method are given in Table 3.13.

Table 3.11 PSO parameters

Number of particles	Population size	Number of iterations	c_1	c_2	ω_{max}	ω_{min}	Maximum velocity
15	20	100	2.5	2.0	0.9	0.4	3

Table 3.12. Capital costs of WTs

WT size	Rated output power (MW)	Capital cost (€/kW)	Total capital cost (M€)
A	1.2	1200	1.44
B	2	1120	2.24
C	3	1050	3.15

Table 3.13 The optimal numbers, sizes and capacities of WTs
obtained by the proposed method

Bus No.	Size	Number	Capacity (MW)
6	B	4	8
9	B	1	2
14	B	2	4
28	B	4	8
30	B	1	2
38	B	4	8
40	A	1	1.2
45	B	4	8
47	C	1	3
54	B	4	8
56	A	4	4.8
62	B	4	8
64	B	2	4
81	B	4	8
83	B	2	4
Total capacity			**81**

It is evident from Table 3.13 that buses 6, 28, 38, 45, 54, 62, and 81 have the largest installed capacities (i.e. 8 MW equal to 4 WTs of size B) while bus 40 has the lowest one (one WT of size A).

In fact, the number of installed WTs is limited by voltage and thermal limits as well as by the bids' values at each bus. For instance, the installed capacity at bus 40 is limited to 1.2 MW (one WT of size A) and this is mainly due to the lowest value of both thermal limit of the line connecting the buses 39-40 (i.e. 90 A) and the bids' values of DLs if compared to those at the other lines and buses.

The installed capacity at buses 56 and 64 is 4.8 MW and 4 MW, i.e. 4 WTs of size A and 2 WTs of size B, respectively. These buses have higher bids and the same thermal limits of the lines H-56 and 63-64 connecting the buses (i.e. 90 A) if compared to previous case.

At buses 45 and 54, the DL bids are higher if compared to previous cases and the thermal limits of the lines 44-45 and 54-55 are respectively 330 A and 180 A. For these reasons, the voltage and thermal limits are not binding and the highest capacity at these buses

is installed if compared to previous cases (i.e. 8 MW equal to four WTs of size B).

As given in Table 3.14, total WTs capacity of 81 MW is installed allowing delivering wind energy of 294550 MWh/year. The total capital cost of the investment is equal to 90.99 M€ while the total NPV is equal to 248.08 M€.

In order to evaluate and compare the obtained results, a GA is used with a population size and a generation number equal to those of the PSO. It can be observed from Table 3.15 that the NPV obtained by PSO is higher than that obtained by GA.

Table 3.14 Results obtained with the proposed method

Total capacity(MW)	Delivered wind energy (MWh/year)	Total capital cost (M€)	NPV (M€)
81	294550	90.99	248.08

Table 3.15 Comparison of the results with GA

Method	Population size	Number of iterations	NPV (M€)
GA	20	100	247.48
PSO	20	100	**248.08**

Fig. 3.17 shows that the total dispatched active power by WTs in different wind/load scenarios. It is observed that it increases proportionally to the both load demand and wind generation. In all scenarios, the dispatched active power is higher if compared to that without WTs in the network.

The energy delivered over the target year has the highest value in the case of 70% load demand and 100% wind generation as shown in Fig.3.18 and it is due to the highest value of corresponding hour in this case as shown in Fig.3.8.

Fig.3.17. Dispatched active power by WTs
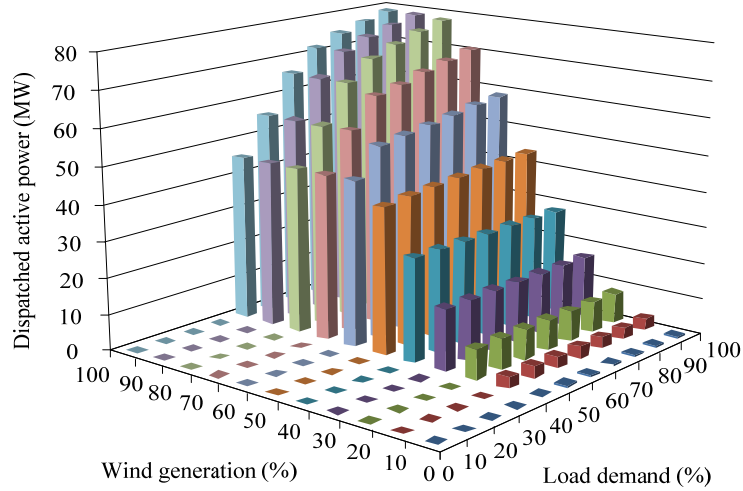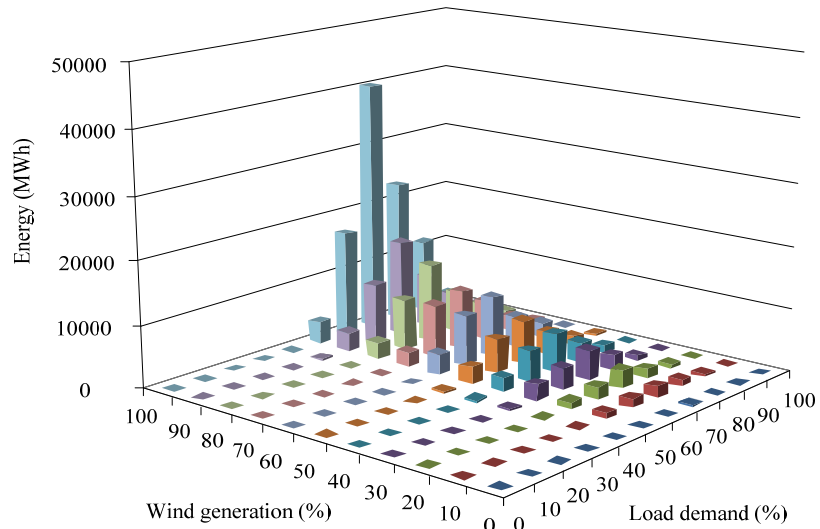

Fig.3.18. Delivered energy over the year

As regards with SW, it increases proportionally to the both load demand and wind generation as shown in Fig.3.19. It is observed that in the case of minimum load, i.e. 40%, and maximum wind generation level, i.e. 100%, the SW is equal to about 2860 €/h and in the case of maximum load and minimum wind generation, the SW is equal to

about 2800 €/h while in the case of maximum wind generation level and maximum load demand this value is equal to around 6300 €/h which is higher if compared to previous cases. It is worth pointing out that, in all cases, the SW is higher if compared to that without WTs in the network: in the case of 100% wind generation and 40% load demand the SW increases about 50% if compared to the case with no WTs in the network.
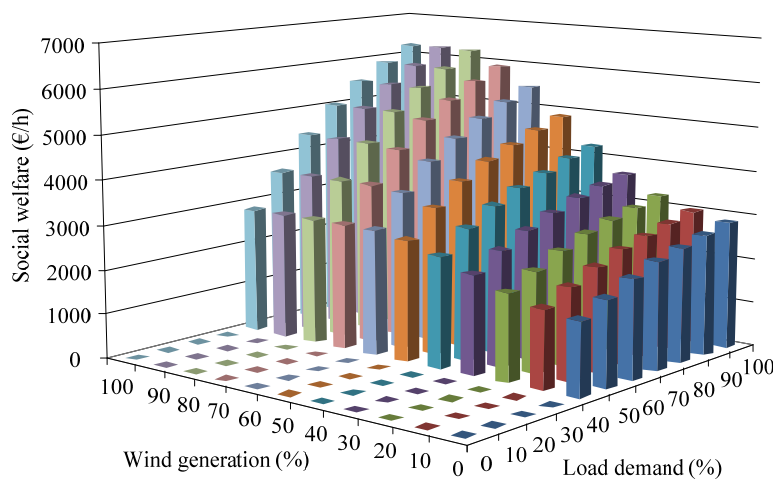
Fig.3.19. Social welfare

It is evident from Fig.3.20 that the revenue increases proportionally to the both load demand and wind generation from minimum to maximum. Furthermore, in the case of maximum load demand and maximum wind generation, revenue has the highest value if compared to other cases while in the case of minimum load and minimum wind generation it has the lowest value. In all cases the revenue is increased if compared to that with no WTs in the network.

The relation of revenue with the wind generation and load demand, shown in Fig. 3.20, is more complex as it depends on the dispatched wind energy and LMPs.

The supplied load, shown in Fig. 3.21, evidences its direct relation with wind generation and its inverse relation with load demand due to the network constraints that limit load increase when constraints are binding. In the cases of maximum wind generation and 40% to 100%

load demand, the values of supplied loads are equal to 100%, 100%, 100%, 98.99%, 95.74%, 91.50% and 87.84% of the maximum load in each case, respectively. It is observed that the value of supplied loads has the lowest and highest values in the cases of maximum and minimum load demand, respectively.

The total active power losses are shown in Fig.3.22. The typical U-shaped relation of power losses with wind generation and the direct relation with load demand can be verified as expected.
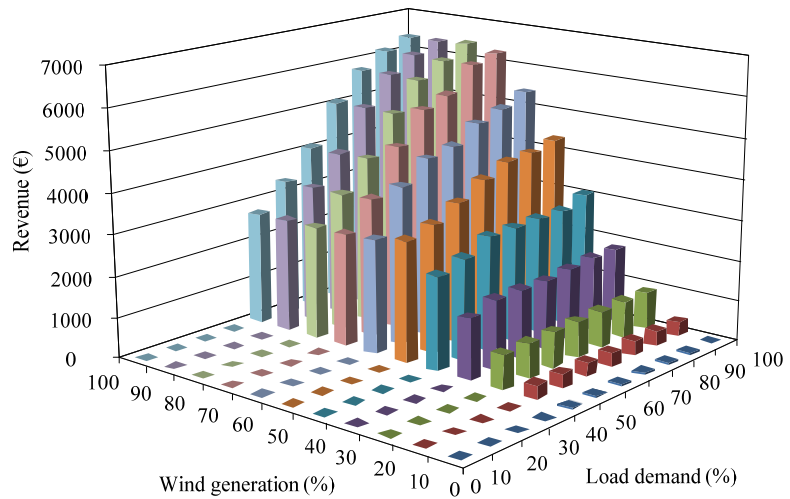
Fig.3.20. Revenue
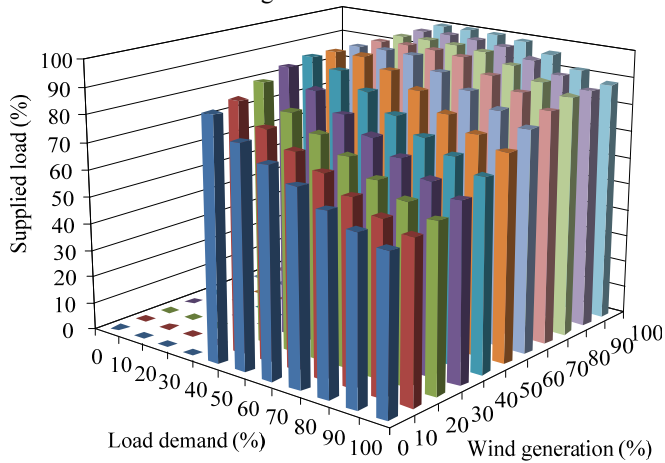
Fig. 3.21. Supplied loads
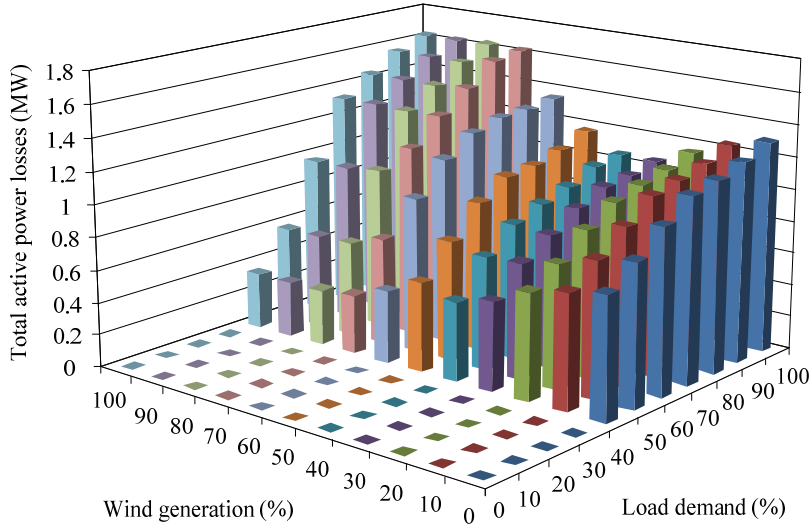
Fig. 3.22. Total active power losses

(a)

(b)
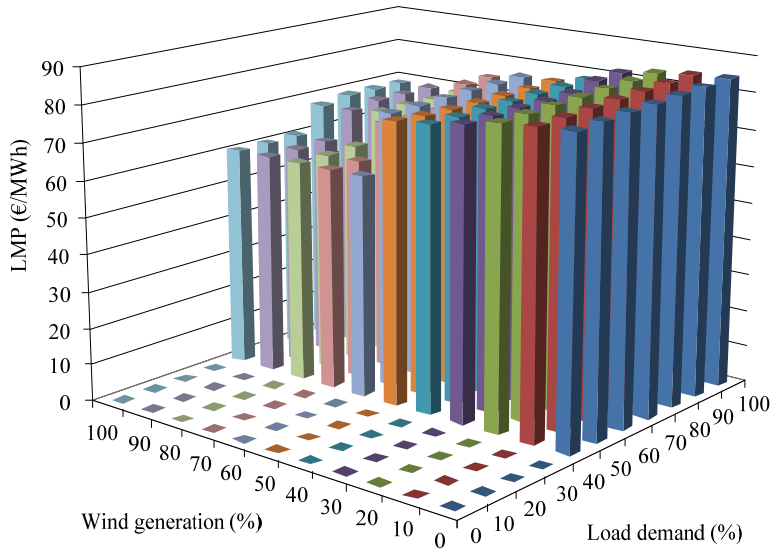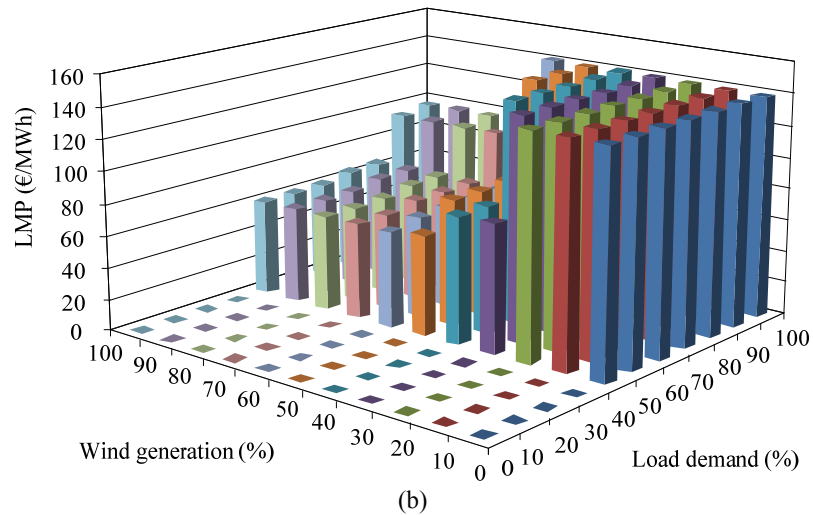
Fig. 3.23. Locational marginal price at (a) bus 6 and (b) bus 47

Figs. 3.23 (a), (b) show the LMP at buses 6, 47, respectively. The LMP at bus 6 has a lower value than that at bus 47 and this is mainly due to the thermal limit of the line 39-40 of 90 A that is lower than that at the lines 5-6 and 6-7 of 480 A.

The LMPs in the cases of high wind generation and low load demand has the lowest values while for low wind generation and high demand are the highest ones. Furthermore, the LMPs in all cases are lower if compared to those with no WTs in the network. Therefore, the optimal allocation of WTs alleviates network congestion and consequently decreases the LMPs.

3.9   Discussion and Conclusion

In the first part of this chapter, a novel method for optimal placement of WTs in distribution networks from the point of view of DNOs was proposed. A market-based OPF is used in a way that maximizes the SW to determine the optimal capacities and numbers of WTs at candidate buses considering different combinations of load demand and wind power generation taking into account network constraints.

With the proposed method not only WTs are optimally allocated but also the SW, dispatched active power and supplied loads are increased if compared to the case with no WTs in the network.

The method can be used to assist DNOs to evaluate the performance of the network and to plan the WTs integration into distribution networks; moreover, it can help DG-owning DNOs to make better decisions to allocate WTs by using a more efficient method.

By yielding location-specific WTs capacity settlement both in terms of cost reduction and consumers' benefits is consistent with actual distribution network topology.

Simulation results verified the capability and effectiveness of the proposed method for optimal placement of WTs.

In the second part, hybrid methods for optimal planning of distribution networks within market environment were proposed. First, a hybrid GA and market-based OPF is used to jointly minimize the annual energy losses, from the point of DNO, and maximize the SW considering different combination of wind generations and load demands to determine the optimal locations, sizes and numbers of WTs to be allocated at candidate buses.

With the proposed method not only WTs are optimally allocated but also the total power losses is decreased and the SW, dispatched active power and supplied loads are increased if compared to the case with no WTs in the network.

The proposed method is consistent with the topology of the distribution system, thus taking into account the demand willingness to buy energy at different buses and can be used to assist DNOs to evaluate the performance of the network and to plan the WTs integration into distribution networks. Simulation results confirmed the capability and effectiveness of the proposed method in optimally allocating WTs in distribution networks.

Second, a hybrid optimization method that combines the PSO and the market-based OPF to jointly maximize the NPV associated to investment made by WTs' developers and the SW in DNO acquisition market environment is proposed.

In both deterministic methods, the GA/PSO is used to select the optimal sizes among different sizes of WTs while the market-based OPF to determine the optimal number of WTs in order to maximize the SW considering network constraints. Furthermore, the DNO acts

as the market operator of the DNO acquisition market that estimates the market clearing price and the optimization process for the active power hourly acquisition. The stochastic nature of both load and wind is modeled by hourly time series analysis. The method is also able to model the correlation among wind resources, i.e. for each range of generation capacity of the first wind profile, a layer with the coincident hours of demand/generation can be created for the second wind power profile.

The proposed hybrid optimization method offers some advantages for WTs investment selection as it is able to integrate the resource adequacy evaluation by considering, through LMPs, the outcomes of WTs allocation in terms of active constraints release, power losses reduction and decrease of the energy imported from the transmission network.

By using the proposed method, WTs can be, in fact, optimally allocated at buses where they are more advantageous, i.e. near higher loads or in parts of the network where the loads have the higher values and the consumers' benefit is higher. The method can help WTs' developers to better allocate WTs taking into account cost reduction and consumers' benefits; moreover, it considers network constraints and LMPs.

The presented case study highlighted that WTs' developers by optimally allocating WTs at buses with the highest LMPs can both improve their profits and increase consumers' benefits by energy cost reduction, power losses decrease and network constraint alleviation.

Chapter 4

Planning of Distribution Networks by Using Probabilistic Methods

This chapter provides a methodology to simulate the amount of wind power that can be injected into the grid as well as the effect of wind power penetration on LMPs through the network considering uncertainties within DNO acquisition market environment. The method is conceived for DNOs to evaluate the amount of wind power that can be injected into the grid. In the proposed approach it has been assumed that WTs and DLs are owned or managed by the DG-owning DNO.

The uncertainties due to the stochastic nature of wind as well as the volatility of WTs' offers quantity and price are modeled by using MCS method. Combined MCS and market-based OPF are used to maximize the SW considering different combinations of wind generation and load demand over a year. The market-based OPF uses CCV approach to generate the appropriate helper variable, cost term, objective function is solved by using SCPDIPM considering network constraints. The effectiveness of the proposed method is demonstrated with an 83-bus 11.4 kV radial distribution system.

The modeling of uncertainties is described in Section 4.1. The structure of the proposed method and simulation procedure are discussed in Sections 4.2 and 4.3, respectively. Section 4.4 explains the 83-bus test system while Section 4.5 presents some numerical results. Discussion and conclusions are presented in Section 4.6.

4.1   Modeling Uncertainty

Wind power is one of the most attractive renewable from the economic point of view but intermittent source for electricity generation; thus, higher amounts of wind power are integrated in into power systems all over the world. A large amount of wind power integration into the network cause operational challenges such as price volatility.

Several difficulties in engineering and science are exposed to uncertainty because of the intrinsic uncertainty of the natural phenomena involved and to the unpredictable evolution of the variables specifying the functional state of human created constructions. Within such a hazardous world, computational approaches able to cope with incomplete information allow engineers to suggest solutions less sensitive to environmental situations and uncontrollable parameters, while concurrently reaching cost reduction, profit gains, and reliability enhancement.

Decision-making problems associated to electricity markets are fairly contrary. Indeed, the own mechanisms leading the operational of these markets can be taken into account responsible for the existence of uncertainties impressing the behavior of market agents. For instance, electricity prices are indefinite when producers and consumers respectively must submit their offers and bids to the pool. Therefore, decisions on the quantity and price of the energy to be sold or purchased are made with imprecise knowledge of the final market result. Similarly, the time gap between contracts on energy trades and their implementation incurs that a producer has to encounter the trading procedure with a specified degree of uncertainty for the power sources accessibility. As the wind power technology can gain the invested costs, wind power producers are interested in participating in electricity markets to maximize their profits. In addition to stochastic nature of wind, the wind producer has to tackle the volatile market prices; thus, the market strategy of a wind producer has to confine the uncertainty to reduce the profit variability due to very significant wind fluctuation. The uncertainty impact of wind production is removed by a balancing mechanism to cover the lack of uncertain production of wind power. The balancing mechanism is usually provided by

expensive dispatchable energy sources. Therefore, a major concern regarding a wind producer is to diminish its need for balancing energy [107-109].

4.1.1   Wind Speed Modeling

Regardless of various wind speed regimes in different places, wind speed differs in a wide range in a given geographic site. Power generated by WT depends on the wind speed that varies with time in a stochastic manner. Thus, it is required to model wind speed properly to study the probabilistic wind power. In some previous works, auto regressive and moving average time series have been used to simulate the hourly wind speed. Then, the probability of each speed level has been calculated by dividing the number of wind speed data in the related range by the total number of wind speed data [110]. In this thesis, Weibull probability density function (PDF) is used to model the wind speed random variations. The Weibull PDF is given by the following equation.

$$f(v) = \frac{k}{c}(\frac{v}{c})^{k-1} e^{(-(v/c)^k)} \qquad (k>0, v>0, c>1) \qquad (4.1)$$

where v, k and c are the wind speed, the shape coefficient and the scale coefficient, respectively.

4.1.2   Wind Turbine Modeling

The power output is calculated from the WT's power curve as shown in Fig. 4.1 (a). A WT is designed to start producing power at cut-in wind speed V_{cin} and reaches its rated power at V_r, and after that, despite increasing wind speed, the power remains constant at P_r up to V_{co}. Mathematical expression of power curve is given as follows [111]:

$$P_{WT} = \begin{cases} 0, & x < V_{cin} \\ P_r \times (A + Bx + Cx^2), & V_{cin} \le x < V_r \\ P_r, & V_r \le x < V_{co} \\ 0, & x \ge V_{co} \end{cases} \qquad (4.2)$$

where *A*, *B*, and *C* are constants determined according to WTs' parameters [112]. Power curve of a 660 kW WT is shown in Fig. 4.1(b).

(a)

(b)
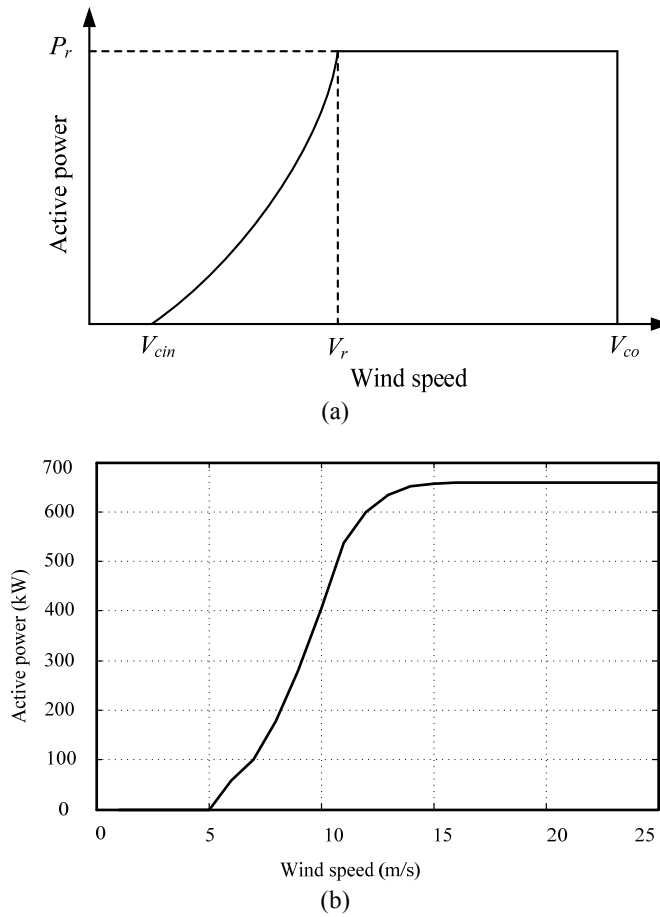
Fig.4.1. (a) Typical power curve of a WT, (b) power curve of 660 kW WT

4.1.3   Modeling of the Quantity and the Price of WT's Offer

4.1.3.1   WT's Offer Quantity Modeling

The power generated by each WT is derived from a Weibull PDF of wind speed and from the WT's power curve. WT's offer quantity is determined according to the power output. It is assumed that at each candidate bus maximum four WTs can be allocated, thus, each WT's offer quantity is supposed to have four blocks with the same size, each equal to the generated power of WTs.

4.1.3.2   WT's Offer Price Calculation and Modeling

The volatility in prices arises from the system balancing market that determines the energy price for substituting the deviation [113]. In the wholesale electricity market, a price for the positive and negative energy deviation are settled for each time period, respectively. Positive energy deviation is defined as higher production or lower consumption than scheduled and negative energy deviation is defined as lower production or higher consumption than scheduled. These prices represent the energy cost needed to counteract the unplanned deviations, and subsequently, they rely on the sign of the imbalance (system imbalance).

Suppose that the price deviation is positive. When there is a generation surplus in the network, production excess is generally paid at a lower price than the day-ahead marginal price. Hence, those market participants causing the positive system imbalance are rewarded for their overproduction at market clearing price. They achieve revenue smaller than that they would have obtained if they had sold their overproduction in the day-ahead market.

Suppose that the price deviation is negative. When there is a generation deficit in the network, those participants responsible for the system imbalance has to pay their imbalance at a higher price. Thus, the balancing process causes to obtain a lower profit for these market

participants compared to that they would have attained by selling only their real production in the day-ahead market [114].

In the following, the way of calculating WTs offer price is explained. Capacity factor (CF) is defined as the ratio of average power output to the rated power output of a WT. The CF is computed as follows [115]:

$$CF = \frac{1}{v_r^3} \int_{v_{cin}}^{v_r} v^3 f(v) dv + \int_{v_r}^{v_{co}} f(v) dv \qquad (4.3)$$

where $f(v)$ is the Weibull PDF. In order to calculate WTs' offers, financial data, i.e. WTs life time, installation cost, depreciation time, interest rate, are considered as summarized in Table 4.1 [98, 99]. The annual cost for WTs was calculated as described in (3.16). The CF is calculated by equation (4.3) and consequently the number of equivalent hours over a year is obtained, as given in Table 1.

Table 4.1 Financial Data for Estimating WT's Offer Price

Life time (years)	20
Installation cost (€/kW)	1700
Depreciation time (years)	10
Interest rate (%)	10
Number of equivalent hours (MWh/MW)	4010
Capacity factor (%)	46
Annual cost (€/kW-year)	280
Calculated offer (€/MWh)	**70**
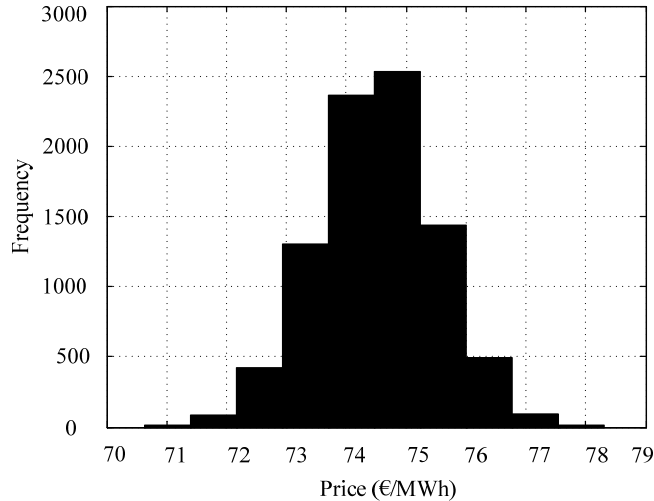
Fig.4.2. Histogram of a 660 kW WT's offer price

By dividing *Ann_Cost* by number of equivalent hours, the offer price for the considered WT is equal to 70 €/MWh. The obtained value, with no subsidy, is assumed as minimum value of Normal PDF. The histogram of Normal PDF of the offer price of a 660 kW WT is shown in Fig. 4.2. The calculated value is considered as the minimum value of Normal PDF in order to cover the annual cost for depreciation also in the case of negative energy deviation.

4.2   Structure of The Proposed Method

The wind speed is modeled by using a Weibull PDF on the basis of the WT's power curve to determine the power output and the offer quantities in a DNO acquisition market environment in order to perform the MCS.

The maximum number of WTs that can be allocated at a given bus is represented by an equivalent number of blocks in the WT's offer. It is assumed that at each candidate bus maximum four WTs can be allocated; therefore, for each generation level there are four blocks with the same size equal to the power output of WTs and the same price for all blocks.

It is assumed that wind power producers do not offer their energy production at zero or fixed price and are penalized in the real-time market for their energy imbalances. The volatile WTs offer price is modeled by using Normal PDF as is explained in following.

With regards to the bids for DLs, it is assumed that there are four blocks per load with different sizes and the same price for all blocks, respectively. Discrete load bands are considered as maximum, normal, medium and minimum load.

The DNO is defined as the market operator of the DNO acquisition market, which determines the price estimation and the optimization process for the hourly acquisition of active power.

The combined MCS and market-based OPF are used to maximize the SW considering different combinations of wind generation and load demand over a year. The market-based OPF uses CCV approach to generate the appropriate helper variable, cost term, and related constraints for any piecewise linear costs. WTs' offers and bids of DLs are taken and treated as marginal cost and marginal benefit functions, respectively, then by using the CCV method they are converted to the equivalent total cost and total benefit functions and plugged into a matrix as piecewise linear costs.

To the best of our knowledge, no probabilistic method for evaluating WTs capacity and LMP in distribution networks from the point of view of DNOs in market environment considering uncertainties has been reported in the literature.

The by-product of the proposed method is the probabilistic capacity of WTs, the SW and the LMP. The structure of the proposed method is shown in Fig.4.3.
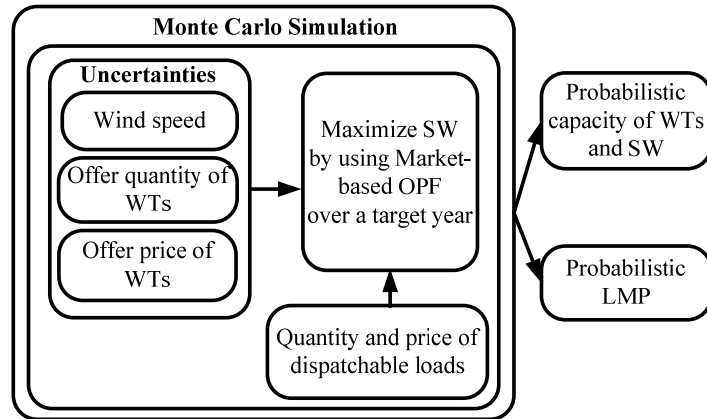
Fig.4.3.The structure of the proposed method

4.3　　Simulation Procedure

  The proposed algorithm, conceived to analyze the amount of wind power that can be injected into the grid and the impact of wind power penetration on LMPs throughout the network, runs as follows.
1) Set the candidate buses according to wind energy availability.
2) Define WTs size and speed-power curve.
3) Model wind speed by using Weibull PDF.
4) Derive the PDF of the WTs power output based on Weibull PDF of wind speed. The power output of WTs is considered as the offer quantity.
5) Calculate the offer price of wind energy producers.
6) Model the WTs offer price by using Normal PDF and consider the calculated value as the minimum value of Normal PDF. It is assumed that at each candidate bus maximum four WTs can be installed; therefore, for each generation level there are four blocks with the same size equal to the power output of WTs and the same price for all blocks.
7) Consider discrete load bands as maximum, normal, medium and minimum load over a year. For each band, four blocks for each DL with different sizes and the same price for all blocks have been assumed.

8) Run MCS taking into consideration aforementioned uncertainties for different combinations of load demands and wind generations.
9) For each sample, maximize the SW by using the market-based OPF subject to network constraints.
10) The by-product of the proposed method is the probabilistic SW, the LMP and the capacity of WTs.

Note that the formulation and description of the DNO acquisition market was provided in Chapter 3.

4.4   Test System Description

In this section, the distribution system to test the proposed method is described. The following analyses are based on an 83-bus 11.4-kV radial distribution system whose data are given in [4]. The eleven feeders are supplied by two 20 MVA, 33/11.4 kV transformers. The one line diagram of the distribution system was shown in Fig. 6.3 (Chapter 3). Discrete load bands are considered as maximum, normal, medium and minimum load. The loading level for each band is given in Table 4.2. In order to test the proposed method, the following assumptions are considered. It is assumed that the considered WTs operate at unity power factor. The Weibull PDF of the considered wind speed is shown in Fig. 4.4(a). In this paper, the parameters of Weibull PDF as explained in Section 3, i.e. c and k, are assumed to be equal to 10 and 3, respectively. The derived PDF of the WT's power output is shown in Fig. 4.4(b).

Here, only WTs of size of 660 kW are considered by DG-owning DNOs even if considering different sizes simultaneously is also possible. The maximum number of WTs that can be allocated at a given bus is represented by an equivalent number of blocks in the WT's offer. At each candidate bus it is assumed that maximum four WTs can be allocated; this requirement is regulated by the accessible land for building WTs. Thus, for each generation level there are four blocks of the same size equal to the power output of WTs and the same offer price for all blocks. The offer price has been modeled by a Normal PDF with a minimum price of 70 €/MWh while for the bus connecting the distribution network to the transmission one the offer

at constant price of 120 €/MWh is assumed. The mean and variance values for Normal PDF are assumed as 75 and 1, respectively.

Voltage limits are taken to be ±6% of nominal value, i.e. V_{max}= 1.06 p.u. and V_{min}= 0.94 p.u., and the feeders' thermal limits are given in Table 4.3 and vary between 40 and 480 A. The total fixed load is 5.4 MW. Regarding the bids for DLs, it is assumed that there are four blocks per demand bid with different sizes as presented in Table 4.4 and the same price of 250 €/MWh for all blocks.

Table 4.2 Loading level

Load Band	Active Power (MW)
Minimum	16.50
Medium	27.50
Normal	39.00
Maximum	55.00

(a)

(b)
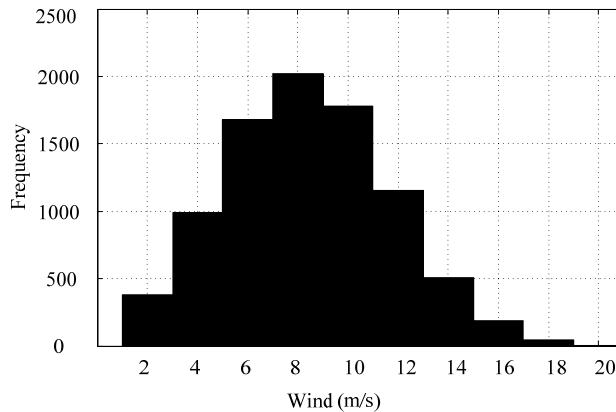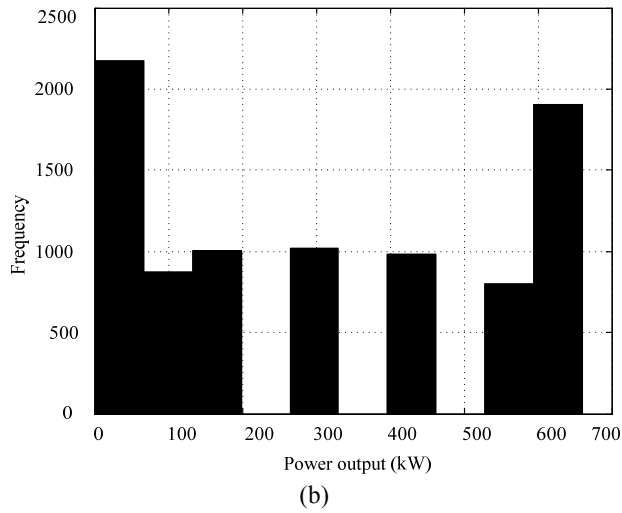
Fig.4.4. (a) Weibull PDF of wind speed, (b) PDF of the WT power output

Table 4.3 Existing wires

Wires	Amps
A-1, 1-2, 2-3, 3-4, 4-5, 5-6, B-11, 12-13, C-15, D-25, E-30, F-43, 44-45, G-47, 48-49, H-56, 57-58, I-65, 66-67, J-73, K-77, 78-79	480
7-8, 15-16,16-17, 17-18, 19-20, 20-21, 26-27, 27-28, 32-33, 33-34, 34-35, 35-36, 36-37, 37-38, 38-39, 49-50, 50-51, 51-52, 52-53,57-58, 58-59, 59-60, 60-61,67-68, 68-69, 79-80, 80-81	330
21-22,21-23, 23-24, 28-29, 41-42, 53-54, 61-62, 62-63, 69-70, 70-71, 71-72, 74-75, 75-76	180
30-31, 56-57, 77-78	60
7-9, 46-47, 63-64	50
7-10, 12-14, 38-39, 39-40, 45-46, 54-55, 81-82, 82-83	40

Table 4.4 Bids of Dispatchable loads

Load No.	Bus No.	Block 1 (MW)	Block 2 (MW)	Block 3 (MW)	Block 4 (MW)
1	6	0.4	0.4	0.4	0.4
2	9	0.4	0.4	0.4	0.4
3	14	0.4	0.4	0.4	0.4
4	28	0.4	0.4	0.4	0.4
5	30	0.4	0.4	0.4	0.4
6	38	0.4	0.4	0.4	0.4
7	40	0.4	0.4	0.4	0.4
8	45	0.4	0.5	0.4	0.4
9	47	0.5	0.5	0.4	0.4
10	54	0.5	0.5	0.4	0.4
11	56	0.5	0.5	0.4	0.4
12	62	0.5	0.5	0.5	0.5
13	64	0.5	0.4	0.5	0.4
14	81	1.0	0.5	0.5	0.5
15	84	0.5	0.5	0.5	0.5
16	44	0.5	0.5	0.5	0.5
17	46	0.5	0.5	0.4	0.4
18	51	0.5	0.5	0.4	0.4
19	53	0.5	0.5	0.5	0.5
20	55	0.5	0.5	0.4	0.4
21	59	0.5	0.5	0.4	0.4
22	63	1.0	0.5	0.4	0.4
23	67	1.0	0.5	0.4	0.4
24	69	0.4	0.4	0.4	0.4
25	73	1.0	1.0	0.4	0.4
26	75	1.0	1.0	0.4	0.4
27	77	0.4	0.4	0.4	0.4
28	79	1.0	0.4	0.4	0.4
29	82	0.4	0.4	0.4	0.4

4.5   Simulation Results

The proposed method was applied to the abovementioned distribution network and implemented in the MATLAB$^®$ environment incorporating some features of MATPOWER. Combined MCS technique and market-based OPF are used to maximize the SW considering different combinations of wind generation and load demand over a year.

The market-based OPF is solved by previously described SCPDIPM considering network constraints. MCS runs for different load bands, as presented in Table 4.2, throughout a year considering a sample every 15 minutes.
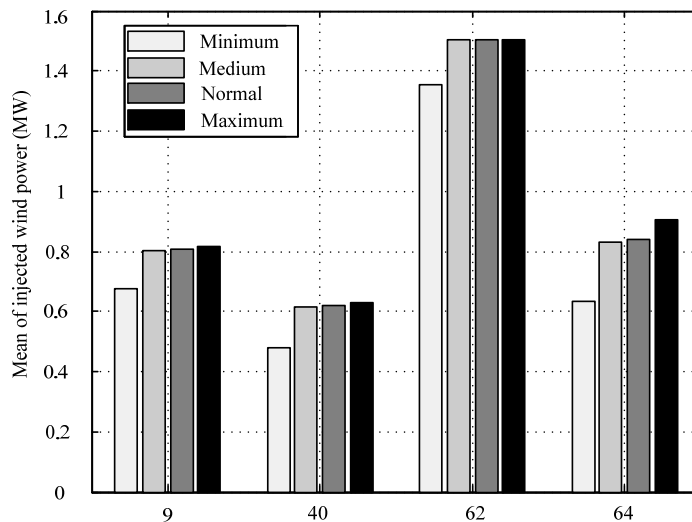
Fig.4.5. Mean of injected wind power for different load bands

Fig.4.5 shows the mean of injected wind power at buses 9, 40, 62, and 64 for different load bands. The amount of wind power that can be injected into the network is limited by the voltage and thermal limits as well as by the bids' values at each bus.

At bus 40 the mean of injected wind power at maximum load has the lowest value (i.e. about 600 kW) if compared to that at other buses. This is mainly due to the lowest value of both thermal limit of the line 39-40 connecting the buses (i.e. 40 A) and the bids' values of DLs if compared to those at the other lines and buses. A higher amount of wind power at maximum load at bus 9 is injected if compared to previous case (i.e. about 800 kW). It is mainly due to the higher thermal limit of the line 7-9 connecting the buses (i.e. 50 A) and higher bids' values at this bus if compared to previous case. At bus 64 with the higher bids' values and the same thermal limit of the line connecting this bus to the network if compared to previous case, a higher amount of wind power is injected that is essentially owing to

the higher bids' values. It is evident from Fig.4.5 that the highest amount of wind power at bus 62 is injected. It is because of the higher thermal limit of the line 61-62 connecting the buses (i.e. 180 A) and the higher bids' values compared to previous cases. It is seen that at all buses by increasing the load, a higher amount of wind power is injected.

Different numbers of WTs, from one to four, have been considered in order to assess their impact on the LMPs. Figs. 4.6(a),(b) show the mean of LMP at buses 14 and 54 for different number of installed WTs and load bands. The mean of LMP at bus 14 for different number of WTs at maximum load vary between 140 and 130 €/MWh, while at bus 54 between 120 and 85 €/MWh.

By increasing the number of installed WTs, from one to four, at bus 54 for all load bands the mean of LMP decreases of about 30% while this value at bus 14 the mean of LMP decreases of about 7%. This is mainly due to the lower thermal limit of line 54-55 of 40 A.

For all load bands, in the case when four WTs are installed the mean of LMP at bus 54 varies between around 80 €/MWh and 90 €/MWh while at bus 14 between 100 €/MWh and 125 €/MWh. The higher thermal limit of 180 A of the line 53-54 connecting the WT at bus 54 to the network allows the injection of about all the generated wind energy into the network for all load bands. Instead, the lower thermal limit of 40 A of the line 12-14 connecting the WT at bus 14 to the network constrains the wind power injection, thus increasing the LMP.

By increasing the number of installed WTs buses connected by congested lines, the decrement in the mean of LMP is small while at the buses connected by uncongested line this value decreases drastically. As a result, the impact of a growing wind generation on LMPs translates into a decrease in the mean of LMP except when some lines are congested, thus limiting wind energy exploitation. Furthermore, the mean of LMP proportionally decreases to the number of installed WTs and increases to the loading level.

(a)

(b)
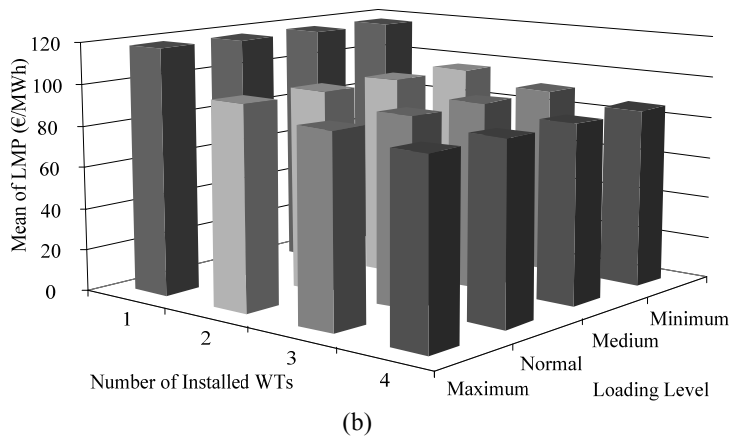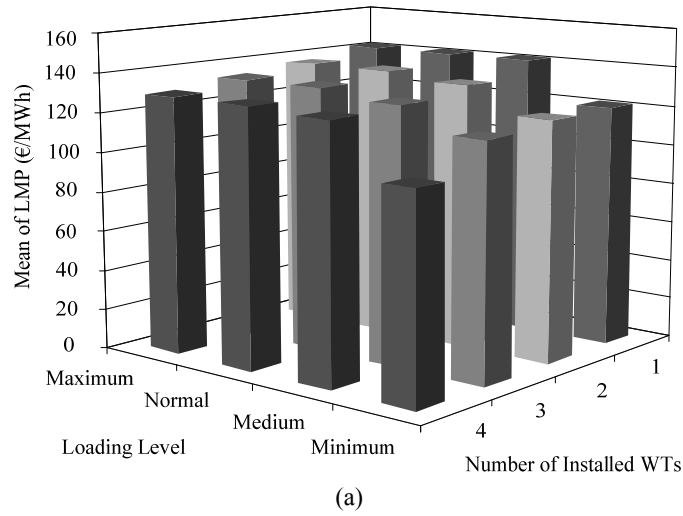
Fig.4.6. Mean of LMP for different number of installed WTs and loading levels at (a) bus 14 and (b) bus 54

The probabilistic SW for different loading levels when maximum four WTs are installed in the network is shown in Fig. 4.7. The increases proportionally to the load demand, in the case of maximum load, the maximum SW is about 3800 €/h while in the case of minimum load it is about 2000 €/h.

(a)

(b)

(c)

(d)
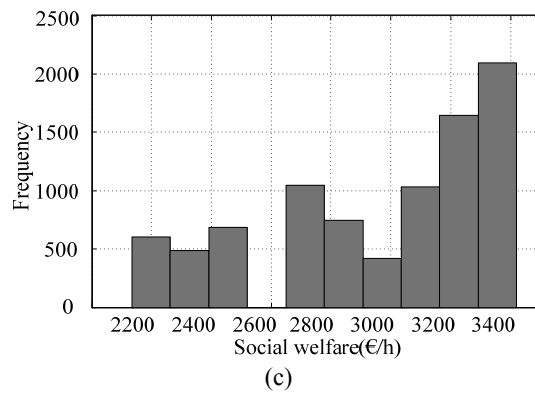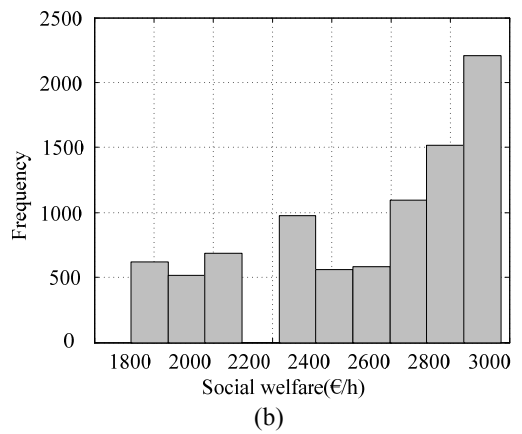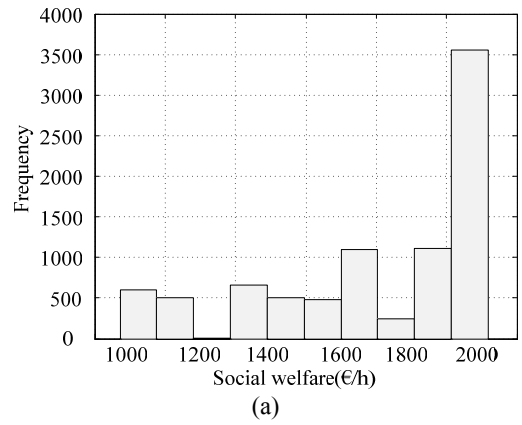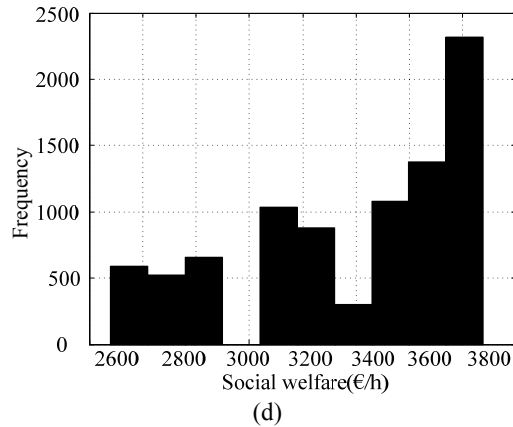
Fig.4.7. Social welfare at (a) Minimum, (b) Medium, (c) Normal and (d) Maximum load

The mean of SW for different number of installed WTs and loading levels is shown in Fig. 4.8. In the case of maximum load and when one WT is installed in the network, the mean of SW is equal to about 2700 €/h while in the case when four WTs are installed it is equal to around 3400 €/h. It is worth pointing out that, for all loading levels, the SW increases by augmenting the wind generation (i.e. the number of installed WTs). It is seen that by increasing the number of installed WTs from one to four, the SW increases about 30%. As a result, the SW increases proportionally to the both load demand and the number of installed WTs.
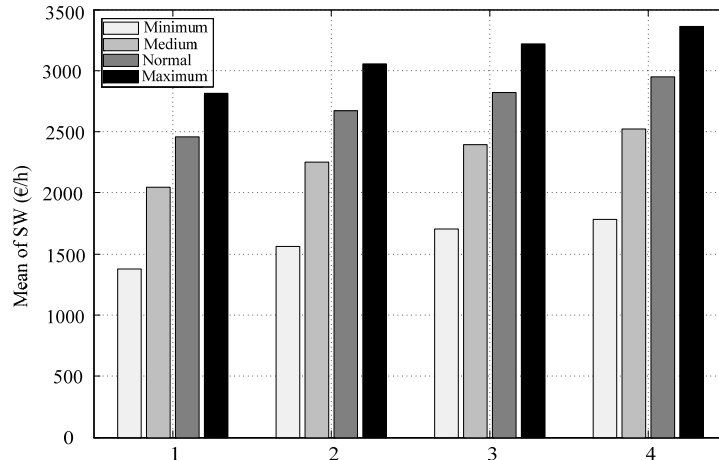
Fig.4.8. Mean of social welfare for different number of WTs and loading levels

4.6   Discussion and Conclusion

In this chapter, a probabilistic method to evaluate the effect of WTs integration into distribution networks within market environment was proposed. Combined MCS and market-based OPF are used to maximize the SW considering different combinations of wind generation and load demand over a year. MCS is used to model the uncertainties related to the stochastic nature of wind and the volatility of WTs' offer quantities and prices.

The main contributions of this chapter are as follows:

1) to provide a probabilistic methodology for assessing the SW and the amount of wind power that can be injected into the grid as well as the impact of wind power penetration on LMPs throughout the network within market environment considering uncertainties;

2) to model uncertainties due to the stochastic nature of wind as well as the volatility of WTs' offer price and quantity through MCS approach;

3) to maximize the social welfare by using market-based OPF considering different combinations of load demand and wind generation over a year;

4) to provide a tool for DG-owning DNOs to better allocate WTs by considering cost reduction and consumers' benefits.

The method can be utilized as a simulation tool to investigate the probabilistic SW and the impact of wind power penetration on LMPs throughout the network. Furthermore, it allows characterizing how LMP varies as a result of increasing wind power penetration. It also can be used as a basic tool for DNOs to estimate the amount of wind power that can be injected into the network considering cost reduction and consumers' benefits.

The proposed probabilistic method can assist DNOs evaluate the performance of the network and to plan the WTs integration into distribution networks. Furthermore, it can help DG-owning DNOs to make better decisions to allocate WTs by using a more efficient method. The method can help DNOs to assess the impact of wind penetration on a given network in terms of both technical and economic effects.

Chapter 5

Control of Distribution Networks

This chapter introduces a fuzzy controller to improve the FRT capability of WTs during both voltage sags and swells in weak distribution networks. Section 5.1 introduces the background of the problem. Grid code requirements and FRT capability are presented in Sections 5.2. The WT generator system and capability limits of DFIG based WTs are explained in Sections 5.3 and 5.4, respectively. The description of the proposed FRT approach and the fuzzy controller design are discussed in Sections 5.5 and 5.6, respectively. Case studies and simulation results are discussed in Section 5.7. Discussion and conclusion are provided in Section 5.8.

5.1   Introduction

Recently, the most popular type of WTs installed worldwide is the variable speed wind turbines, which has better advantages such as controllability of speed and flexible operation compared with fixed speed wind turbines. Other advantages of using variable speed generators include improved power quality, speed control, reduced mechanical stresses, decoupled control of active and reactive power as well as more power generation than fixed speed generator under the same circumstances [116]. Two types of variable speed generator are commonly used. First type is direct-drive synchronous generator which is completely decoupled from the grid by a power electronics converter connected to the stator winding. The grid side of this converter is a voltage source converter. The generator side can be a voltage-source converter or diode rectifier. The direct-drive generator is excited using an excitation winding or permanent magnets. Another type is DFIG which also uses power electronics. One end of a back-to-back voltage-source converter feeds the three-phase rotor winding and

other end connected to stator winding or power grid. Among the two types, DFIG is more favorable due to the following facts.

- Economical converter cost, because converter rating generally can be 10-40% of total system power, while the speed range is also 33% around the synchronous speed.
- Cost effective converter filters and EMI filters since filters are rated for 0.1-0.4 p.u. of the total system power, and converter harmonics represent a smaller fraction of total system harmonics.
- DFIG converter is able to decouple control of active and reactive power.

During the fault, disconnection of wind generator can take place if the wind generator does not support the voltage dip or sag.

Disconnecting a wind generator too quickly could have a negative impact on the power system grid, especially with large wind farms.

Another issue is the mechanical power output from wind generator which is directly proportional to the torque of WT. During wind speed fluctuation, the output voltage will also fluctuate. If voltage fluctuation is out of the limit, it introduces negative impact on the power system. From economic point of view, tracking optimum power from wind is economically effective for wind turbine operators. Present day technology is available to ensure that the WT is connected to the grid during fault or network disturbance. Additional circuitry is utilized in order to overcome FRT capability or voltage regulation but at the expense of additional cost.

To enhance the FRT capability of WTs, several methods have been proposed.

A novel control strategy for FRT capability improvement of DFIG based WTs based on a controller using H_∞ technique and μ-analysis was proposed in [117]. In [118], the authors studied the performance of the DFIG based WTs during voltage sag caused by an external short circuit fault.

A comprehensive time domain model of DFIG using decoupled dq controller was described in [119], which was proposed to keep generator operating during transient grid faults. In [120], the authors investigated the FRT capability of WFs and the performance of converter protection schemes based on various resistor protections with crowbar and series dynamic resistor. In [121], the authors used a

real time digital simulator (RTDS) to introduce a new control strategy for FRT enhancement of WTs with DFIG and as well as used current limiters which are controlled by Thyristor switches to counter the effect of fault on DFIG operation. In [122], the authors utilized a five-level cascade multilevel inverter based STATCOM to enhance the FRT control strategy of WFs as well as to alleviate voltage fluctuation. The improvement of dynamic model of DFIG wind generator and controllers for network unbalance gird FRT capability using PI-R current regulators was analyzed in [123]. The improvement includes control of the GSC and RSC, respectively during voltage unbalance. Authors in [124] discussed the enhancement of the fault ride through capability, which was achieved by inserting a series-connected voltage-source converter during the fault.

5.2   Grid Code Requirements and FRT Capability

In recent years, the increasing penetration of WTs into power systems has led power system operators to develop new grid code requirements for WTs in many countries. These requirements impose WTs operators to deal with some aspects such as FRT capability, reactive power control, and voltage control. This implies that the WTs connection into a distribution system requires coordination with voltage and reactive power control. Several countries have provided different grid codes depending on their system characteristics and operation standards such as the codes from E. ON Netz Germany, Denmark, Belgium, the U.K., Spain, the Netherlands, USA, and Canadian TSO Hydro-Quebec [125]. The Nordic grid code from Nordel [126] specifies the technical requirements that new WTs should have in order to be connected at the transmission network and provide acceptable safe operation and reliability. Belgium grid code [127], provided by the Belgian TSO, Elia, applies to the grids with the voltage levels 30–70 kV and 150–380 kV. This code discriminates different kinds of voltage disturbances. German grid code from E.ON Netz [128,129] applies to the grids with the voltage levels 110, 220 and 380 kV.

Denmark grid code [130] relates to the WTs connected to the grids with the voltages below 100 kV. Fig. 5.1 illustrates the FRT requirements of the Danish grid code. Apart from the FRT requirements of Fig.1, WFs must disconnect if the voltage increases above 1.2 p.u.. Additional requirements for voltages below 100 kV define that a WT must remain connected after the faults in the distribution system as listed below.

- Three-phase short circuit lasting 100 ms (five cycles),
- two-phase short circuit with/without earth lasting 100, ms (five cycles), followed by a new fault 300–500 ms (15–25 cycles), lasting also 100 ms (five cycles),
- at least two two-phase short circuits within 2 min,
- at least two three-phase short circuits within 2 min,
- at least six two-phase short circuits at 5-min intervals,
- at least six three-phase short circuits at 5-min intervals.

When the voltage at the PCC is above the FRT curve, i.e. the area labeled: "must stay connected", the WT must remain connected. The curve can be divided into four areas according to the voltage variations. In area 1, the faults last up to 0.1 s and the voltage magnitude at the PCC is equal to or greater than 0.2 p.u. and WTs must remain connected to the network. Area 2, between 0.1 to 0.75 seconds, defines a growth recovery voltage from 0.2 to 0.7 p.u. in a mentioned period. The main challenge in this area is adjusting of protection system to ensure the voltage change during the voltage restoration. Area 3, between 0.75 to 10 seconds, describes the system recovery with voltage sag to 0.7 p.u.. Area 4, between 10 to 100 seconds, describes the full normalization after 10 seconds voltage sag, the voltage should be no less than 0.9 p.u.. Regarding voltage swells, in the area between 0.2 to 90 seconds if the voltage increases above 1.1 p.u., the WTs must be disconnected.

When the voltage at the PCC is above the FRT curve, i.e., the area labeled "must stay connected," the WT must remain connected. The curve can be divided into four areas according to the voltage variations. In area 1, the faults last up to 0.1 s, the voltage magnitude at the PCC is equal to or greater than 0.2 p.u., and WTs must remain connected to the network. Area 2, between 0.1 and 0.75 s, defines a growth recovery voltage from 0.2 to 0.7 p.u. in a mentioned period. The main challenge in this area is adjusting of the protection system to

ensure the voltage change during the voltage restoration. Area 3, between 0.75 and 10 s, describes the system recovery with voltage sag to 0.7 p.u. Area 4, between 10 and 100 s, describes the full normalization after the 10 s voltage sag; in this case, the voltage should not be less than 0.9 p.u. Regarding the voltage swells, in the area between 0.2 and 90 s, if the voltage increases above 1.1 p.u., the WTs must be disconnected. The aim of modern grid codes is supporting voltage during a voltage drop by compensating the reactive power. During voltage sag, the additional reactive current is relied on the value of the voltage sag. The minimum limit according to the Danish grid code for voltage sags is described by the following formulation:

$$(\Delta I_q / I_n)/(\Delta V / V_n) \geq 2 \quad \text{for} \quad 0.5 \leq (\Delta V / V_n) \leq 2$$
$$(\Delta I_q / I_n) = 1 \qquad \text{for} \quad (\Delta V / V_n) \leq 0.5 \qquad\qquad (5.1)$$

where
$$\Delta I_q = I_q - I_{q0} \quad , \qquad \Delta V = V - V_0$$

I_n is the rated current, I_q is the quadratic axis current (reactive component), I_{q0} is the pre-fault reactive component, V_n is the rated terminal voltage, V is the generator terminal voltage during fault, and V_0 is the pre-fault terminal voltage.

It is assumed that the pre-fault voltage and pre-fault reactive current are 1 and 0 p.u., respectively. According to Fig. 5.2, the wind power plant in area B must have a controller to control the reactive power in the presence of fault sequences. When voltage drops by 50%, the maximum reactive current must be injected by the system. As a larger amount of reactive current during the fault is needed, the controller's objective is, therefore, increasing the amount of reactive current during voltage sag.
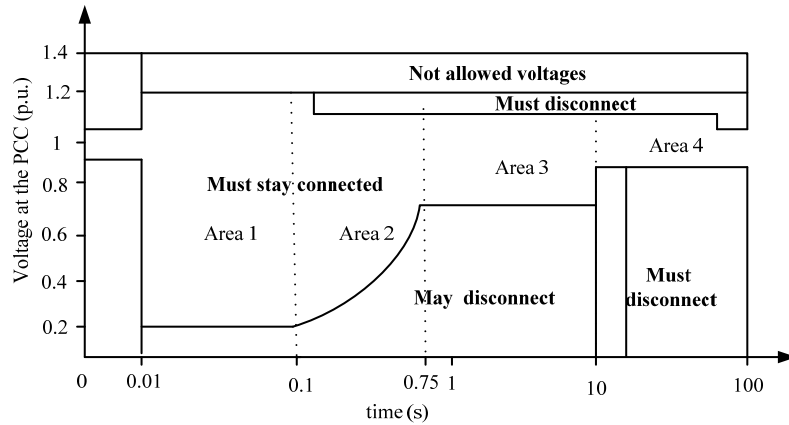
Fig.5.1. FRT requirements of the Danish grid code for grids below 100 kV
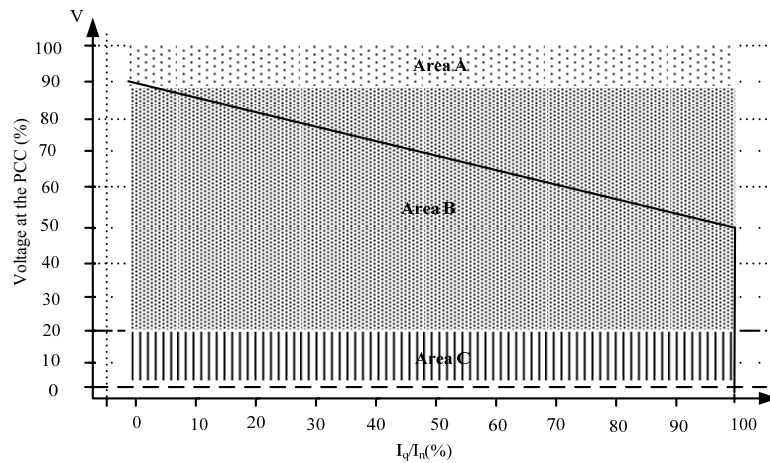

Fig.5.2. Requirement for reactive power supply during voltage drops

5.3   Power Electronics for Generators

Nowadays, the WTs in the market mix different advanced notions with proven technologies for generators and power electronics. In this Section, the existing status of generators and power electronics in WT concepts from an electrical viewpoint is described. It explains

traditional and new notions of generators and power electronics concerning technical and economic aspects [59].

5.3.1   Overview of WT topologies

WTs can operate either with a fixed speed or a variable speed.

5.3.1.1   Fixed-Speed WTs

In the past, the typical WTs operated at fixed speed. This means that regardless of the wind speed, the rotor speed of WT is fixed and specified by the network frequency, the gear ratio and the generator design. Fixed-speed WTs (FSWTs) are equipped with an induction generator i.e. squirrel cage or wound rotor that is directly connected to the grid by means of a soft-starter and a capacitor bank in order to compensate reactive power.

These are designed to reach maximum efficiency at a specific wind speed. The FSWTs generator has two winding sets: one of them is utilized at low wind speeds (usually 8 poles) and the other one at medium and high wind speeds (usually 4-6 poles). The FSWT has some advantages and disadvantages. The advantages are simple, robust and reliable and well-proven and the low cost of its electrical parts and disadvantages are an uncontrollable reactive power consumption, mechanical stress and limited power quality control. Because of the fixed-speed operation, the wind speed variations are transferred in the mechanical torque and consequently into the grid power. In weak grids, the power variations cause huge voltage oscillations, which result in substantial line losses.

5.3.1.2   Variable-Speed WTs

Recently, the variable-speed WT (VSWTs) has become the dominant type among the installed WTs. VSWTs are designed to reach maximum efficiency within a large variety of wind speeds. In variable-speed operation mode, it is possible to adapt the rotating speed ω of the WT to the wind speed v. This way, the tip speed ratio λ

is retained constant at a pre-specified value that relates to the maximum power coefficient.

In a VSWT the generator torque is preserved constant and the wind fluctuations are absorbed by variations in the generator speed. The electrical system of a VSWT is more complex than that of a FSWT. It is usually equipped with an induction or synchronous generator and connected to the grid via a power converter. The generator speed is controlled by the converter which the power variations resulted from wind fluctuations are absorbed generally by variations in the speed of rotor and accordingly in the rotor speed of WT. The advantages of VSWTs are an augmented energy capture, enhanced power quality and reduced mechanical stress on the WT. The disadvantages are power losses in power converters, the utilization of additional components and the tools augmented cost owing to the power electronics. The presentation of VSWT types augments the number of appropriate types of generator and presents several degrees of freedom in the mixture of generator and converter types.

5.3.2   State of the Art Generators

The classification of WTs' configurations are explained in the following in terms of speed control and the of power control type. There are four diverse types of WTs, as shown in Figure 5.3. WT configurations can be classified regarding the type of power (blade) control: stall, pitch, active stall. Table 5.1 shows the various types of WT configurations, taking into consideration speed and power control criteria. Every combination of these two criteria obtains a label; for instance, Type A0 represents the fixed-speed stall-controlled WT. The grey zones in Table 5.1 demonstrate the combinations that, nowadays, are not utilized in the WT manufacturing (e.g. Type B0).
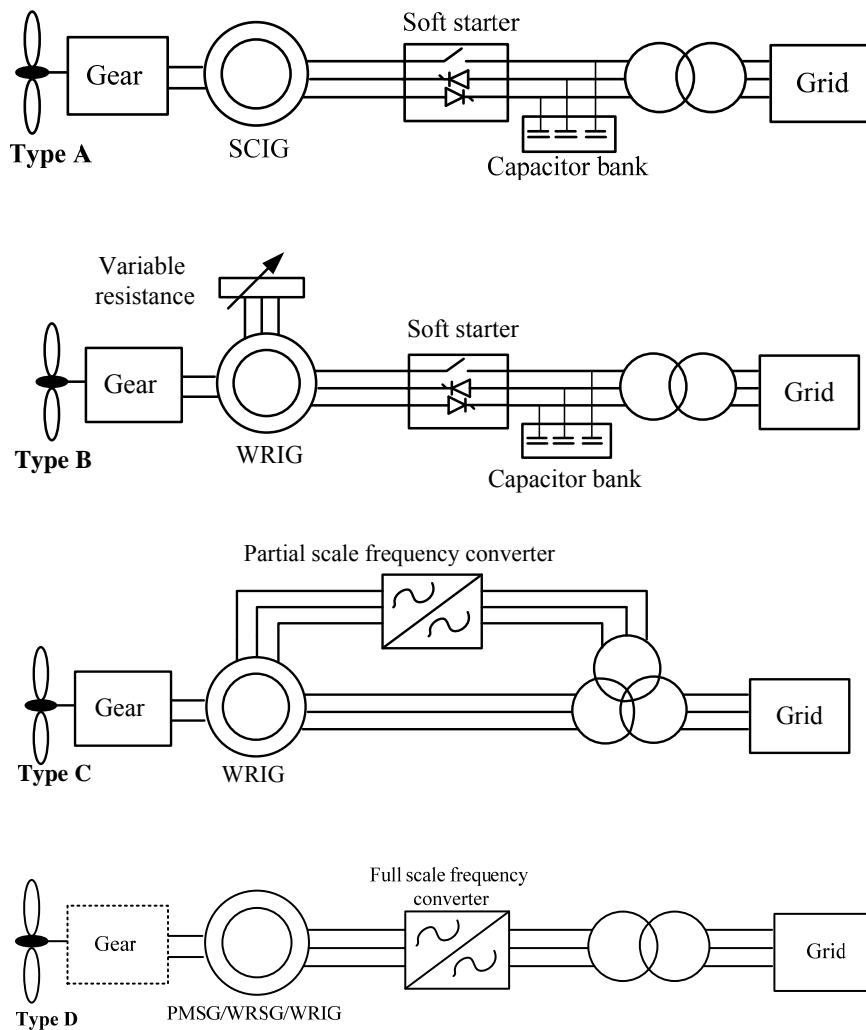
Fig.5.3. Typical wind turbine configurations. SCIG= squirrel cage induction generator; WRIG= wound rotor induction generator; PMSG= permanent magnet synchronous generator; WRSG= wound rotor synchronous generator. The broken line around the gearbox in Type D configuration indicates that there may or may not be a gearbox.

In this Section, the standard WT types, as shown in Figure 5.3 and Table 5.1 are investigated. The typical WT configurations, their advantages and disadvantages are introduced in the following.

Table 5.1 Wind turbine concept

Speed control		Power control		
		Stall	Pitch	Active stall
Fixed speed	Type A	Type A0	Type A1	Type A2
Variable speed	Type B	Type B0	Type B1	Type B2
	Type C	Type C0	Type C1	Type C2
	Type D	Type D0	Type D1	Type D2

Note: The grey zones indicate combinations that are not in use in the wind turbine industry today.

5.3.2.1   Type A: Fixed Speed

This configuration represents the FSWT with an asynchronous squirrel cage induction generator (SCIG) directly connected to the grid through a transformer as shown in Fig.5.1. Since the SCIG draws reactive power from the grid, this configuration uses a capacitor bank for reactive power compensation. A smoother grid connection is achieved by using a soft-starter. Without concerning of the power control fact in a FSWT, the wind oscillations are converted into mechanical variations and thus into power oscillations. Owing to the voltage variations, the FSWT draws variable quantities of reactive power from the utility grid that augments the voltage variations and the line losses. Therefore, the major disadvantages of this configuration are that it doesn't provide speed control, it needs a stiff grid and its mechanical structure has to be capable to bear high mechanical stress. All three types of the fixed-speed WT of Type A i.e. Types A0, A1 and A2 are used in the WT industry and can be described as follows.

5.3.2.2   Type A0: Stall Control

This is the formal notion applied by numerous Danish WT manufacturers through the 1980s and 1990s. It has become so much popular due to its comparatively low price, easiness and robustness. Stall-controlled WTs cannot perform aided startup, which means that the power of the WT cannot be controlled through the connection sequence.

5.3.2.3   Type A1: Pitch Control

The key advantages of a Type A1 WT are that it simplifies power controllability, controlled startup and emergency stopping. Its main disadvantage is that, at high wind speeds, even small variations in wind speed cause large fluctuations in output power. The pitch mechanism is not fast enough to avoid such power fluctuations. By controlling the blade, slow fluctuations in the wind can be compensated.

5.3.2.4   Type A2: Active Stall Control

This configuration mainly keeps all the power quality features of the stall-regulated system. The enhancements demonstrate a better use of the whole system, accordingly the usage of active stall control. One disadvantage is the high price resulting from the pitch control mechanism. As shown in Fig. 5.1 and Table 5.1, the variable speed notion is utilized by all three configurations including Types B, C and D. Because of power restriction considerations, the variable speed concept is used actually nowadays along with a fast-pitch mechanism. Variable speed stall or variable speed active stall controlled WTs are not taken into account here as potentially they don't have the ability to rapidly reduce the power. Hence, as presented in Table 5.1, Types B0, B2, C0, C2, D0 and D2 are not utilized nowadays in WT industry.

5.3.2.5   Type B: Limited Variable Speed

This configuration relates to the restricted VSWT with variable generator rotor resistance, known as OptiSlip. It utilizes a wound rotor induction generator (WRIG). The generator is directly connected to the grid and a capacitor bank does the reactive power compensation. A soft-starter is used in order to have a smoother grid connection. The distinctive characteristic of this configuration is that it has a variable extra rotor resistance, which can be altered by controlled converter mounted on the rotor shaft. The rotor resistance can be altered and therefore controls the slip. Therefore, the power output in the system is controlled. The range of the dynamic speed control depends on the

size of the variable rotor resistance. Usually, the speed range is 0–10% above synchronous speed.

5.3.2.6 Type C: variable speed with partial scale frequency converter

This configuration, known as the DFIG concept, corresponds to the limited variable speed WT with a WRIG and partial scale frequency converter in the rotor circuit. The partial scale frequency converter carries out the reactive power compensation and the smoother grid connection. Normally, the speed varies in the range of synchronous speed of -40 to +30 %. The lesser frequency converter makes this notion interesting from an economical perspective. The key disadvantages are the usage of slip rings and protection in the case of grid faults.

5.3.2.7 Type D: Variable Speed with Full- Scale Frequency Converter

This configuration relates to the VSWT, with the generator connected to the grid throughout a full-scale frequency converter. The frequency converter carries out the reactive power compensation and the smoother grid connection. The generator can be excited electrically by wound rotor synchronous generator (WRSG) or WRIG or by a permanent magnet synchronous generator (PMSG). Some VSWT systems haven't gearbox (see the dotted gearbox in Figure 5.1). In these cases, a direct driven multi-pole generator with a large diameter is used.

5.3.3 State of the Art Power Electronics

The VSWT notion needs a power electronic system that is able to adjust the frequency and voltage of the generator. Prior to demonstrating the existing status regarding power electronics, it is essential to know why it is attractive to utilize power electronics in future WTs. Table 5.2 shows the advantages and disadvantages of

using power electronics in WTs for both the WT and the grid to which the WT is connected.

Table 5.2 Advantages and disadvantages of using power electronics in WT systems

Power electronics properties	Advantages	Disadvantages
Controllable frequency (important for the wind turbine)	▪ Energy optimal operation ▪ Soft drive train ▪ Load control ▪ Gearless option ▪ Reduced noise	Extra costs Additional losses

Power plant characteristics (important for the grid)	▪ Controllable active and reactive power
	▪ Local reactive power source
	▪ Improved network (voltage) stability
	▪ Improved power quality
	  ➢ reduced flicker level
	  ➢ filtered out low harmonics
	  ➢ limited short circuit power
		High harmonics

5.4   Wind Turbine Generator System

A DFIG is a wound rotor induction generator with the stator connected to the grid directly and with the rotor connected to the network through a back to back converter. The schematic of DFIG based WT is shown in Fig. 5.4. The aim of the RSC is to control the active and reactive power on the grid separately, while the GSC has to maintain the DC-link voltage at a set value [131]. A detailed description of the control systems for both the converters can be found in [132].

The relation between the wind speed and aerodynamic torque in a turbine can be described by the following equation:

$$P_w = \frac{1}{2}\rho\pi R^2 V_w^3 C_p(\theta, \lambda) \tag{5.2}$$

$$T_w = \frac{1}{2}\rho\pi R^2 V_w^2 C_p(\theta, \lambda)/\lambda \tag{5.3}$$

where P_w and T_w are the power and aerodynamic torque extracted from the wind in (W, N.m). ρ is the air density (kg/m^3), R is the wind turbine rotor radius (m), V_w is the equivalent wind speed (m/s), θ is the pitch angle wind turbine blade (deg), $\lambda = (\omega_{rot} R)/V_w$ is the tip speed ratio, where ω_{rot} is the wind turbine rotor speed (rad/s) and C_P is the aerodynamic efficiency of the rotor. C_P may be expressed as a function of the tip speed ratio (λ) and pitch angle (θ) by the following equation:

$$C_P = 0.22(116/\beta - 0.4\theta - 5)e^{-12.5/\beta} \tag{5.4}$$

where β is defined as follow:

$$\beta = \frac{1}{\dfrac{1}{\lambda + 0.08\theta} - \dfrac{0.035}{\theta^3 + 1}}$$
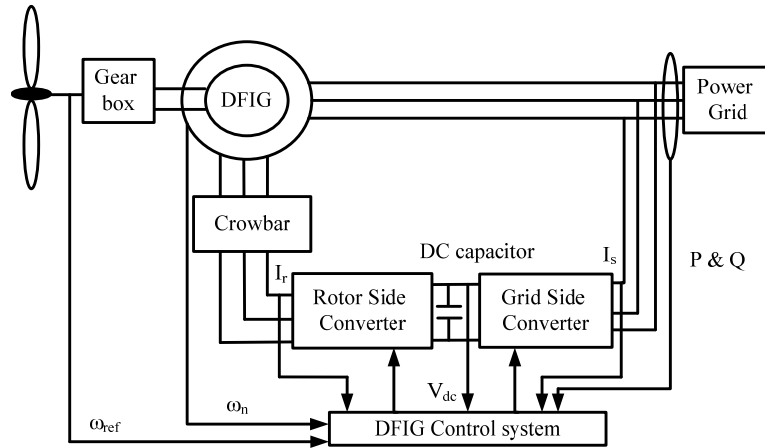

Fig.5.4. Configuration of DFIG based WT connected to a grid

5.4.1   DFIG-Based WT Capability Limits

In steady state, the DFIG capability limits are obtained by considering the stator- and rotor-rated currents as well as calculating the total capacity limits of WT. These currents are related to stator and rotor heating because of Joule's losses.

5.4.1.1   Stator Current Limit

The limit of stator current considers the heating owing to the Joule's losses of stator winding. When the rated current and voltage of stator are considered in p.u., the stator current limit can be expressed as follows.

$$P_S^2 + Q_S^2 = (3U_S^2 I_S^2) \tag{5.5}$$

where U_S, I_S, P_S, and Q_S are the voltage, current, active power and reactive power of the stator, respectively. Eq. (5.5) expresses that the locus of maximum stator current in the *PQ* plane is a circle centred at the origin, with a radius equal to the apparent power of stator as shown in Fig. 5.5.

5.4.1.2   Rotor Current Limit

The rotor current limit considers the heating owing to the Joule's losses of the rotor winding. The active and reactive powers of stator can be formulated at the rated voltage of stator as follows:

$$P_S = \frac{X_M}{X_S} U_S I_R \sin d \quad , \quad Q_S = \frac{X_M}{X_S} U_S I_R \cos d - \frac{U_S^2}{X_S} . \tag{5.6}$$
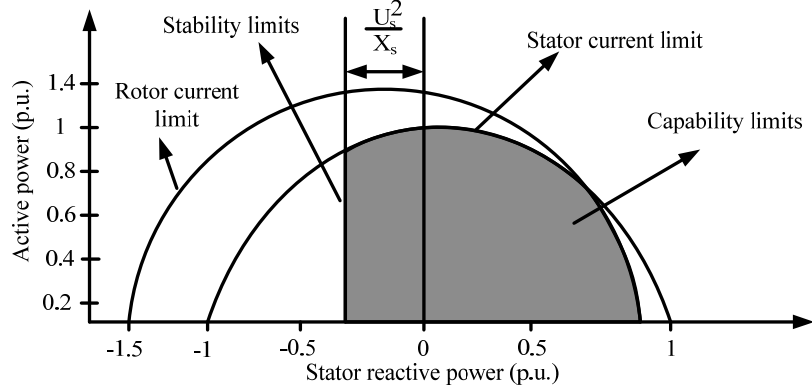
Fig.5.5. DFIG capability limits

5.4.1.3   Total Capability Limits

The total active power of the DFIG fed into the grid is the sum of the stator and rotor active power.

$$P_T = P_S + P_R \tag{5.7}$$

where

$$P_R = -sP_S \tag{5.8}$$

$$P_T = (1-s)P_S \tag{5.9}$$

where P_T is the total active power of the DFIG fed into the grid, P_S is the stator active power, and P_R is the rotor active power.

5.4.1.4   Maximum and Minimum Reactive Power Limits

From (5.6), the following equation can be obtained:

$$P_S^2 + (Q_S + \frac{U_S^2}{X_S})^2 = (\frac{X_M}{X_S} U_S I_R)^2 . \tag{5.10}$$

As shown in Fig.5.5, equation (5.10) is a circle centered at $[-\frac{U_S^2}{X_S}, 0]$ with a radius equal to $\frac{X_M}{X_S} U_S I_R$. The active and reactive power of

stator can be expressed as a function of the maximum allowable current of rotor and stator [133]:

$$P_S^2 + Q_S^2 = (3U_S^2 I_S^2) \tag{5.11}$$

$$P_S^2 + (Q_S + 3\frac{U_S^2}{X_S})^2 = (3\frac{X_M}{X_S}U_S I_R)^2 \tag{5.12}$$

Equation (11) represents a circumference centered equal to the stator rated apparent power. Equation (12) represents a circumference centered at $[-3\frac{U_S^2}{X_S}, 0]$. Substituting (5.8) and (5.9) into (5.11) and (5.12) can be expressed as:

$$(\frac{P_T}{1-s})^2 + Q_T^2 = (3U_S I_S)^2 \tag{5.13}$$

$$(\frac{P_T}{1-s})^2 + (Q_T + 3\frac{U_S^2}{X_S})^2 = (3\frac{X_M}{X_S}U_S I_R)^2 \tag{5.14}$$

The DFIG capability limits according to (5.13) and (5.14) can be achieved by taking into consideration the stator and rotor maximum currents $I_{S\max}$ and $I_{R\max}$, respectively.

The capability curve of a 9 MW WF considered in this work during normal operation is shown in Fig. 5.6. According to the capability curve of the considered WFs, the limits of the reactive power that the WFs can inject or absorb are 2.5 and 8 MVAr, respectively and they have been considered for designing the fuzzy controller.
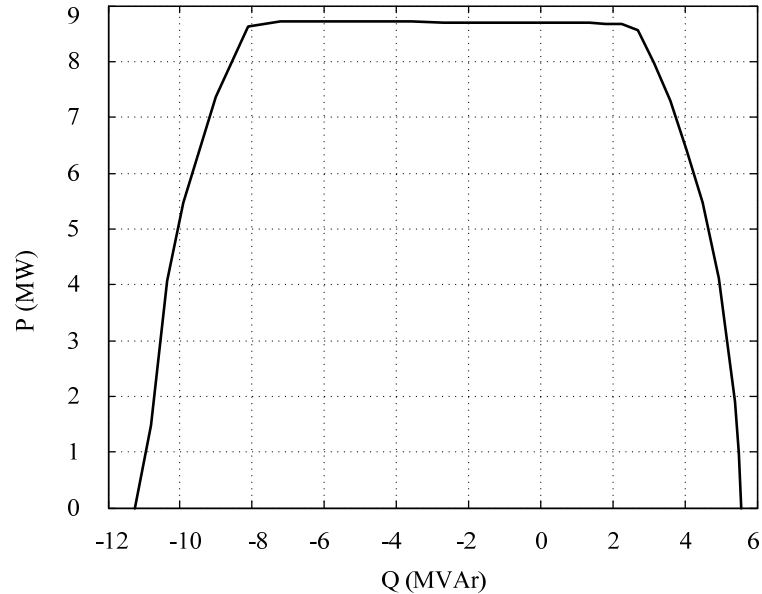
Fig.5.6. Capability curve of a 9 MW wind farm in normal operation

5.5   Proposed FRT approach

5.5.1 Strategy

In this chapter, a fuzzy controller for improving FRT capability in variable speed WTs is designed in order to compensate the voltage variations at the PCC by controlling simultaneously the reactive and active power generated by WFs. The schematic and the strategy of the proposed fuzzy controller are shown in Figs. 5.7, 5.8, respectively.

In the case of voltage sag, the reference signal for the reactive power (Q_{ref}) is sent by fuzzy controller in order to compensate voltage sag effects.

In the case of voltage swell, when the absorbed reactive power is enough to compensate voltage swell, there is no need to reduce the active power by using the reference signal for the active power production (active power modulator). The active power modulator,

that is sent by fuzzy controller to the RSC of WTs, varies in the range [0 1] to reduce the active power production. Furthermore, during a voltage swell, when the absorbed reactive power is not enough to lower the voltage at the PCC, the active power modulator is regulated to decrease the active power and increase the absorbed reactive power according to the following formula:

$$|Q| = \sqrt{S^2 - P^2} \tag{5.15}$$

where S is the power converter size, given as maximum apparent power, P and Q are the generated active and reactive power, respectively.
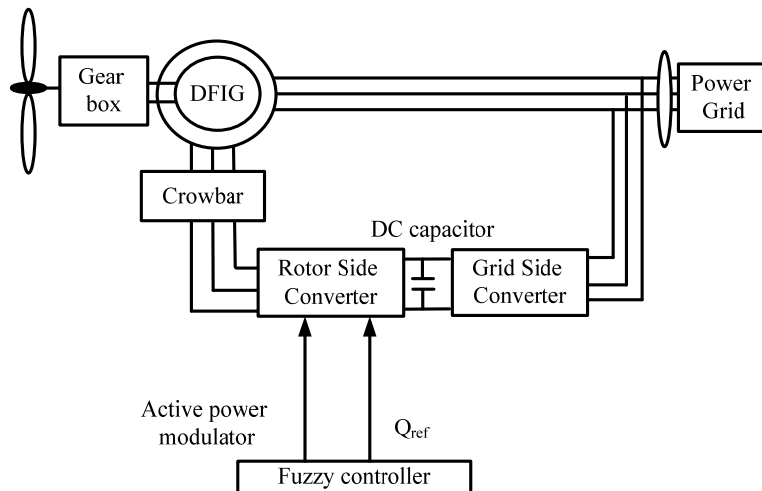
Fig.5.7. Schematic diagram of the proposed FRT approach

In this case, WFs will not generate the maximum active power, but this will positively affect the voltage regulation at the PCC: 1) within the limited size of the power converters of DFIG, the active power reduction will increase the maximum reactive power that can be absorbed by WFs, 2) the active power reduction, in low or medium voltage weak networks with long feeders characterized by a high R/X ratio, can affect the voltage drop on the feeders, therefore, contributing to decrease the voltage at the PCC.

Note that the proposed method is also able to compensate voltage variations in the normal operation if some network constraints are violated. For instance, in normal operation when the voltage

constraints are violated at the connection buses of the WFs, the controller is able to inject or absorb the reactive power according to capability curve of WFs up to 2.5 or 8 MVAr, respectively in order to compensate voltage variations.

Fig.5.8. Strategy of the proposed method

5.5.2   Grid Code Requirement and Reactive Power Compensation

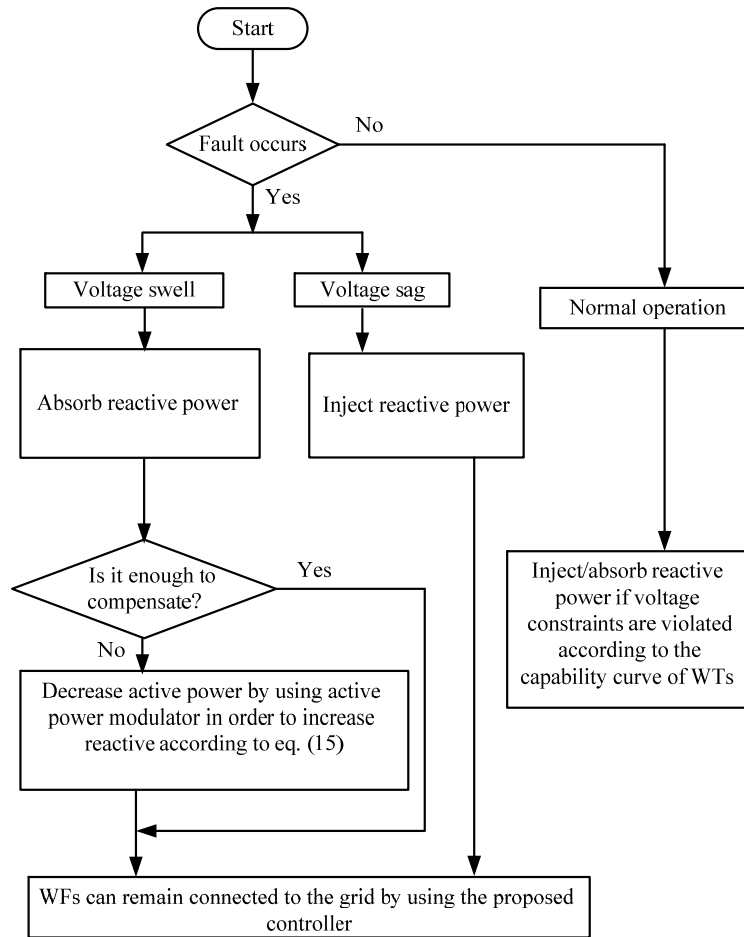Reactive power must be injected to the grid to support grid voltage recovery during voltage sag. According to Danish grid code, as shown in Fig.5.2, when the depth of voltage sags is 50%, the maximum reactive power (100% of the generation system rating) must be injected into the grid in order to compensate voltage variations. In the proposed control strategy, when voltage drops by 50%, the maximum reactive power (current) can be injected by DFIG converters. According to Fig.5.1, with the proposed method all WFs in different cases can successfully fulfill the FRT requirements and remain connected to the grid.

5.6   Description of Fuzzy Logic Controller

Due to nonlinearity of power system and linearization problems, the control of variable speed WTs may not be performed correctly with conventional control methods. For example, a PI controller design may require identifying the WT transfer function, the linear model of the network and defining an accurate tuning process.

The use of a fuzzy logic controller (FLC) can overcome these problems and deal with the nonlinearities as well as time variances of the system without the need of an accurate model. In the case of WTs control, for example, inaccurate aerodynamic calculations, tolerance in mounting the turbine, dirt or ice on blades, time-varying aerodynamic parameters, and other unpredictable parameter variations can make fuzzy logic control preferable if compared to conventional control methods [134, 135]. The fuzzy controller presents many advantages if compared to a PI controller [136]: 1) it is easy obtaining variable gains depending on the error; 2) it is simple solving problems affected by uncertain models, 3) it gives fast convergence, 4) it is parameter insensitive, and accepts noisy and inaccurate signals.

A FLC includes three blocks namely Fuzzification, Inference engine and Defuzification and is explained as follows.

5.6.1   Fuzzification

Fuzzification is a procedure to process the input variables with membership functions (MFs) and determines the degree of input variables belonging to one of the fuzzy sets through MFs. In order to convert the value of input variables into a value between 0 and 1, MFs are used and can take random shapes such as Gaussian, Sigmoidal and Triangular shape curves. In fact, MFs should be selected in a proper way to reflect the input variables' characteristics and meet the controller's requirements. MFs' overlapping is needed as it means more than one rule is fired at each time that is a main characteristic of a fuzzy controller.

In the proposed fuzzy controller, as shown in Fig.5.9, the selection of the best MFs has been performed on the basis of a prior knowledge and on experimentation with the system and its dynamics. Moreover, in order to design the FLC, shrinking span MFs have been chosen: this guarantees smoother results with less oscillations, large and fast control actions when the system state is far from the set point, and moderate and slow adjustments when it is near to the set point. Thus, when the system is closer to its set point, the MFs, for those specific linguistic terms, have narrower spans.
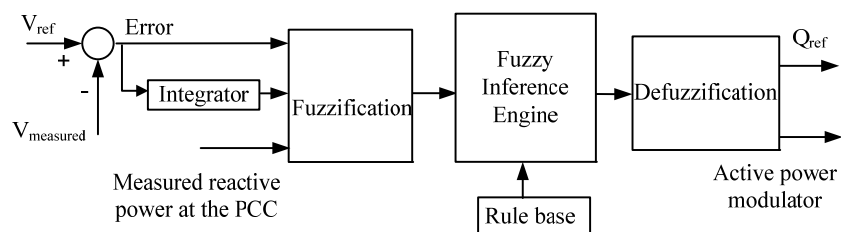
Fig.5.9. Fuzzy controller

The type of MFs is frequently chosen to fit an expected input data distribution or clusters and can influence both the tracking accuracy and the execution time. Triangular, Trapezoidal, and Gaussian MFs are the common choice even if any convex shape can be adopted. In particular, for the proposed controller, Triangular and Gaussian MFs have been compared and Triangular has been selected as type of MFs for input and output variables. Although most researchers are inclined

to design the input/output MFs using equal span mathematical functions, these do not always guarantee the best solution. Among all the parameters associated with a FLC, MFs have a dominant effect in changing its performance.

The proposed fuzzy controller presents three inputs: the error, the integral of error, and the measured reactive power at the PCC and two outputs that are the reference values for both the reactive and the active power production. The reference signal for the reactive power (Q_{ref}), varying in the range [-1 1], and the reference signal for the active power production (active power modulator), varying in the range [0 1] to decrease active power production and consequently increase the reactive power according eq. (5.15), both are sent by the fuzzy controller to the RSC of WTs.

Before fuzzification, all the input and output variables except active power modulator are normalized by using their base values.

The error is defined as the difference between the reference voltage (V_{ref}) and the measured voltage at the PCC.

The third input, the reactive power measured at the PCC, is used in order to determine when the active power modulator is required to be regulated by the fuzzy controller.

Here, the fuzzy sets of the inputs and outputs assume the following names: "NVB"= Negative-Very-Big, "NB"= Negative-Big, "NM" = Negative-Medium, "NS" = Negative-Small, "ZE" = Zero, and so forth. Triangular MFs have been selected for the inputs and outputs as shown in Fig.5.10.

5.6.2   Fuzzy Inference Engine

The fuzzy inference engine consists of the operation process, fuzzy rule implication and aggregation process. The fuzzified input variables are processed with fuzzy operators and IF-THEN rule implementation. The output fuzzy sets for every rule are aggregated into a single output fuzzy set. Input fuzzy sets are related to a fuzzy rule by a logical AND operator. Although each rule may have various weights, all the rules used here have the same weight.

Aggregation is the process to represent the outputs of each rule that is combined into a single fuzzy set. The input of aggregation

process is the output of fuzzy sets and its output is a fuzzy set for each output variable. The implementation of the fuzzy controller requires an adequate knowledge.

(a)

(b)

(c)

(d)
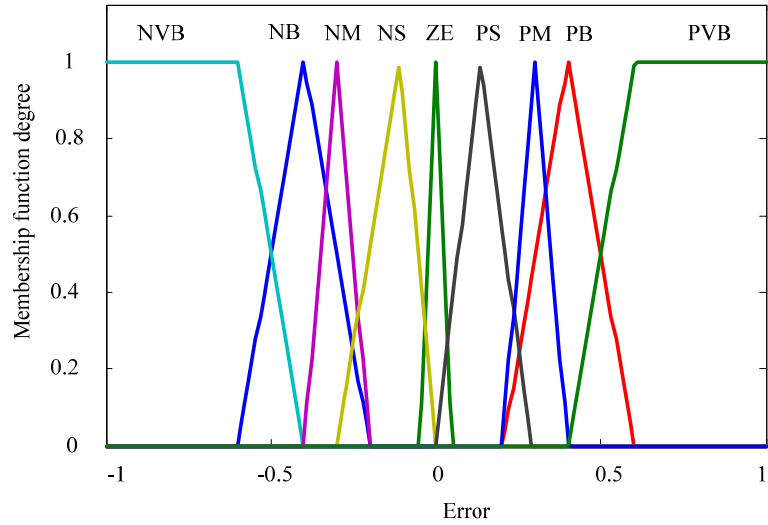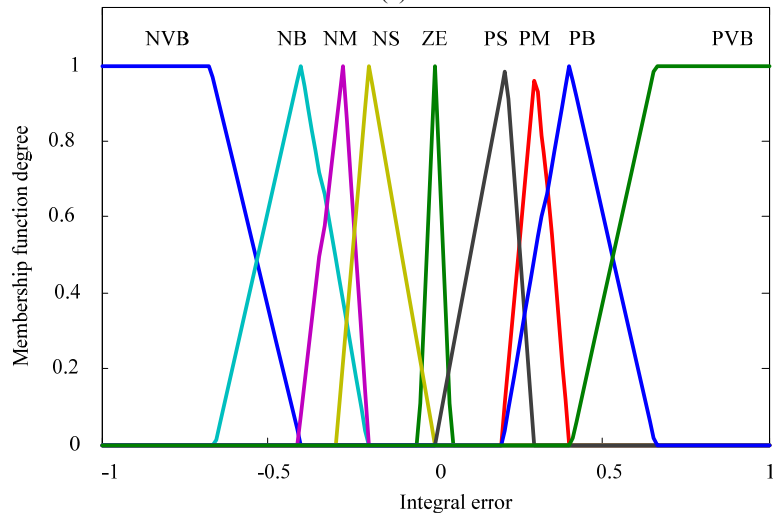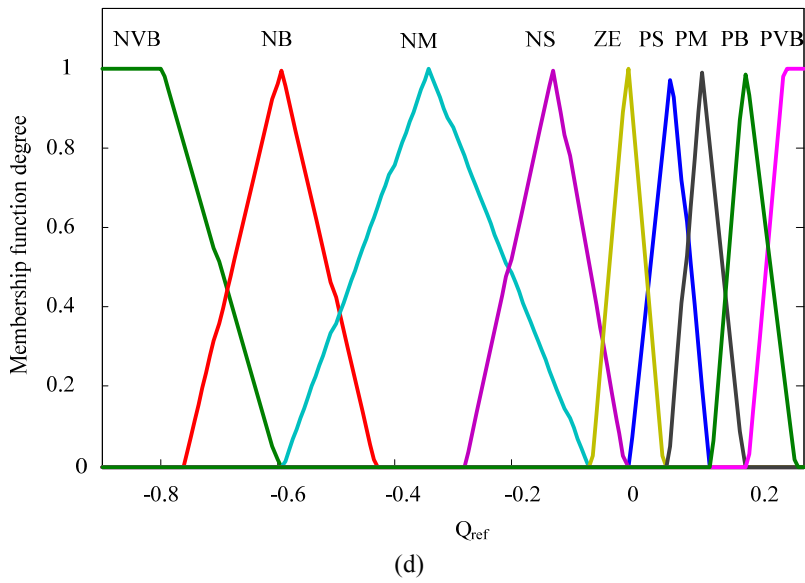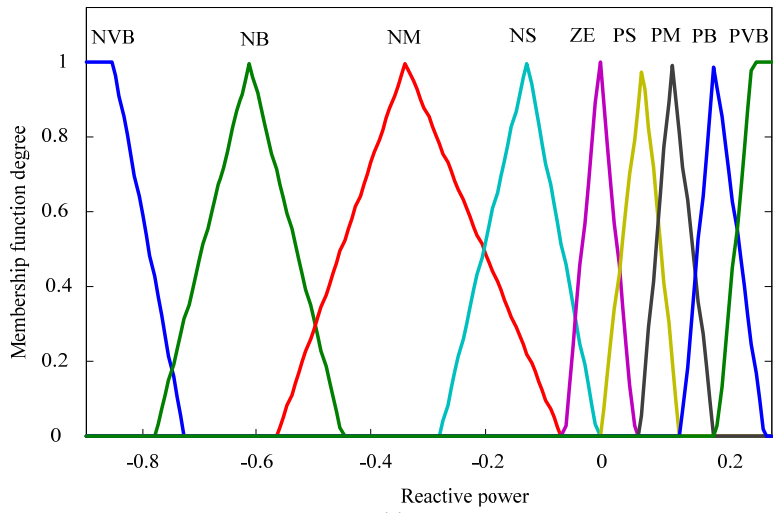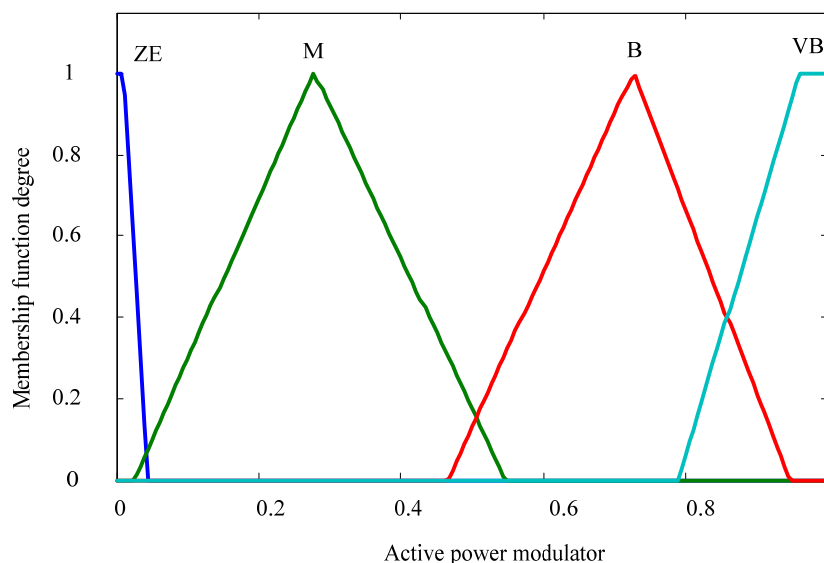
(e)

Fig.5.10. Membership functions of fuzzy controller. (a) Input signal error, (b) input signal integral error, (c) input signal reactive power measured at the PCC, (d) output reference reactive power, (e) output active power modulator

The knowledge base has been coded in a set of rules consisting of linguistic statements linking a finite number of conditions with a finite number of conclusions.

Such a knowledge can be collected and delivered by human experts and expressed by a finite number (r = 1, 2,…, n) of heuristic Multiple Input Single Output (MISO) fuzzy rules, is written as following form:

$$R^r_{MISO} : \text{IF}\,(x\,is\,A_i^{(r)})\,\text{AND}\,(y\,is\,B_i^{(r)})...$$
$$\text{AND}\,(z\,is\,C_i^{(r)})\,\text{THEN}\,(u\,is\,U_j^{(r)}) \tag{5.16}$$

where $A_i^{(r)}$, $B_i^{(r)}$, ..., $C_i^{(r)}$ are the values of linguistic variables (conditions) $x, y, ...z$, defined in the universes of discourse: $X, Y, ..., Z$, respectively, and $U_j^{(r)}$ is the value of independent linguistic variable u in the universe of discourse U.

Inference rules for the proposed controller can be derived by the control surfaces and some of these rules are provided in Table 5.3. 86 rules are used in order to design the fuzzy controller. Mamdani-based

system architecture is realized; Max-Min method is used in the inference engine.

Considering that, for a given combination of the active and reactive power, the maximum reactive power that can be injected/ absorbed by a WT depends on both the power converter size and the generated active power; the maximum reactive power that the WT can inject/absorb can be increased by decreasing the generated active power according to eq. (5.15).

Table 5.3 Rules of fuzzy controller

No.	Error	Integral error	Reactive power	Reference reactive power	Active power modulator
1	NVB	~PS	NVB	NB	B
2	NVB	~PVB	~NVB	NVB	ZE
3	NVB	NVB	~NVB	NVB	VB
4	NB	NS	~NVB	NVB	M
5	NM	PM	~NVB	NM	ZE
6	NS	PS	~NS	NS	ZE
7	ZE	ZE	ZE	ZE	ZE
8	PS	PVB	~PS	PS	ZE
9	PVB	NVB	~PB	PB	ZE
~ means NOT					

It's worth noting that the fuzzy controller identifies both the active and reactive power reference set points to send to the RSC of WTs described in Section 5.4.

The proposed controller is designed in order to compensate the voltage at the PCC by injecting/absorbing the Q_{ref} to the RSC as well as by regulating the active power modulator. Note that both signals, i.e. Q_{ref} and active power modulator, are sent by fuzzy controller to the RSC. The active power modulator is sent by the fuzzy controller to the RSC in order to decrease the injected active power with the aim of increasing the absorbed reactive power in the case of voltage swell.

An easy understanding of the proposed fuzzy controller can be summarized as follows.

1) If error is positive and integral of error is positive and reactive power measured at the PCC is positive, then Q_{ref} is positive and active power modulator is zero. In other words, in the case of voltage sag only Q_{ref} is sent by the fuzzy controller to the RSC in order to inject reactive power.

2) If error is negative and integral of error is negative and reactive power measured at the PCC is not NVB, then Q_{ref} is negative and the active power modulator is zero. In other words, in the case of voltage swell, when the absorbed reactive power is enough to decrease the voltage swell effects, there is no need to regulate the active power.

3) If error is negative and integral of error is negative and reactive power measured at the PCC is NVB, both reactive and active power are regulated in order to decrease the voltage swell effects. In this case, when the Q_{ref} is not enough to compensate the voltage swell effects, the active power modulator is sent by the fuzzy controller to the RSC in order to decrease the active power, and consequently increase the absorbed reactive power according to eq. (5.15).

Two fuzzy surfaces of the controller have been provided in Fig. 5.11. As evidenced from Fig. 5.11 (b), in the case of voltage swell when the absorbed reactive power reaches 80% of its maximum value the active power is decreased by the fuzzy controller in order to increase the maximum reactive power that WTs can absorb. Moreover, it is used in combination with a protection system for disconnecting the WTs from the grid when the controller is unable to compensate the voltage variations.

5.6.3   Defuzzification

The input for the defuzzification process is a fuzzy set and the output is a single value. Here, the centroid method is used for defuzzification. It can be evidenced that the controller does not need a mathematical model of the system; however, an understanding of the control requirements is needed.
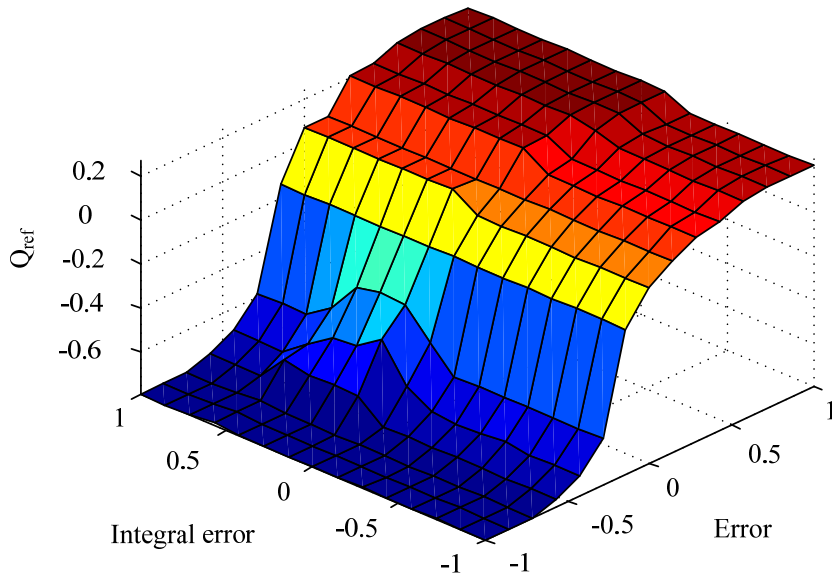
(a)
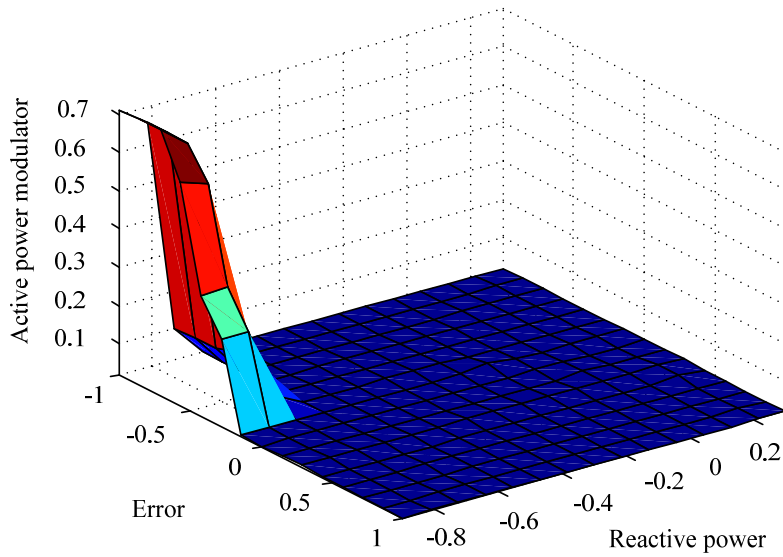
(b)

Fig.5.11. Fuzzy surfaces of the controller

5.7   Case Study and Simulation Results

A DFIG based WT, shown in Fig.5.4, has been considered [137]. In order to test the proposed controller three 9-MW WFs (6×1.5 MW WTs) connected to a real 25 kV weak distribution system, as shown in Fig.5.12, at buses 12, 16, and 35 are considered. The network is characterized by lines with high resistances and low X/R ratios. The base value for the power and voltage are 9 MVA, operating at power factor 0.9 lagging, and 575 V, respectively. According to the capability curve of the considered WFs, the limits of the reactive power that the WT can absorb or inject are about 8 MVar and 2.50 MVar, respectively. Real wind data sets acquired by the Wind Engineering Research Field Laboratory [138] are considered. The wind speed time history consists of 17500 observations within 50 seconds interval with sampling rate of 25 Hz. The wind profile and generated active power profile are shown in Fig. 5.13.

In order to test the FRT capability of the WFs endowed with the proposed fuzzy controller considering minimum and maximum load, two different cases are studied for the following load conditions.
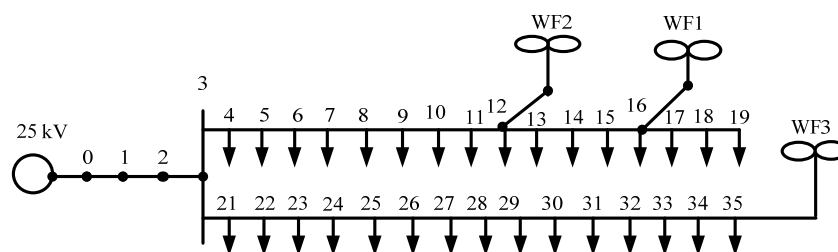

Fig.5.12. 25kV weak distribution network
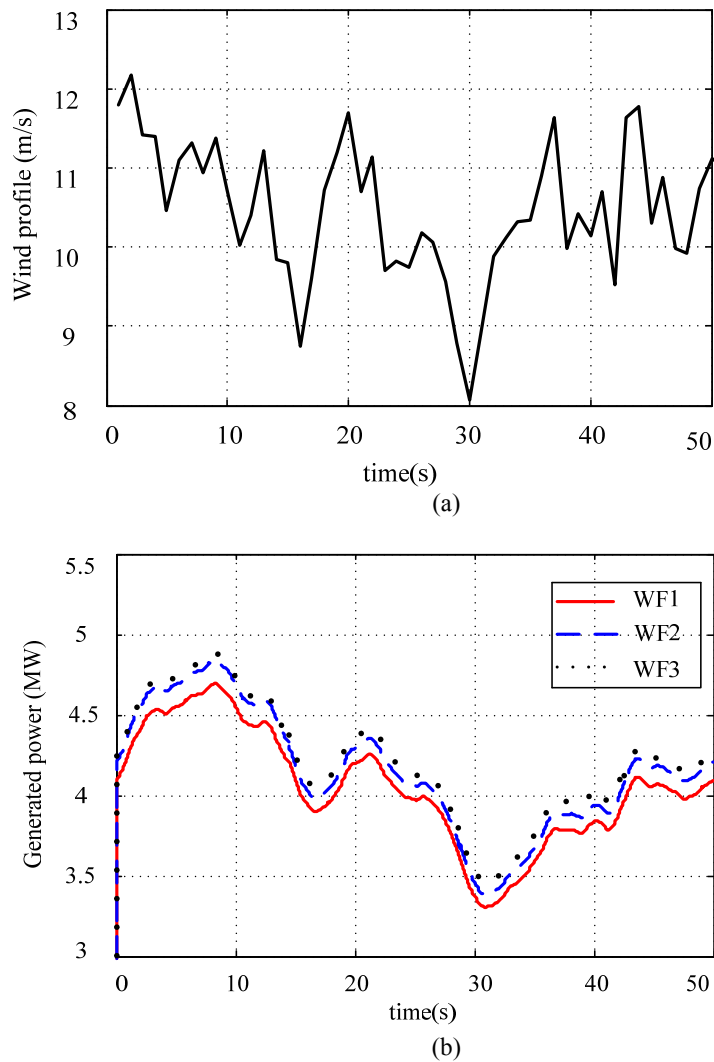
(a)

(b)

Fig.5.13. (a) wind profile (m/s), (b) generated power (MW)

5.7.1   Minimum load

The total network loads are 18 MW and 12.5 MVAr assumed as minimum load.

- Case study 1: a 30% voltage sag with a duration of 1 second starting at t=5, considering

i. three WFs at buses 12, 16 and 35,

ii. two WFs at buses 16 and 35.

- Case study 2: a 15% voltage swell with a duration of 1 second starting at t=5, considering

i. three WFs at buses 12, 16 and 35,

ii. two WFs at buses 16 and 35.

A1) Case study A1

(i)- When the voltage drops by 30%, each WF injects reactive power during the voltage sag in order to help increasing the voltage to 0.725, 0.730, and 0.741 p.u. for WF2, WF1 and WF3, respectively (see Fig. 5.14(a)).

The injected reactive power, as shown in Fig. 5.14 (b), varies between about 2.25 MVAr for WF3 to about 2.40 MVAr for WF2 according to the voltages at the connection buses. According to Danish grid code, all WFs can successfully fulfill the FRT requirement and, consequently, remain connected to the grid. In order to evaluate the effectiveness of the proposed controller, both the case without any controller and with a classical PI controller as designed in [139] are evaluated. The results are given in Table 5.4. It can be evidenced that with the fuzzy controller, all WFs can successfully fulfill the FRT requirement and remain connected to the grid while with the PI controller only WF3 can successfully fulfills the FRT requirement and remain connected to the grid while WF1 and WF2 disconnect. Moreover, without any controller all WFs disconnect.

Table 5.4 Results obtained with PI controller and without controller for all WFs

WF No.	Proposed Controller		PI Controller		Without Controller	
	Voltage (p.u.)	WF's situation	Voltage (p.u.)	WF's situation	Voltage (p.u.)	WF's situation
1	0.745	Connected	0.698	Disconnected	0.688	Disconnected
2	0.740	Connected	0.695	Disconnected	0.685	Disconnected
3	0.715	Connected	0.715	Connected	0.691	Disconnected
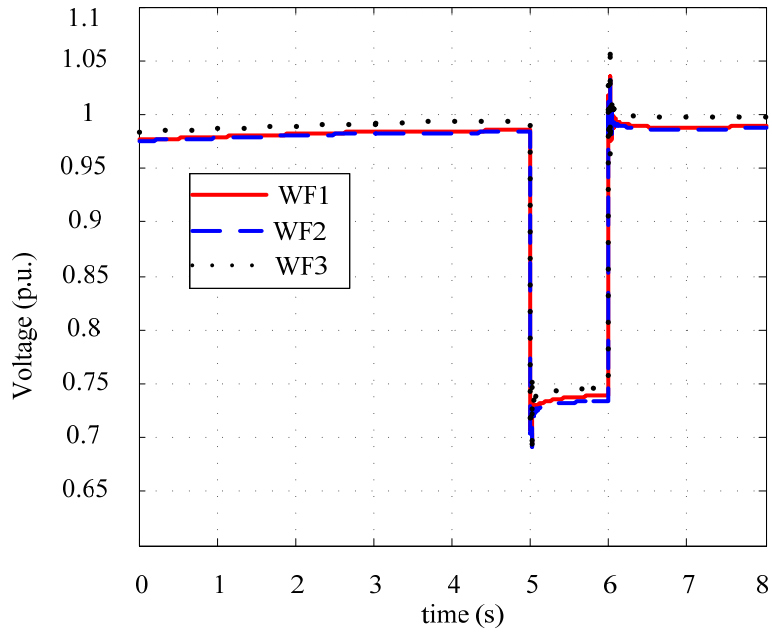
(a)
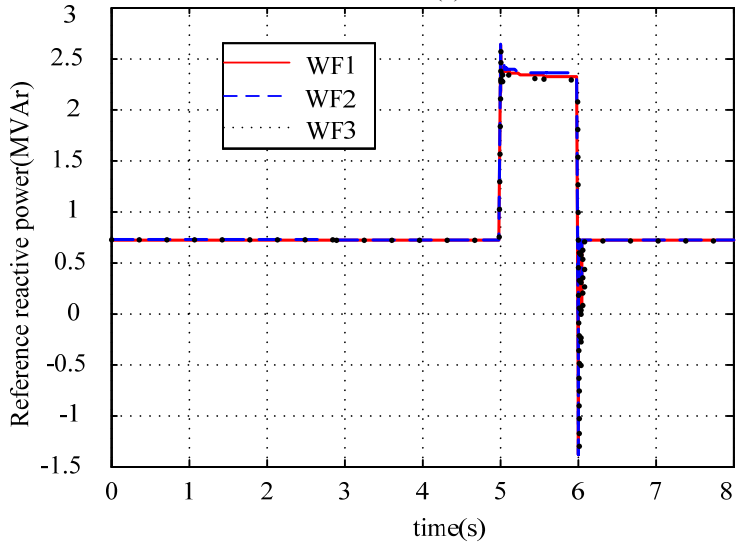
(b)

Fig.5.14. (a) Voltage at the PCC, (b) reference reactive power at the PCC

According to Danish grid code, as shown in Fig.5.2, when voltage drops by 50%, the maximum reactive power can be injected (100% of the generation system rating) by DFIG converters. In the case of 30% voltage sag, the proposed controlled controller injects about 50% of maximum reactive power (2.5 MVAr) in order to compensate voltage sag effects that can meet the requirements of Danish grid code. Note that the proposed controller is able to compensate voltage sags with deeper magnitudes than those assumed in the abovementioned case study up to 80% and meet the requirements of Danish grid code according to Fig.5.1.

  (ii) In this case, only WF1 and WF3 are considered. The reactive powers injected by the WFs increase if compared to the previous case and only WF3 can fulfill grid code requirements and remain connected to the grid (see Table 5.5).

Table 5.5 Results Obtained with proposed Controller in the case of 2 WFs

WF No.	Voltage (p.u.)	WF's situation
1	0.690	Disconnected
3	0.721	Connected

A2) Case study A2
  (i) Considering three WFs during a 15% voltage swell, they absorb reactive power in order to help lowering the voltage as shown in Fig.14. The absorbed reactive power varies between about 7 MVAr for WF1 to about 8 MVAr for WF3, as shown in Fig.15 (a), according to the voltages at the connection buses. The voltage, as shown in Fig. 14, at buses 16, 12, and 35 is about 1.060, 1.070, and 1.076 p.u., respectively. Moreover, when the absorbed reactive power reaches 80% of its maximum value and is not enough for compensating voltage variations, the active power modulator is regulated in order to decrease the generated active power to increase the absorbed reactive power generated by WFs. Therefore, in order to increase the absorbed reactive power for compensating the voltage swell, the active power modulator is regulated in order to decrease the generated active power for increasing the absorbed reactive power generated by WFs (see Fig. 15 (b)). The relation between measured reactive power, active power modulator and fuzzy controller surface is shown in Fig. 15. It is

evidenced that when the fault starts at t=5, for a period of 0.2 seconds, i.e. until 5.2 seconds, the absorbed reactive power is enough to compensate the voltage swell and the active power modulator is not regulated. According to Figs.5.16 (a), (b) and the fuzzy controller surface (Fig. 5.16 (c)), it can be observed that the active power modulator regulation starts at t=5.2s. The combined regulation of both active and reactive power generated by WFs allows in this case reducing the voltage swell effects. It can be observed in Fig.5.17 that the active power generated by the WFs during voltage swell is decreased by the fuzzy controller in order to increase the absorbed reactive power. In other words, when the absorbed reactive power reaches 80% of its maximum value, the active power is started decreasing by the fuzzy controller in order to increase the maximum reactive power that the WFs can absorb.

According to Danish grid code all WFs can successfully fulfill the FRT requirement and, consequently, remain connected to the grid. In order to assess the effectiveness of the proposed controller, the performance of the fuzzy controller is compared with that of a PI controller as designed in [139] and without any controller. As shown in Table 5.6, with the PI controller, WF1 and WF2 can successfully fulfill the FRT requirement and remain connected to the grid while WF3 disconnects; moreover, without any controller all WFs are disconnected.
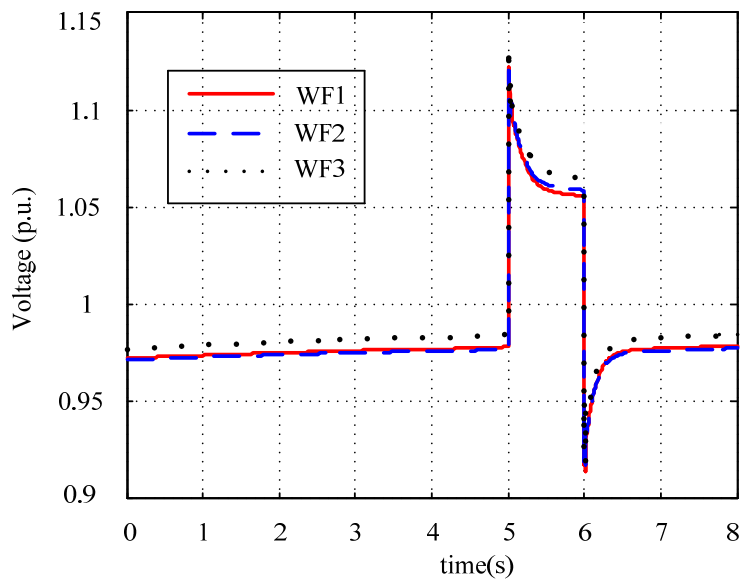
Fig.5.15. Voltage at the PCC
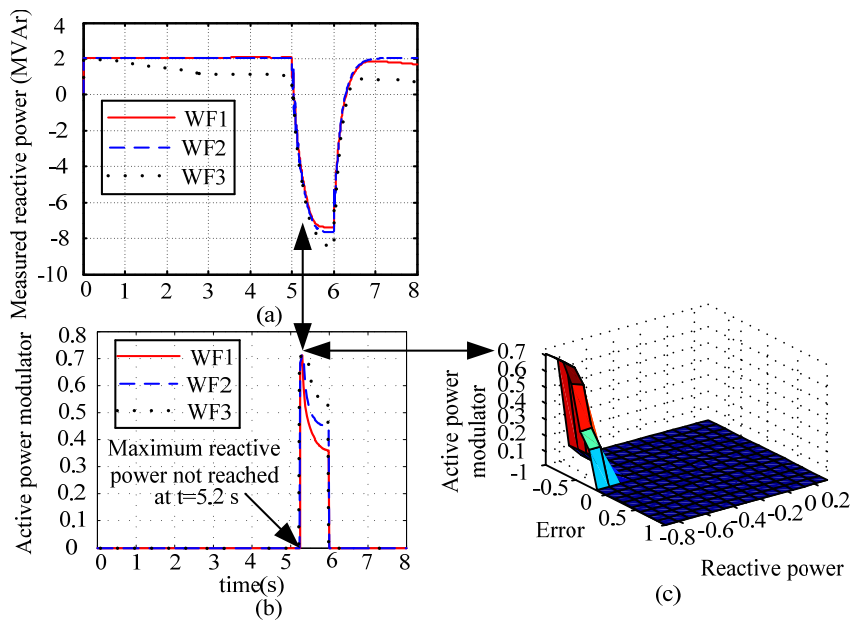
Fig.5.16 (a) Voltage at the PCC, (b) measured reactive power at the PCC (c) fuzzy controller surface
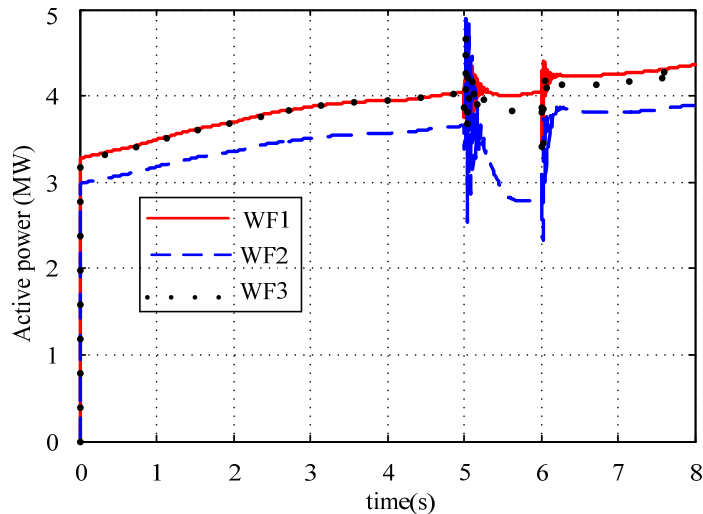
Fig.5.17. Active power generated by WFs at the PCC

Table 5.6 Results Obtained with PI Controller and Without Controller for All WFs

WF No.	Proposed Controller		PI Controller		Without Controller	
	Voltage(p.u.)	WF's situation	Voltage(p.u.)	WF's situation	Voltage(p.u.)	WT's situation
1	1.056	Connected	1.085	Connected	1.112	Disconnected
2	1.059	Connected	1.090	Connected	1.115	Disconnected
3	1.067	Connected	1.111	Disconnected	1.125	Disconnected

(ii) When considering only WF1 and WF3, it can be observed that the reactive power absorbed by the WFs is increased if compared to the previous case, while more active power is reduced. For example for WF3, in case (i) the absorbed reactive power is about 7.8 MVAr while a reduction of about 55% of active power is achieved. In case (ii) these values are about 8 MVAr and 62%, respectively. According to Table 5.7, both WF1 and WF3 can successfully fulfill the grid code requirements and remain connected to the grid. Therfore, by increasing the number of WFs their probability of remaining connected is increased.

Note that during the normal operation of network, the proposed controller is also able to compensate voltage constraints' violiations. As shown in Fig.5.18, for WF2 the voltage drop is higher than the other WFs and therefore the reactive power injected by fuzzy

controller in order to compensate voltage sag effect is higher than the others.

Table 5.7 Results Obtained with proposed controller in the case of 2 WFs

WF No.	Voltage (p.u.)	WF's situation
1	1.071	Connected
3	1.062	Connected
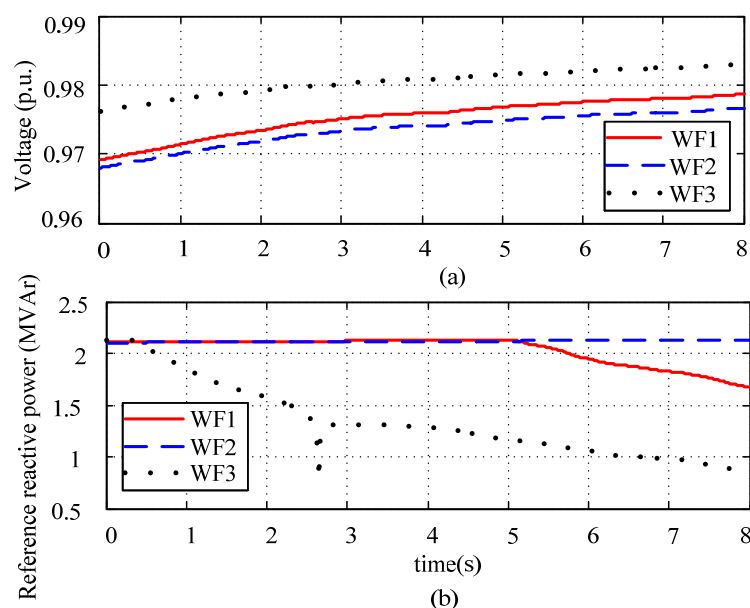
Fig.5.18. (a) Voltage and (b) reference reactive power at the PCC during the normal operation

5.7.2 Maximum load

A total maximum load of 24 MW and 15 MVAr has been assumed. The same case studies investigated in section A for minimum load are also studied for maximum load.

B1) Case Study B1

(i) When the voltage drops by 30%, each WF injects reactive power during the voltage sag in order to help increasing the voltage. The injected reactive power varies between about 2.35 MVAr for WF3 to

about 2.50 MVAr for WF2 according to the voltages at the PCC. By increasing the value of the loads, the voltage at the PCC decreases and the reactive powers injected by WFs increase. As shown in Fig.5.19, all WFs can fulfill the grid code requirements and can remain connected to the grid.
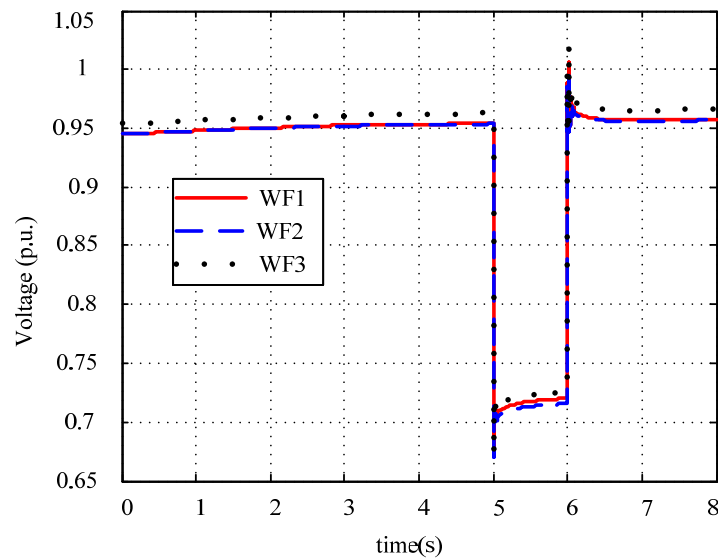
Fig.5.19. Voltage at the PCC

B2) Case Study B2

  (i) Considering three WFs during a 15% voltage swell, the absorbed reactive power varies between about 6 MVAr for WF1 to about 7 MVAr for WF3. A reduction of about 28% and 46% of active power is achieved for WF1 and WF3, respectively. According to Danish grid code, all WFs can successfully fulfill the FRT requirements and, consequently, remain connected to the grid.

  (ii) In this case, both WF1 and WF3 can fulfill the grid code requirement and remain connected to grid.

5.8   Discussion and Conclusion

This chapter proposed a fuzzy controller for improving FRT capability of variable speed WTs; it is designed in order to

compensate the voltage at the PCC by controlling both the reactive and active power generated by WFs. The FRT capability improvement considering both voltage sag and voltage swell effects is investigated considering Danish grid code. The proposed method is able to simultaneously regulate active and reactive power during voltage variations. During voltage sag only the reactive power is injected by using the controller in order to improve the voltage sag effects while during a voltage swell, when the absorbed reactive power is not enough, the active power generated by WFs is decreased by using the active power modulator that is sent by fuzzy controller to the RSC to increase the absorbed reactive power. In this case, according to both the WTs' power curve and capability curve, the WFs will not generate the maximum active power.

The novelty of the proposed fuzzy controller includes simultaneously considering active and reactive power regulation, for example, during a voltage swell, the absorbed reactive power is not adequate to lower the voltage at the PCC within its statutory limits, and the reference signal for the active power production is decreased by the fuzzy controller in order to increase reactive power. In this case the WTs will not generate the maximum active power according to the WTs' power coefficient, but this will determine two positive effects of the voltage regulation at the PCC: firstly, within the limited size of the power converters of DFIGs, the active power reduction will allow increasing the maximum reactive power that can be absorbed by WTs. Furthermore, in medium voltage weak networks with long feeders characterized by a high R/X ratio, the active power reduction can also increase the voltage drop on the feeders thus contributing to lower the voltage at the PCC.

In the previous research works, authors have investigated the FRT capability improvement only considering voltage sag while in this chapter the voltage swell effect is also considered to investigate FRT capability improvement according to Danish grid code.

The performances of the proposed fuzzy controller were analyzed for both voltage sags and swells considering different load values as well as different numbers and locations of WFs. The performances of the proposed controller were compared with a previously designed PI controller in *SymPowerSystems* toolbox of MATLAB [139]. The results revealed that the performances of the proposed controller are

better than those of the PI controller for both compensating voltage sag and swell effects. In other words, with the proposed controller all the WFs in different cases fulfill the FRT requirement and remain connected to the grid while with the PI controller in some cases WFs cannot fulfill the FRT requirement. Note that during the normal operation of the network (without faults), the proposed controller is also able to compensate bus voltage when its constraints are violated.

Chapter 6

Conclusion and Future Works

6.1   Summary

In this thesis, several aspects of planning, management and control of renewable energy source based distribution systems are investigated. The contents of the thesis consist of the following topics:

6.1.1 Planning of distribution network

6.1.2 Deterministic methods

    6.1.3 Modeling uncertainties of load and wind as well as the correlation among different wind speeds by using time series analysis.

    6.1.4 Providing a hybrid optimization method for wind power investment in distribution level by using market-based OPF and GA/PSO within a DNO acquisition market environment.

    6.1.5 Maximizing NPV related to the investment made by WTs' developers and SW over a target year.

    6.1.6 Minimizing annual energy losses from the point of view of DG-owning DNOs and maximizing SW over a target year.

    6.1.7 Using the GA/PSO to choose the optimal size and the market-based OPF to determine the optimal number of WTs.

6.1.2 Probabilistic methods

6.1.2.1 Providing a probabilistic methodology for assessing the SW and the amount of wind power that can be injected into the grid as well as the impact of wind power penetration on LMPs throughout the network within market environment considering uncertainties.

6.1.2.2 Modeling uncertainties due to the stochastic nature of wind as well as the volatility of WTs' offer price and quantity through MCS approach.

6.1.2.3 Maximizing the social welfare by using market-based OPF considering different combinations of load demand and wind generation over a year.

6.1.2.4 Providing a tool for DG-owning DNOs to better allocate WTs by considering cost reduction and consumers' benefits.

6.1.3 Management and control of distribution networks

6.1.3.1 Designing a fuzzy controller to improve FRT capability of DFIG based WTs according to Danish grid code. The controller is designed to compensate the voltage sags and swells at the PCC by simultaneously controlling the reactive and active power generated by WTs.

6.2 Conclusions

In this thesis, deterministic and probabilistic methods are developed for optimal planning of distribution networks with integration of WTs within a market environment.

With regards to the deterministic methods, hybrid optimization methods for optimal allocation of WTs from viewpoints of DG-owning DNOs and WTs' developers respectively for jointly minimizing annual energy losses and maximizing SW as well as maximizing NPV and SW are proposed:

(i) The method jointly minimizes the annual energy losses and maximizes the SW considering different combination of wind generations and load demands to determine the optimal locations,

sizes and numbers of WTs to be allocated at candidate buses. The GA is used to select the optimal locations and sizes among different sizes of WTs while the market-based OPF is used to determine the optimal number of WTs. DNO acts as the market operator of the DNO acquisition market that estimates the market clearing price and the optimization process for the active power hourly acquisition. The stochastic nature of both load and wind is modeled by hourly time series analysis. The method is also able to model the correlation among wind resources, i.e. for each range of generation capacity of the first wind profile, a layer with the coincident hours of demand/generation can be created for the second wind power profile.

The method can help DNOs to assess the performance of the network and to plan the WTs integration into distribution networks. Simulation results confirmed the capability and effectiveness of the proposed method in optimally siting and sizing of WTs in distribution networks.

 (ii) The method combines the PSO and the market-based OPF to jointly maximize the NPV associated to investment made by WTs' developers and the SW in DNO acquisition market environment. The PSO is used to select the optimal sizes among different sizes of WTs while the market-based OPF to determine the optimal number of WTs in order to maximize the SW considering network constraints.

The presented case study highlighted that WTs' developers by optimally allocating WTs at buses with the highest LMPs can both improve their profits and increase consumers' benefits by energy cost reduction, power losses decrease and network constraint alleviation.

 With regards to probabilistic methods, a probabilistic method to evaluate the effect of WTs integration into distribution networks within market environment was proposed. Combined MCS and market-based OPF are used to maximize the SW considering different combinations of wind generation and load demand.

The method can be utilized as a simulation tool to study the probabilistic SW and the impact of wind power penetration on LMPs throughout the network. Furthermore, it characterizes how LMP changes by increasing wind power penetration. It also can be used as a tool for DNOs to approximate the amount of wind power that can be injected into the network taking into account cost reduction and consumers' benefits.

The proposed probabilistic method can help DNOs to evaluate the performance of the network and to plan the WTs integration into distribution networks. Furthermore, it can help DG-owning DNOs to make better decisions to allocate WTs by using a more efficient method. The method can help DNOs to evaluate the impact of wind power penetration into the network in terms of both technical and economic effects.

Regarding the control and management of distribution networks, a fuzzy controller for improving FRT capability of WTs is designed to compensate the voltage sags and swells at the PCC by controlling both the reactive and active power generated by WFs. The FRT capability improvement is investigated considering Danish grid code. The proposed method is able to simultaneously regulate active and reactive power during voltage variations. During voltage sag only the reactive power is injected by using the controller in order to improve the voltage sag effects while during a voltage swell, when the absorbed reactive power is not adequate, the active power generated by WFs is decreased by using the active power modulator that is sent by fuzzy controller to the RSC to increase the absorbed reactive power. In this case, according to both the WTs' power curve and capability curve, the WFs will not generate the maximum active power but it has positive effects on voltage regulation at the PCC, i.e. within the limited size of the DFIG converters, the reduction of active power increases the maximum reactive power absorbed by WTs.

The simulation results showed that the performances of the proposed controller are better than those of the previously designed PI controller for both compensating voltage sag and swell effects. The proposed controller is also able to compensate bus voltage during normal operation when its constraints are violated.

6.3 Future Works

During the process of the research work, a number of interesting and promising research topics are identified. These research topics may deserve a further investigation in the future:

1) Modeling the correlation among different wind speeds by using autoregressive integrated moving average (ARIMA) method.

2) Developing the proposed hybrid deterministic methods in active networks and smart grids by using active network management schemes such as coordinated voltage control (CVC) and power factor control (PFC) within market environment.

3) Developing the proposed probabilistic method active networks by using CVC and PFC schemes considering also the correlation among different wind speeds.

4) Utilizing bilevel optimization and other efficient approaches such as mixed integer programming.

5) Study the reliability issues of distribution systems considering wind and load uncertainties within market environment.

6) Extending the proposed FRT approach for active distribution network and smart grids by applying active management schemes.

7) Developing other advanced control methods such as nonlinear and digital control techniques to improve FRT capability in active distribution network and smart grids.

References

[1] R. Banosa, F. Manzano-Agugliaro, F.G. Montoya, C. Gila, A. Alcayde, J. Gómez, "Optimization methods applied to renewable and sustainable energy: A review", Renewable and Sustainable Energy Reviews, vol. 15, no.4, pp. 1753-1766, 2011.

[2] D. Kirschen and G. Strbac, Fundamentals of Power System Economics. New York: Wiley, 2004.

[3] G. P. Harrison, A. Piccolo, P. Siano, A. R. Wallace, "Exploring the tradeoffs between incentives for distributed generation developers and DNOs", IEEE Trans. Power Syst., vol. 22, no.2, pp. 821-828, 2007.

[4] A. Piccolo, P. Siano, "Evaluating the impact of network investment deferral on distributed generation expansion", IEEE Trans. Power Syst., vol. 24, no.3, pp.1559-1567, 2009.

[5] P. Siano, L. F. Ochoa, G. P. Harrison, A. Piccolo, "Assessing the strategic benefits of distributed generation ownership for DNOs", IET Gener. Transm. Distrib., vol.3, no.3, pp. 225-236, 2009.

[6] I. M. de Alegría, J. Andreu, J. L. Martín, P. Ibañez, J. L. Villate, and H. Camblong, "Connection requirements for wind farms: A survey on technical requirements and regulation", Renewable Sustainable Energy Rev., vol. 11, no. 8, pp. 1858–1872, 2007.

[7] J. O. G. Tande, "Exploitation of wind-energy resources in proximity to weak electric grids", Applied Energy, vol.65, no. 1-4, pp. 395-401, 2000.

[8] G.P. Harrison, A. Piccolo, P. Siano, A.R. Wallace, "Hybrid GA and OPF evaluation of network capacity for distributed generation connections", Elect. Power Syst. Res., vol. 78, no.3, pp. 392-398, 2008.

[9] G.P. Harrison, A. Piccolo, P. Siano, A.R. Wallace", Distributed generation capacity evaluation using combined genetic algorithm and OPF", Int. J. Emerg. Electr. Power Syst., vol.8, no.2, pp. 1-13, 2007.

[10] K. Nara, Y. Hayashi, Y. Ikeda, K. Ashizawa, "Optimal allocation of distributed generation and reactive sources considering tap positions of voltage regulators as control variables", Euro. Trans. Electr. Power, vol.17, no.3, pp. 219-239, 2007.

[11]H. Falaghi, M.R. Haghifam, "ACO based algorithm for distributed generation sources allocation and sizing in distribution systems", IEEE Power Tech, pp. 555- 560, 2007.

[12]C.L.T. Borges, D.M. Falcao, "Optimal distributed generation allocation for reliability, losses, and voltage improvement", Int. J. Electr. Power Energy Syst., vol.28, no.6, pp. 413- 420, 2006.

[13]A.M. El-Zonkoly, "Optimal placement of multi-distributed generation units including different load models using particle swarm optimization", Swarm and Evolutionary Computation, vol. 1, no.1, pp. 50-59, 2011.

[14] P. Siano, P. Chen, Z. Chen, A. Piccolo, "Evaluating maximum wind energy exploitation in active distribution networks," IET Gener. Transm. Distrib., vol.4, no.5, pp. 598-608, 2010.

[15]C. Cecati, C. Citro, A. Piccolo, P. Siano, "Smart operation of wind turbines and diesel generators according to economic criteria", IEEE Trans. Industrial Electronics, vol. 58, no.10, pp. 4514 - 4525, 2011.

[16]C. Cecati, C. Citro, P. Siano, "Combined operations of renewable energy systems and responsive demand in a smart grid", IEEE Trans. Sustainable Energy, vol.2, no.4, pp. 468- 476, 2011.

[17]D.J. Burke, M. O'Malley, "Maximizing firm wind connection to security constrained transmission networks", IEEE Trans. Power Syst. vol.25, pp.749-59, 2010.

[18]J.K. Kaldellis, K.A. Kavadias, A.E. Filios, "A new computational algorithm for the calculation of the maximum wind energy penetration in autonomous electrical generation systems" Appl. Energy, vol.86, pp.1011-1023, 2009.

[19]B. Snyder, M.J. Kaiser, "A comparison of offshore wind power in Europe and the US: patterns and drivers of development", Appl. Energy vol.86, pp.1845-1856, 2009.

[20]S.A. Akdag, O. Guler, "Evaluation of wind energy investment interest and electricity generation cost analysis for Turkey", Appl. Energy, vol.87, pp.2574-2580, 2010.

[21]C. De Jonghe, E. Delarue, R. Belmans, W. D'Haeseleer, "Determining optimal electricity technology mix with high level of wind power penetration" Appl. Energy, vol.88, pp. 2231-2238, 2011.

[22] E. Haesen, C. Bastiaensen, J. Driesen, R. Belmans, "A probabilistic formulation of load margins in power systems with stochastic generation," IEEE Trans. Power Syst., vol. 24, no.2, pp. 951-958, 2009.

[23] T. H. M. El-Fouly, H. H. Zeineldin, E. F. El-Saadany, and M. M. A. Salama, "Impact of wind generation control strategies, penetration level and installation location on electricity market prices," IET Renew. Power Gen., vol. 2, no. 3, pp. 162–169, Sep. 2008.

[24] J. Choi, T. Tran, A. A. El-Keib, R. Thomas, H. Oh, R. Billinton, "A method for transmission system expansion planning considering probabilistic reliability criteria", IEEE Trans. Power Syst., vol. 20, no.3, pp. 1606-1615, 2005.

[25] M. Zhao, Z.Chen, F. Blaabjerg, "Probabilistic capacity of a grid connected wind farm", 31st IEEE Annual Conference of Industrial Electronics Society (IECON), pp.774- 779, 2005.

[26] P. Chen, P. Siano, B. Bak-Jensen, Z. Chen, "Stochastic optimization of wind turbine power factor using stochastic model of wind power", IEEE Trans. Sust. Energ., vol. 1, no.1, pp. 19-29, 2010.

[27] W. Wangdee, R. Billinton, "Considering load-carrying capability and wind speed correlation of WECS in generation adequacy assessment", IEEE Trans. Energy Convers., vol. 21, no.3, pp.734-741, 2006.

[28] P. Chen, P. Siano, Z. Chen Z, B. Bak-Jensen, "Optimal allocation of power-electronic interfaced wind turbines using a genetic algorithm-Monte Carlo hybrid optimization method", Wind Power Systems, Springer, Berlin, pp. 1–23, 2010.

[29] T. Jónsson, P. Pinsson, and H. Madsen, "On the market impact of wind energy forecasts," Energy Econ., to be published.

[30] Y.M. Atwa, E.F. El-Saadany, "Probabilistic approach for optimal allocation of wind-based distributed generation in distribution systems", IET Renew. Power Gener., vol. 5, no.1, pp. 79-88, 2011.

[31] K. Skytte, "The regulating power market on the Nordic power exchange Nord Pool: An econometric analysis," Energy Econ., vol. 21, no. 4, pp. 295–308, Aug. 1999.

[32] P. E. Morthorst, "Wind power and the conditions at a liberalized power market," Wind Energy, vol. 6, no. 3, pp. 297–308, 2003.

[33] R. Moesgaard and P. E. Morthorst, "The impact of wind power on electricity prices in Denmark," presented at the Eur. Wind Energy Conf. (EWEC), Brussels, Belgium, Apr. 2008.

[34] A. Ceña, "The impact of wind energy on the electricity price and on the balancing powers costs: The Spanish case," presented at the Eur.Wind Energy Conf. (EWEC), Marseille, France, Mar. 2009.

[35] D. Connolly, H. Lund, B. V. Mathiesen, and M. Leahy, "A review of computer tools for analyzing the integration of renewable energy into various energy systems," Appl. Energy, vol. 87, no. 4, pp. 1059–1082, 2010.

[36] A. Soroudi, "Possibilistic-scenario model for DG impact assessment on distribution networks in an uncertain environment", IEEE Trans. Power Syst., vol. 27, no. 3, pp. 1283–1293, 2012.

[37] F. Wu, X. P. Zhang, P. Ju, and M. J. H. Sterling, "Decentralized nonlinear control of wind turbine with doubly fed induction generator," IEEE Trans. Power Syst., vol. 23, no. 2, pp. 613–621, May 2008.

[38] G. Tapia, A. Tapia, and J. X. Ostolaza, "Two alternative modeling approaches for the evaluation of wind farm active and reactive power performances," IEEE Trans. Energy Convers., vol. 21, no. 4, pp. 909–920, Dec. 2006.

[39] G. Wenzhong, G. Wang, and J. Ning, "Development of low voltage ride through control strategy for wind power generation using real time digital simulator," in Proc. IEEE Power Syst. Conf. Exposit., Mar. 2009, pp. 1–6.

[40] L. Jerbia, L. Krichen, and A. Oualia, "A fuzzy logic supervisor for active and reactive power control of a variable speed wind energy conversion system associated to a flywheel storage system," Electric Power Syst. Res., vol. 79, no. 6, pp. 919–925, 2009.

[41] R. Sakamoto, T. Senjyu, T. Kaneko, N. Urasaki, T. Takagi, S. Sugimoto, and H. Sekine, "Output power leveling of wind turbine generator by pitch angle control using Hinf control," IEEE PES Power Systems Conf. and Exposition, , pp. 2044–2049, 2006.

[42] T. Senjyu, Y. Kikunaga, A. Yona, H. Sekine, A. Y. Saber, and T. Funabashi, "Coordinate control of wind turbine and battery in wind power generator system," IEEE Power and Energy Society General Meeting, Pittsburgh, PA, Jul. 20–24, vol. 2, pp. 1–7, 2008.

[43] W. Qiao and R. G. Harley, "Power quality and dynamic performance improvement of wind farms using a STATCOM," in Proc. IEEE Power Electronics Specialists Conf., pp. 1832–1838, Jun. 2007.

[44] M. Tsili and S. Papathanassiou, "A review of grid code technical requirements for wind farms," IET Renew. Power Gener., vol. 3, no.3, pp. 308–332, 2009.

[45] S. M. Muyeen, R. Takahashi, T. Murata, J. Tamura, M. H. Ali, Y. Matsumura, A. Kuwayama, and T. Matsumoto, "Low voltage ride through capability enhancement of wind turbine generator system during network disturbance," IET Renew. Power Gener., vol. 3, no. 1, pp. 65–74, 2009.

[46] C. Zhan and C. Barker, "Fault ride-through capability investigation of a doubly-fed induction generator with an additional series-connected voltage source converter," in Proc. 8th IEE Int. Conf. AC DC Power Transmission, Mar. 2006, pp. 79–84.

[47] L. Qu and W. Qiao, "Constant power control of DFIG wind turbines with supercapacitor energy storage," IEEE Trans. Ind. Applicat., vol. 47, no. 1, pp. 359–367, Jan.–Feb. 2011.

[48] J. Liang, W. Qiao, and R. G. Harley, "Feed-forward transient current control for low-voltage ride-through enhancement of DFIG wind turbines," IEEE Trans. Energy Convers., vol. 25, no. 3, pp. 836–843, Sep. 2010.

[49] H. Karimi-Davijani, A. Sheikholeslami, H. Livani, and M. Karimi-Davijani, "Fuzzy logic control of doubly fed induction generator wind turbine," World Appl. Sci. J., vol. 6, no. 4, pp. 499–508, 2009.

[50] E. Denny and M. O'Malley, "Wind generation, power system operation, and emissions reduction. IEEE Trans. Power Syst., vol.21, no.1, pp.341–347, Feb. 2006.

[51] H. A. Gil and G. Joos. Generalized estimation of average displaced emissions by wind generation. IEEE Trans. Power Syst., vol.22, no.3, pp.1035–1043, Aug. 2007.

[52] US Department of Energy (DOE). 20%Wind Energy by 2030: Increasing Wind Energy's Contribution to US Electricity Supply. DOE Office of Energy Efficiency and Renewable Energy Report, Jul. 2008, Available at http://www1.eere.energy.gov/windandhydro/wind 2030.html.

[53]European Union (EU). Climate change: Commission welcomes final adoption of Europe's climate and energy package. Europa press releases RAPID.

[54]European Wind Energy Association (EWEA). Making 180 GW a reality by 2020. Position Paper. Available at http://www.ewea.org/index.php?id=182, Oct. 2007.

[55]European Wind Energy Association (EWEA). Pure Power: Wind energy targets for 2020 and 2030. Report. Available at http://www.ewea.org/index.php?id=178, Dec. 2009.

[56]North American Electric Reliability Corporation (NERC). Accommodating High Levels of Variable Generation. Special Report. Available at http://www.nerc.com/news_pr.php?npr=283, Apr. 2009.

[57]Global Wind Energy Council. Global Wind 2009 Report. Available at http://www.gwec.net., 2010.

[58]T. Ackermann, J. Rivier Abbad, I. M. Dudurych, I. Erlich, H. Holttinen, J. Runge Kristoffersen, and Ejnar Sørensen. European Balancing Act. IEEE Power & Energy Magazine, vol.5, no.6, pp. 91–103, 2007.

[59] T. Ackermann (Ed). Wind Power in Power Systems. John Wiley & Sons, Chichester, England, 2005.

[60]E. A. DeMeo, W. Grant, M. R. Milligan, and M. J. Schuerger, "Wind plant integration", IEEE Power & Energy Magazine, vol.3, no.6, pp. 38–46, 2005.

[61]E. A. DeMeo, G. A. Jordan, C. Kalich, J. King, M. R. Milligan, C. Murley, B. Oakleak, and M. J. Schuerger, "Accommodating wind's natural behavior", IEEE Power & Energy Magazine, vol.5, no.6, pp. 68–77, 2007.

[62]H. Holttinen, "Hourly Wind Power Variations and their Impact on the Nordic Power System Operation", PhD thesis, Helsinki University of Technology, Helsinki, Finland. Available at http://www.regie-energie.qc.ca/audiences/3526-04/ MemoiresParticip3526/Memoire_CCVK_15_hh_lic_thesis finalpub.pdf, 2003.

[63]J. M. Morales, R. Minguez, and A. J. Conejo, "A methodology to generate statistically dependent wind speed scenarios", Applied Energy, vol.87, no.3, pp.843–855, 2010.

[64] E. Denny and M. O'Malley, "Quantifying the total net benefits of grid integrated wind", IEEE Trans. Power Syst., vol.20, no.2, pp.605–615, 2007.

[65] W.G. Früh, "Long-term wind resource and uncertainty estimation using wind records from Scotland as example", Renewable Energy, vol. 50, pp. 1014-1026, 2013.

[66] National Renewable Energy Laboratory (NREL), "Wind Energy Curtailment: Case Studies", Available at http://www.nrel.gov/docs/fy10osti/46716.pdf, Oct.2009.

[67] S. Borenstein, "The long-run efficiency of real-time electricity pricing", Energy Journal, vol.26, no.3, pp.93–116, 2005.

[68] S. Borenstein, S. P. Holland, "On the efficiency of competitive electricity markets with time-invariant retail prices", RAND Journal of Economics, vol.36, no.3, pp.469–493, 2005.

[69] The Brattle Group, "Quantifying Demand Response Benefits in PJM", Cambridge, MA. Available at http://sites.energetics.com/MADRI/pdfs/brattlegroupreport.pdf, Jan. 2007.

[70] S. P. Holland and E. T Mansur, "The short-run effects of time-varying prices in competitive electricity markets", Energy Journal, vol.27, no.4, pp.127–155, 2006.

[71] Smart Grids: European Technology Platform for the Electricity Networks of the Future, Available at http://www.smartgrids.eu/, 2010.

[72] T. H Bradley and A. A. Frank, "Design, demonstrations and sustainability impact assessments for plug-in hybrid electric vehicles", Renewable & sustainable energy reviews, vol.13, no.1, pp.104–117, 2009.

[73] J. Kiviluoma and P. Meibom, "Influence of wind power, plug-in electric vehicles, and heat storages on power system investments", Energy, vol.35, no.3, pp.1244–1255, 2010.

[74] P. Denholm, E. Ela, B. Kirby, and M. Milligan, "The Role of Energy Storage with Renewable Electricity Generation", National Renewable Energy Laboratory (NREL), Available at http://www.nrel.gov/docs/fy10osti/47187.pdf, 2010.

[75] H. Ibrahim, A. Ilinca, and J. Perron, "Energy storage systems – characteristics and comparisons", Renewable & Sustainable Energy Reviews, vol.12, no.2, pp.1221–1250, 2008.

[76] M. Ilic, F. D. Galiana, and L. Fink, "Power System Restructuring: Engineering and Economics" Springer, Massachusetts, 2010.

[77] C. K. Ekman and S. H. Jensen, "Prospects for large scale electricity storage in Denmark", Energy Conversion and Management, vol.51, no.6, pp.1140–1147, 2010.

[78] W. F. Pickard, A. Q. Shen, and N. J. Hansing, "Parking the power: Strategies and physical limitations for bulk energy storage in supply demand matching on a grid whose input power is provided by intermittent sources", Renewable & sustainable energy reviews, vol.13, no.8, pp.1934–1945, 2009.

[79] Market Operator of the Electricity Market of the Iberian Peninsula, OMEL. Available at http://www.omel.es, 2010.

[80] F. C. Schweppe, M. C. Caramanis, R. D. Tabors, and R. E. Bohn, "Spot Pricing of Electricity", Springer, Norwell, Massachusetts.

[81] S. Stoft, "Power System Economics: Designing Markets for Electricity", IEEE-Wiley, New York, 2002.

[82] Electricity Tariff Structures Review: International Comparisons Commission for Energy Regulation, CER, Ireland, 2004, CER/04/101.

[83] The Operating Environment for Distribution Companies Working Group on Distribution Issues, Union of the Electricity Industry – EURELECTRIC, Brussels, Belgium, 2005, Report 2004-233-0005.

[84] Electricity Distribution Price Control Review – Final Proposals. London, U.K.: Office of Gas and Electricity Markets (OFGEM), 2004.

[85] G. Strbac, N. Jenkins, P. Djapic, M. Hurd, and G. Nicholoson, "Benefits of Active Management", London, U.K.: Dept. Trade and Industry (DTI), 2003.

[86] G. P. Harrison and A. R.Wallace, "OPF evaluation of distribution network capacity for the connection of distributed generation," Proc. Inst. Elect. Eng.-Gen. Transm. Dist., vol. 152, no. 1, pp. 115–122, 2005.

[87] P. N. Vovos, G. P. Harrison, A. R.Wallace, and J. W. Bialek, "Optimal power flow as a tool for fault level constrained network capacity analysis," IEEE Trans. Power Syst., vol. 20, no. 2, pp. 734–741, May 2005.

[88] A. Keane and M. O'Malley, "Optimal allocation of embedded generation on distribution networks," IEEE Trans. Power Syst., vol. 20, no. 3, pp. 1640–1646, Aug. 2005.

[89] N. S. Rau and Y. H.Wan, "Optimum location of resources in distributed planning" , IEEE Trans. Power Syst., vol. 9, no. 4, pp. 2014–20,1994.

[90] Electricity Distribution Microsite Office of Gas and Electricity Markets [Online]. Available: http://www.ofgem.gov.uk/

[91] V. H. Mendez, J. Rivier, J. I. de la Fuente, T. Gomez, J. Arceluz, and J. Marin, "Impact of distributed generation on distribution losses," in Proc. 3rd Mediterranean Conf. Power Generation, Transmission, Distribution and Energy Conversion, Athens, Greece, 2002.

[92] S. Grenard and G. Strbac, "Effect of regulation on distribution companies investment policies in the UK," in Proc. IEEE Bologna PowerTech Conf., Bologna, Italy, Jun. 23–26, 2003.

[93] R.D. Zimmerman, Manual MATPOWER 2011, http://www.pserc.cornell.edu/matpower/manual.pdf.

[94] R.D. Zimmerman, C.E.Murillo-Sánchez, R.J. Thomas, "MATPOWER: Steady-State Operations, Planning, and Analysis Tools for Power Systems Research and Education", IEEE Trans. Power Syst., vol.26, no.1, pp.12-19, 2011.

[95] H. Wang, C.E. Murillo-Sánchez, R.D. Zimmerman, R.J. Thomas, "On Computational Issues of Market-Based Optimal Power Flow", IEEE Trans. Power Syst., vol. 22, no. 3, pp. 1185-1193, 2007.

[96] E. D. Castronuovo, J. M. Campagnolo, R. Salgado, "On the application of high performance computation techniques to nonlinear interior point methods," IEEE Trans. Power Syst., vol. 16, no. 3, pp.325-331, 2001.

[97] R. A. Jabr, A. H. Coonick, B. J. Cory, "A primal-dual interior point method for optimal power flow dispatching", IEEE Trans. Power Syst., vol. 17, no. 3,pp. 654-662, 2001.

[98] A.G. Tsikalakis, N.D. Hatziargyriou, "Centralized control for optimizing microgrids operation", IEEE Trans. Energy Convers., vol.23, no.1, pp. 241-248, 2008.

[99] MICROGRIDS-Large Scale Integration of Micro-Generation to Low Voltage Grids, May 2002, EU Contract ENK5-CT-2002-

00610, Tech. Annex [Online]. Available: http://microgrids.power.ece.ntua.gr.

[100] C. Schwaegerl, M. H. J.Bollen, K. Karoui, A. Yagmur, "Voltage control in distribution systems as a limitation of the hosting capacity for distributed energy resources ", IET CIRED conference, pp. 1-5, 2005.

[101] L. F. Ochoa, C. J. Dent, G. P. Harrison, " Distribution Network Capacity Assessment: Variable DG and Active Networks, IEEE Trans. Power Syst., vol. 25, no. 1, pp. 87-95, 2010.

[102] D. Das, "Optimal placement of capacitors in radial distribution system using a Fuzzy-GA method", Electrical Power and Energy Systems, vol. 30, no.6, 2008, pp.361-367.

[103] R. Palma-Behnke, J. L. A. Cerda, L. Vargas, A. Jofre, "A distribution company energy acquisition market model with the integration of distributed generation and load curtailment options," IEEE Trans. Power Syst., vol. 20, no. 4, pp. 1718-1727, 2005.

[104] MathWorks, Genetic algorithms and direct search toolbox: User Guide, 2004.

[105] J. Kennedy, R. Eberhart, "Particle swarm optimization," IEEE Int. Conf. Neural Networks, 1995, pp. 1942-1948.

[106] T. A. A. Victoirea, A. E. Jeyakumar, "Deterministically guided PSO for dynamic dispatch considering valve-point effect", Electr. Power Syst. Res., vol. 73, no. 3, 2005, pp. 313-322.

[107] N. Hatziargyriou and A. Zervos, "Wind power development in Europe", Proc. IEEE, vol. 89, no. 12, pp. 1765–1782, Dec. 2001.

[108] E. A. DeMeo et al., "Accommodating wind's natural behavior", IEEE Power Energy Mag., vol. 5, no. 6, pp. 59–67, 2007.

[109] Global Wind Energy Council, Global Wind 2008 Report. [Online]. Available: http://www.gwec.net.

[110] R. Karki, P. Hu, R. Billiton, "A simplified wind power generation model for reliability evaluation," IEEE Trans. Energy Convers., vol. 21, no. 2, pp. 533–540, 2006.

[111] G. C. Ejebe, J. Tong, J. G. Waight, J. G. Frame, X. Wang, W. F. Tinney, "Available transfer capability calculations," IEEE Trans. Power Syst., vol. 13, no. 4, pp. 1521-1527, 1998.

[112] P. Giorsetto, K. F. Utsurogi, "Development of a new procedure for reliability modeling of wind turbine generators," IEEE Trans. Power Apparatus Syst., vol. PAS-102, no. 1, pp. 134–143, 1983.

[113] K. Skytte, "The regulating power market on the Nordic power exchange Nord Pool: An econometric analysis," Energy Econ., vol. 21, no. 4, pp. 295–308, Aug. 1999.

[114] W.Hu, Z. Chen, B. Bak-Jensen, "The relationship between electricity price and wind power generation in Danish electricity markets", Asia-Pacific Power and Energy Engineering Conference (APPEEC), pp. 1-4, 2010.

[115] S.H. Jangamshetti, V. G. Rau, "Optimum Siting of Wind Turbine Generators", IEEE Trans. Energy Convers.,vol.16, no.1, pp. 8-13, 2001.

[116] M. Molinas , J.A. Suul, T. Undeland, "Low voltage ride through of wind farms with cage generators: STATCOM versus SVC", IEEE Trans. Power Electronics vol.23, no.3, pp.1104-1117, 2008.

[117] M.R. Rathi, N. Mohan, "A novel robust low voltage and fault ride through for wind turbine application operation in weak grids", Industrial Electronics Society, IECON 2005. 31st Annual conference of IEEE; 2005. pp. 2481-2483.

[118] H.Zou, H. Sun, J. Zou, "Fault ride-through performance of wind turbine with doubly fed induction generator: Industrial electronics and applications", 2nd IEEE conference ICIEA, pp. 1607-161, 2007.

[119] A.H. Kasem, E.F. El-Saadany, H.H. El-Tamaly, M.A.A. Wahab, " An improved fault ride-through strategy for doubly fed induction generator-based wind turbines", IET Renew. Power Gener., vol.2, no.4, pp.201-214, 2008.

[120] J.Yang, D.DG, J.E. Fletcher, "Fault ride-through of doubly-fed induction generator with converter protection schemes", IEEE International Conference in Sustainable Energy Technologies, pp. 1211-1216, 2008.

[121] W. Gao, G.Wang, J. Ning, "Development of low voltage ride through control strategy for wind power generation using real time digital simulator", IEEE PES Power system conference and exposition, pp. 1-6, 2009.

[122] Y.Liu, H. AQ, T. Guojun, S. Bhattacharya, "Control strategy improving fault ride-through capability of cascade multilevel inverter based STATCOM", IEEE Industry applications society annual meeting, 2008, pp. 1-6, 2008.

[123] J. Hu, Y. He, L. Xu, B.W. Williams, "Improved control of DFIG systems during network unbalance using PI-R current regulators". IEEE Trans. Industrial Electronics, vol.56, no.2, pp.439-451, 2009.

[124] C. Zhan, C. Barker, "Fault ride-through capability investigation of a doubly-fed induction generator with an additional series-connected voltage source converter", 8th IEE Int. Conf. AC and DC power transmission, ACDC 2006; pp. 79-84, 2006.

[125] M. Tsili, S. Papathanssiou, "A review of grid code technical requirements for wind farms", IET Renew. Power Gener., vol.3, no.3, pp. 308–332, 2009.

[126] 'Nordic grid code', Nordel, January 2007.

[127] Grid code for the local transmission system operator (Arreˆteʹ du Gouvernement wallon relatif a` la reʹ vision du re`glement technique pour la gestion du reʹseau de transport local d'eʹ lectriciteʹ en Reʹgion wallonne et l'acce`s a` celui-ci)'. Walloon Energy Commission (Commission Wallone pour l' Energie-CWaPE),Wallonia, Belgium, May 2007.

[128] 'Grid code–high and extra high voltage' E.ON Netz GmbH, Bayreut Germany, April 2006.

[129] 'Requirements for offshore grid connections in the E.ON Netz Network' E.ON Netz GmbH, Bayreuth, Germany, April 2008.

[130] 'Grid connection of wind turbines to networks with voltages below 100 kV, Regulation TF 3.2.6, Energinet, Denmark, May 2004.

[131] A. Tapia, G. Tapia, J. X. Ostolaza, and J. R. Saenz, "Modeling and control of a wind driven doubly fed induction generator," IEEE Trans. Energy Convers., vol. 18, no. 2, pp. 194–204, Jun. 2003.

[132] J. M. Carrasco, L. G. Franquelo, J. T. Bialasiewicz, E. Galvan, R. C. P. Guisado, and M. A. M. Prats, "Power-electronic systems for the grid integration of renewable energy sources: A survey," IEEE Trans. Ind. Electron., vol. 53, no. 4, pp. 1002–1016, Jun. 2006.

[133] M. E. Montilla-DJesus, D. Santos-Martin, S. Arnaltes, and E. D. Castronuovo, "Optimal operation of offshore wind farms with line commutated HVDC link connection," IEEE Trans. Energy Convers., vol. 25, no. 2, pp. 504–513, Jun. 2010.

[134] V. Galdi, A. Piccolo, and P. Siano, "Exploiting maximum energy from variable speed wind power generation systems by using an adaptive Takagi–Sugeno–Kang fuzzy model," Energy Conversion Manage., vol. 50, no. 2, pp. 413–421, 2009.

[135] V. Calderaro, V. Galdi, A. Piccolo, and P. Siano, "A fuzzy controller for maximum energy extraction from variable speed wind power generation systems," Electric Power Syst. Res., vol. 78, no. 6, pp. 1109–1118, 2008.

[136] V. Galdi, A. Piccolo, and P. Siano, "Designing an adaptive fuzzy controller for maximum wind energy extraction," IEEE Trans. Energy Convers., vol. 23, no. 2, pp. 559–569, Jun. 2008.

[137] C. Feltes, H. Wrede, F. W. Koch, and I. Erlich, "Enhanced fault ride through method for wind farms connected to the grid through VSC based HVDC transmission", IEEE Trans. Power Syst., vol. 24, no. 3, pp. 1537–1546, Aug. 2009.

[138] K. S. Hansen and G. C. Larsen, "Extreme wind characteristics from a Danish offshore site," in Proc. Offshore Wind Energy Mediterranean Other European Seas: Technol. Potential Application, pp. 441–454, 2000.

[139] SimPower Systems User's Guide, Hydro-Québec, MathWorks, 2009.